

165
-16-81
APPD

(3)

PC-2268

NTIS - 55
Bind - 108

DOE/ET/26917-T1

ENERGY

MASTER

CONSERVATION

ADVANCED ON-BOARD ELECTRIC VEHICLE CHARGER

Final Report

By
R. W. Johnson

December 31, 1979

Work Performed Under Contract No. AC01-78ET26917

ESB Technology Company
Yardley, Pennsylvania



U. S. DEPARTMENT OF ENERGY

Division of Transportation Energy Conservation

DISCLAIMER

This report was prepared as an account of work sponsored by an agency of the United States Government. Neither the United States Government nor any agency Thereof, nor any of their employees, makes any warranty, express or implied, or assumes any legal liability or responsibility for the accuracy, completeness, or usefulness of any information, apparatus, product, or process disclosed, or represents that its use would not infringe privately owned rights. Reference herein to any specific commercial product, process, or service by trade name, trademark, manufacturer, or otherwise does not necessarily constitute or imply its endorsement, recommendation, or favoring by the United States Government or any agency thereof. The views and opinions of authors expressed herein do not necessarily state or reflect those of the United States Government or any agency thereof.

DISCLAIMER

Portions of this document may be illegible in electronic image products. Images are produced from the best available original document.

825509

DISCLAIMER

"This book was prepared as an account of work sponsored by an agency of the United States Government. Neither the United States Government nor any agency thereof, nor any of their employees, makes any warranty, express or implied, or assumes any legal liability or responsibility for the accuracy, completeness, or usefulness of any information, apparatus, product, or process disclosed, or represents that its use would not infringe privately owned rights. Reference herein to any specific commercial product, process, or service by trade name, trademark, manufacturer, or otherwise, does not necessarily constitute or imply its endorsement, recommendation, or favoring by the United States Government or any agency thereof. The views and opinions of authors expressed herein do not necessarily state or reflect those of the United States Government or any agency thereof."

This report has been reproduced directly from the best available copy.

Available from the National Technical Information Service, U. S. Department of Commerce, Springfield, Virginia 22161.

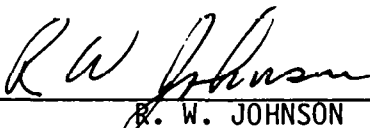
Price: Paper Copy \$10.00
Microfiche \$3.50

ADVANCED ON-BOARD ELECTRIC VEHICLE CHARGER
DOE CONTRACT NO. EM-78-C-01-5158

FINAL REPORT
31 DECEMBER, 1979

PREPARED FOR THE DEPARTMENT OF ENERGY
by
ESB TECHNOLOGY COMPANY

REPORT PREPARED BY



R. W. JOHNSON
Design and Development Engineer

Approved: 
W. K. BENNETT
Program Manager

THIS PAGE
WAS INTENTIONALLY
LEFT BLANK

ABSTRACT

This report describes the design and development of an on-board charger power module for use in electric vehicles. The module operates at 20KHz in a series resonant, half bridge configuration.

The report details circuit design trade-offs, module performance, and solutions to the problems of acoustic noise, maintaining high power factor, circuit protection and operating reliability.

The power module operates from a single phase, 240 V, 50/60 Hz utility line. Average power factor is 0.90; efficiency at maximum power output is 86 percent. The module is rated to charge a bank consisting of 20 Exide EV-106 batteries (60 cells) to an end voltage of 2.42 V/cell.

Physically, the module weighs less than 17 Kg. Projected manufacturing cost at the thousand unit level is \$394.00 (1978 dollars).

TABLE OF CONTENTS

	<u>Page No.</u>
ABSTRACT.....	iii
ILLUSTRATIONS.....	vi
FORWARD.....	vii
1.0 BACKGROUND.....	1
1.1 Elements of Charging Equipment.....	1
1.2 High Frequency Power Conversion.....	3
2.0 TECHNOLOGY DESCRIPTION.....	7
2.1 Basic Operation.....	7
2.2 Circuit Characteristics.....	11
3.0 MODULE DEVELOPMENT.....	12
3.1 Specification Goals.....	12
3.2 Conceptual Design.....	13
3.2.1 Power Factor.....	13
3.2.2 Power Circuit Configuration.....	13
3.2.3 Control Circuit.....	16
3.2.4 Circuit Protection.....	19
3.3 Implementation of the Development Goals.....	21
3.4 Major Characteristics of Power Components.....	26
3.4.1 Input Capacitor (C3).....	26
3.4.2 Series Resonant Capacitors.....	27
3.4.3 Current Sense Transformer.....	27
3.4.4 Anti-Parallel (Ringback) Diode.....	27
3.4.5 Snubber Components.....	28
3.4.6 Fault Survival Configuration.....	28
3.4.7 Main Power Transformer.....	29

TABLE OF CONTENTS (cont'd)

	<u>Page No.</u>
3.4.8 Output Filter Capacitors.....	29
3.4.9 SCR's (Silicon Controlled Rectifiers).....	30
4.0 RESULTS.....	31
4.1 Performance Evaluation.....	31
4.2 Achievements Against Goals.....	32
4.2.1 The Output.....	32
4.2.2 Efficiency.....	34
4.2.3 Power Factor.....	37
4.2.4 Input Requirements.....	42
4.2.5 Size and Weight.....	42
4.2.6 Estimated Cost.....	46
4.2.7 Circuit Protection Features.....	47
4.2.8 Additional Data.....	47
APPENDIX A: PROJECT CHRONOLOGY.....	
APPENDIX B: DOCUMENTATION.....	
APPENDIX C: BIBLIOGRAPHY.....	
APPENDIX D: SNUBBER CIRCUIT COMPUTER SIMULATION.....	
APPENDIX E: DATA AND DATA REDUCTION.....	
APPENDIX F: ESTIMATED MATERIAL COSTS.....	
APPENDIX G: POWER MODULE OPERATION AND CALIBRATION.....	

ILLUSTRATIONS

<u>Figure No.</u>		<u>Page No.</u>
1-1	Ferroresonant Charger Output Characteristic.....	2
1-2	Typical Closed Loop Charger Output Characteristic.....	4
2-1	Basic Power Module.....	8
2-2	Basic Current Waveform.....	9
3-1	Typical Charger Operation.....	14
3-2	Typical Series Resonant Charger.....	17
3-3	1Ø Series Resonant Charger Current Control.....	25
4-1	Closed Loop V-I Response.....	33
4-2	Efficiency (η) vs. Battery Voltage.....	35
4-3	Efficiency (η) vs. Line Voltage	36
4-4	Output Power Data Reduction.....	38
4-5	Power Factor vs. Battery Voltage.....	39
4-6	Power Factor vs. Line Voltage.....	40
4-7	Power Factor vs. Input Watts.....	41
4-8	Line Current vs. Battery Voltage.....	43
4-9	Power Module Front View.....	44
4-10	Power Module Rear View.....	45
4-11	Photograph of Typical Line Current.....	48
4-12	Photograph of Typical Resonant Current Envelope, High.....	48
4-13	Photograph of Typical Resonant Current Envelope, Med.....	49
4-14	Photograph of Typical Resonant Current Envelope, Low.....	49
4-15	Photograph of Typical Resonant Current Cycle, High.....	50
4-16	Photograph of Typical Resonant Current Cycles, Medium & Low....	50
4-17	Photograph of Typical Input Capacitor Voltage.....	51
4-18	Photograph of Typical Resonant Capacitor Voltage (at point "A" in Schematic Diagram, Fig. 2-1) at Medium and Low Current.....	51
4-19	Photograph of Typical Resonant Capacitor Voltage (at point "A" in Schematic Diagram, Fig. 2-1) at High Current.....	52
4-20	Component Weights.....	53

FORWARD

Existing battery charger technology is built around magnetics operating at power line frequencies, which are often very costly, large and heavy. These chargers are often largely dominated by raw material costs and therefore closely follow the rising cost of copper and iron.

One technique that can be used to reduce the cost of 60Hz magnetics is to eliminate the transformer. Such chargers connect the battery directly to the utility line. These chargers require protective features to prevent electrical shock hazards during operation. In addition, as with many 60Hz chargers, the power factor presented to the utility line is very low.

A second approach to reducing the cost and weight of magnetic components is the use of high frequency power conversion techniques. This report describes the concept, designs and operation of a specialized battery charger for electrical vehicles that is based on a high frequency series resonant power conversion circuit.

We believe that it is advantageous to use high frequency power conversion techniques to achieve size and weight reduction. With presently available components, a high frequency charger can be made more flexible, and more sophisticated charge regimes are possible with little additional cost. The use of SCR's with their inherently high surge current capability and high power gain can result in equipment with excellent efficiency as well as competitive cost. The series resonant inverter has been used for years in aerospace applications. With the recent development of fast turn-off SCR's, a major barrier to a successful high frequency charger has been eliminated. These semi-conductors have fast turn-on time, high rate of change of reapplied

voltage (dv/dt) and fast turn-off time. Similar advances are being made in other component designs, notably capacitors and transformer core materials. With these developments, there will be available components to produce high frequency chargers at a cost competitive to that of 60Hz chargers. In addition, the performance of the high frequency charger can be superior, in line power factor and efficiency, to standard 60Hz chargers.

1.0 BACKGROUND

1.1 Elements of Charging Equipment

Most storage batteries are recharged from the commercial utility line using equipment dedicated to charging a specific battery type and size. Two of the essential elements of this equipment are a rectifier, for charging the AC delivered by the utility line to DC required by the battery, and some means of changing the voltage of the utility line to that required for efficient charging of the battery. The vast majority of chargers that operate from the utility line employ magnetic transformers to change the line voltage level to that required by the rectifier and battery with minimum losses. The transformer also serves to isolate the battery from the utility line to reduce the risk of shock hazard from accidental contact with a battery terminal.

A third element normally included in charging equipment is a means for controlling the amount of charge delivered to the battery, or for measuring or sensing the battery state of charge, and terminating the charging process when the battery is determined to be fully charged. Both open-loop and closed-loop control systems are in use.

Open-loop control systems are best exemplified by the ferro-resonant (or constant-voltage) transformer class of charger. This charger is characterized by a well-regulated open-circuit output voltage and an inherently limited starting current. The result is a tapered charging characteristic, as shown in figure 1-1.

Closed-loop control systems operate by controlling the flow of charging current to the battery in response to some measured battery parameter, such as terminal voltage. Closed-loop systems have been implemented with many types of circuits. Two of the most common are

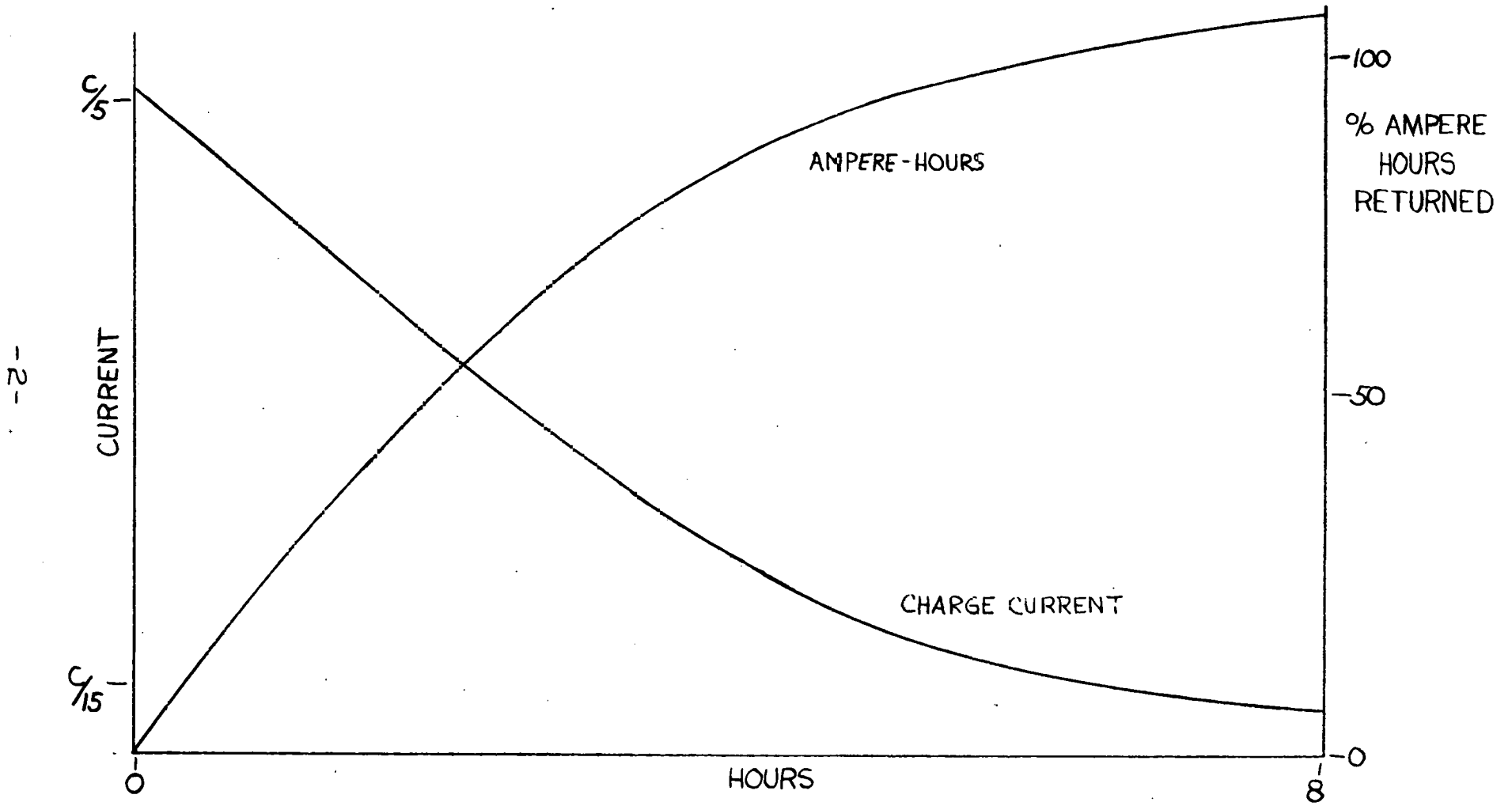


FIGURE 1-1
FERRORESONANT CHARGER OUTPUT CHARACTERISTIC

magnetic amplifiers and semiconductor switching circuits using SCR's (silicon controlled rectifiers) or transistors. Because of the greater degree of control permitted, closed-loop systems usually have a charge profile characterized by a constant starting current rate and a well-controlled finish voltage, as shown in figure 1-2.

1.2 High Frequency Power Conversion

In all conventional chargers, the transformer operates at the power line frequency (60 Hz in the U. S.); therefore, for chargers rated at over a few tens of watts, the transformer required becomes very large and heavy. Consequently, by addressing the transformer design, significant savings could be obtained in the areas of size, weight and cost of a charger.

The size and weight of a transformer are very much a function of the power line frequency. As the frequency increases, the required core cross-sectional area decreases. While the wire size will not decrease for a given current-carrying capacity, fewer turns and shorter length per turn result in reduced wire content. A transformer operating at a power line frequency in the range of 5 to 20KHz can be designed to be less than 1/10 the size of a 60Hz transformer of comparable power rating.

Realizing the size and weight savings that can accompany high frequency transformer operation requires that a high frequency power line be made available. Since the power line is fixed at 60Hz, the usual method used for high frequency power conversion is to rectify and filter the 60Hz line, and use the resulting DC to operate a local AC generator (inverter). For charge operation, the output of the transformer would be rectified for application to the battery. Thus the total conversion steps consist of AC-DC conversion, DC-AC inversion, transformation, and finally, AC-DC conversion.

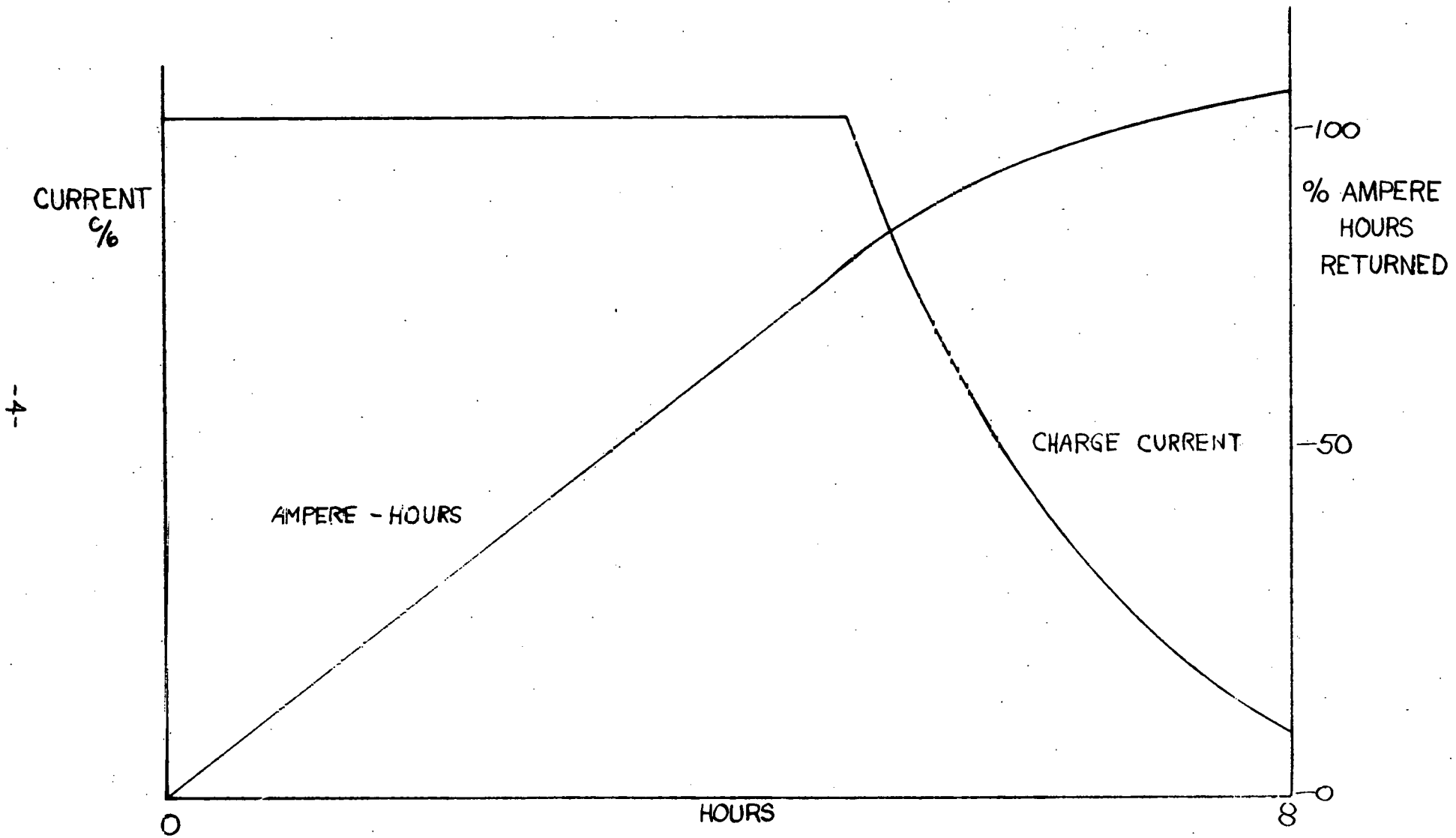


FIGURE 1-2
 TYPICAL CLOSED LOOP CHARGER OUTPUT CHARACTERISTIC

-4-

Conversion of power at high frequency offers certain advantages. The most obvious is reduction in transformer size and weight. Another is the reduced filter component requirements for the rectified output (output filtering reduces output RMS current and therefore internal heat loss of the battery being charged).

One of the most important benefits is cost; even with the extra stage of AC-DC conversion, a high frequency charger with power line isolation has slower rising cost trends than 60Hz equipment, because of the greatly reduced raw materials requirement. Finally, output power control can be achieved by controlling parameters (such as frequency) of the DC-AC inverter, thus reducing fixed power losses when the converter is in the "standby" mode (no output power demand).

Several circuit approaches have been developed for power conversion at high frequencies. The basic circuits are the parallel and bridge inverter circuits, originally designed for 60 Hz operation, adapted to operation at higher frequencies. These circuits are compatible with either transistors or SCR's. Variations of the parallel transistor inverters, using square-loop steel transformer core materials to control the operating parameters, have been used for many years in aerospace power supply applications. More recently, circuits designed especially for high-frequency operation have been applied to switching power supplies (so-called "off-line" switchers). These circuits include "buck" and "boost" regulators, variations of blocking oscillators, and parallel and series resonant switching circuits.

The series resonant circuit is particularly suitable for operation with SCR's, because SCR commutation occurs naturally every half cycle of operation, without the use of auxiliary commutation components. For

this, and other advantages, ESB developed a charger for industrial applications based on the series resonant circuit, operating from a three-phase utility line.

The common characteristic of all of the circuits described above is that they operate from a relatively constant DC voltage -- a battery, rectified and filtered AC line, etc. The three-phase utility line, when rectified, provides a DC voltage with only 5 percent ripple without filtering. The series-resonant circuit, as configured for 3-phase operation, cannot operate from a widely and rapidly fluctuating voltage supply, such as would be encountered in a rectified, but unfiltered, single phase utility line.

The power converter that ESB proposed to develop for this contract is an expansion of the technology developed at the ESB Technology Center in the past several years. Until recently, this circuit was either experimental or depended on high-cost components and techniques for its success. ESB's contribution has been to develop an inverter for three-phase applications that uses economical components and techniques to achieve a highly reliable and stable charger. Our goal for this contract is to extend this basic technology to a power conversion circuit that will operate from a rectified, unfiltered single-phase utility line while maintaining efficiency and input power factor goals.

2.0 TECHNOLOGY DESCRIPTION

2.1 Basic Operation

The basic operation of the controllable power module will be presented here. The specific implementation is discussed in Section 3.0.

The power stage of the controllable power module is an SCR series resonant inverter. In this type of inverter, the load (in our case a battery) is placed in series with a resonating inductor (L) and capacitor (C). This prevents the user, who has only the output terminals available, from inadvertently placing any high current stress (e.g., short circuit) on any of the semi-conductor switches.

Referring to figure 2-1, assume that a DC supply voltage is applied to the Input Capacitor (C3). When one of the main switching elements (e.g., SCR1) is turned on, a series resonant current pulse will flow through SCR1, L1, T1, into C1 and C2, charging point A above the DC supply voltage. This portion of the current waveform is called the "main" current pulse. Point A is now higher than the DC supply voltage. Now, a series resonant current pulse will flow in reverse from C1 and C2 through T1, L1, and CR1 into the DC supply. This portion of the current waveform is called the "ringback" current pulse, as shown in figure 2-2. It is important to note that the main current pulse is always larger in amplitude than the ringback current pulse. The SCR is conducting during the main current pulses. To shut off this device, it is required that the current be reduced below some minimum value (holding current) and remain below that value for a period of time (commutation time) before the SCR will switch to the forward blocking state. The ringback current pulse provides a natural, convenient method to achieve SCR commutation.

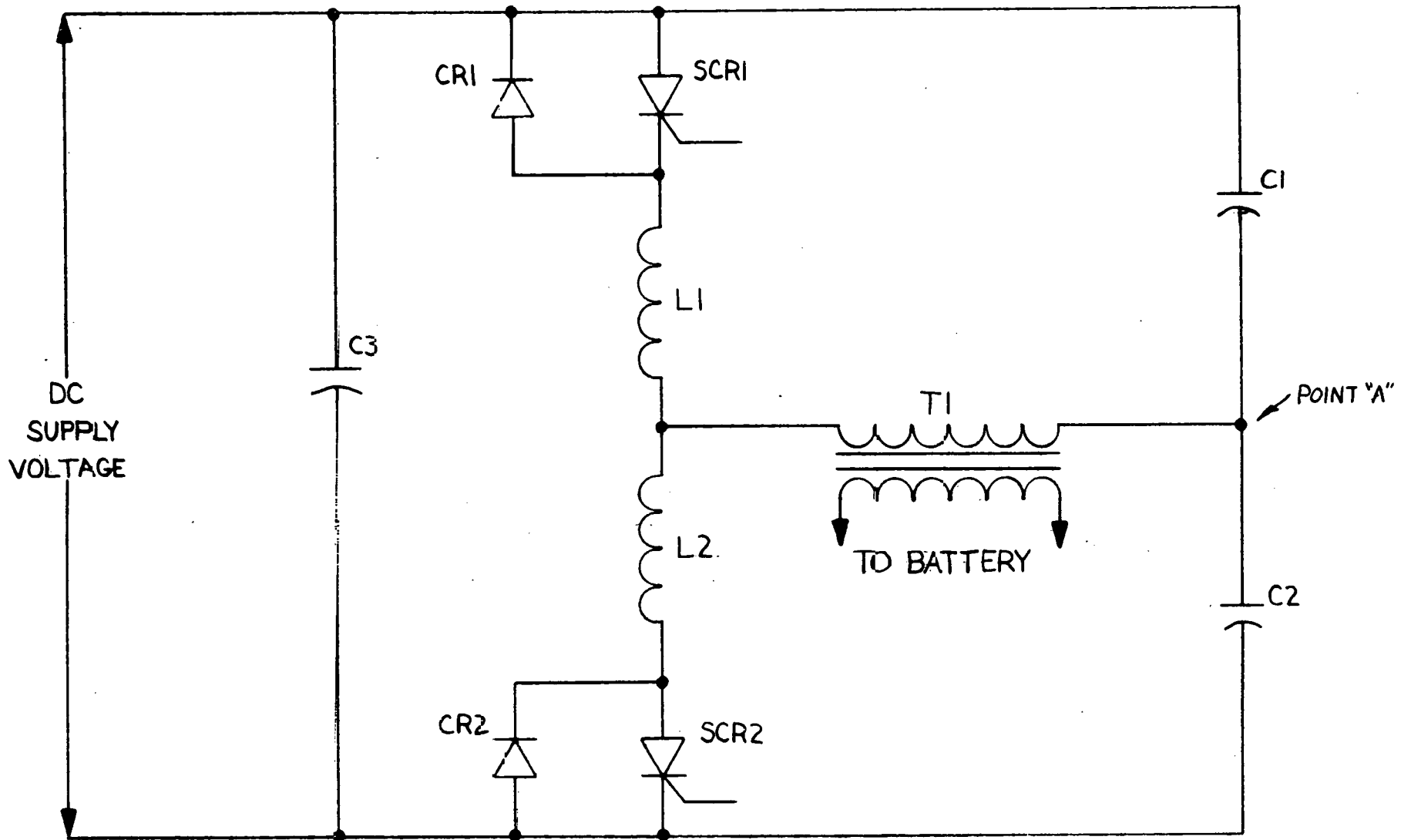


FIGURE 2-1
BASIC POWER MODULE

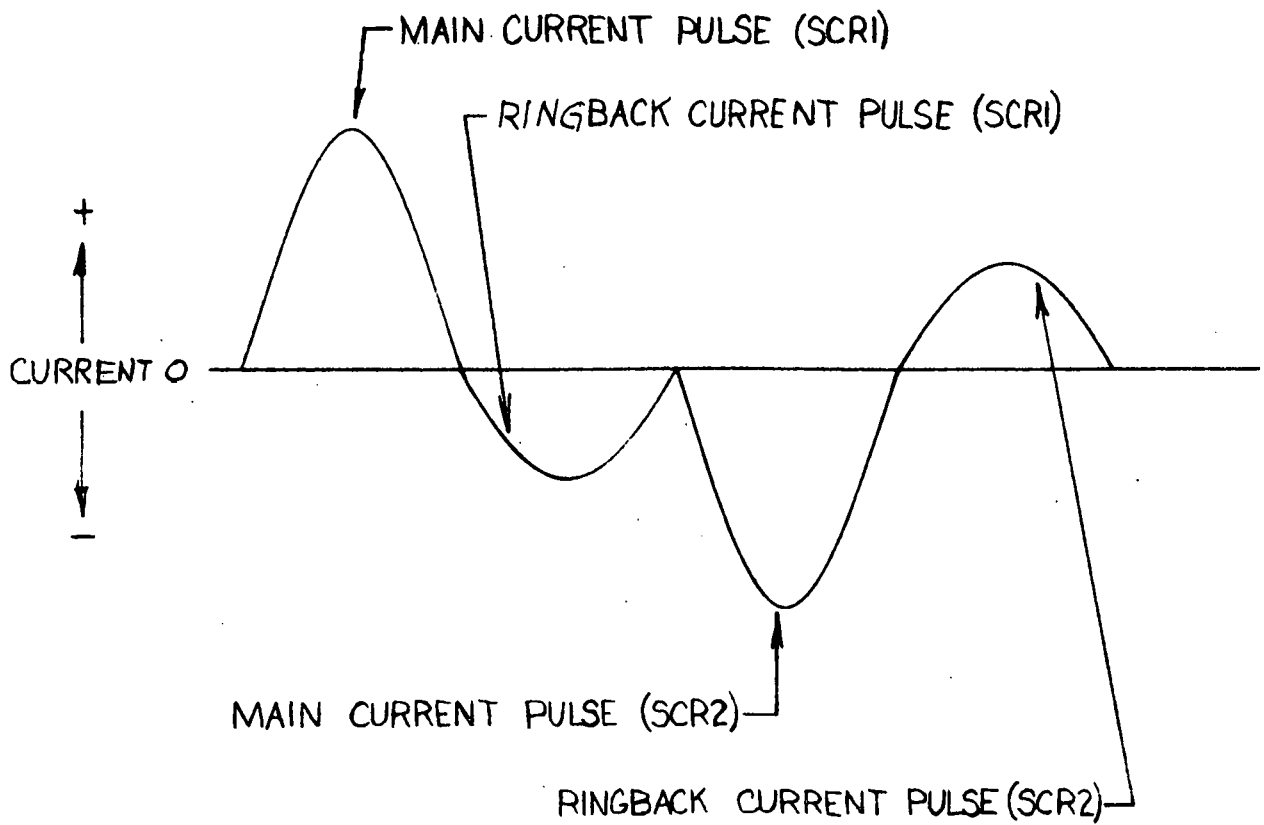


FIGURE 2-2
BASIC CURRENT WAVEFORM

The only requirement is that no other action will cause the SCR to conduct until the minimum commutation interval has passed. The main resonant current and subsequent ringback current pulses are similar, but negative, when the lower SCR is turned on, as shown in figure 2-2.

If we neglect the small resistive components in the circuit and the DC power source, we can describe the main current flowing when SCR1 is fired:

$$i = \frac{V_{C1} - V_{BAT}}{\sqrt{\frac{L_1}{C_1 + C_2}}} \sin \frac{t}{\sqrt{L_1(C_1 + C_2)}}$$

where V_{C1} is the voltage across C1 at the instant the SCR is turned on, V_{BAT} is the load voltage reflected into the resonant circuit and the input capacitor (C3) is much larger than capacitors C1 or C2.

In addition, we now can see that the current is sinusoidal in nature, and therefore the SCR will see a low rate of change of current or di/dt , minimizing the power dissipation during the first 1 or 2 microseconds of SCR conduction, when the forward conducting voltage can be high.

It is obvious that if we decrease the number of current pulses within a fixed period of time, we can control the average current into the battery. It is not obvious that if we fire the next SCR during the ringback current pulse of the previous SCR, we obtain an added advantage. As we move from the end of the ringback pulse toward the beginning of this pulse, we will achieve an apparent increase in supply voltage. The main current pulse (resulting from firing SCR1, for example) causes the voltage at point A to rise above the supply voltage;

during the ringback current pulse, the voltage at point A returns sinusoidally to a point below the supply voltage. Firing SCR2 before this cycle is complete will increase its apparent supply voltage. A similar relationship exists in the next half-cycle. The only restriction to this technique is that at no time can either SCR be fired until the minimum commutation time has elapsed.

2.2 Circuit Characteristics

The series resonant inverter allows high speed inverter SCR's to be run at their maximum operating frequency while minimizing switching losses for that frequency. A half-resonant cycle can be used for commutation, while the resonant inductors limit di/dt . High operating frequencies are desirable because they permit reduction in the cost, size and weight of power conversion equipment. Off-line switching power supplies illustrate this well. The cost savings in power transformers and inductors at higher conversion frequencies can more than offset the increased complexity and cost of generating the high frequency.

The series resonant inverter has the advantage of simplicity when compared to parallel or bridge type SCR inverters. The auxiliary commutation SCR(s) inherent in the latter inverters are not required in the series resonant inverter. Compared to transistor inverters, the series resonant SCR inverter has much better power handling capability without the necessity of paralleled semiconductor switches. Compared to transistorized off-line switching regulators of the buck-boost type, the series resonant inverter is more rugged and reliable and, in the multikilowatt power range, more economical. This is especially true when operating from 240 Vrms or higher since high voltage transistors with the same power handling capabilities are more expensive than SCR's at present.

One penalty that must be paid for the above benefits is higher peak operating currents than in the other inverter types. Despite the current peaks, efficiencies of 88-90 percent are obtainable.

Another disadvantage to the series resonant converter is the generation of acoustic noise when output power is reduced. Noise can be reduced through careful control of component design and circuit operating parameters.

A third disadvantage, also in common with all high frequency converters, is the generation of RFI/EMI. This problem will yield to classical solutions.

3.0 MODULE DEVELOPMENT

3.1 Specification Goals

The development of a basic controllable power module, suitable for on-board installation, is presented here. The power module will be capable of charging a 20KWH battery in 6-8 hours. The power module will be operating from any standard 240V, 2-wire, single phase utility line. Although it is capable of being completely controllable (to a user defined charge control regime) this model will be equipped with a fixed function control circuit that provides constant current, constant voltage with automatic crossover, to permit an evaluation against known standards.

The power module goals are:

OUTPUT: 145 volts DC, 23 amperes, 0-3300W continuously variable

SIZE: 20,000-26,000 cm³ (1200-1600 in²)

WEIGHT: 16-20 Kg (35-45 lbs)

EFFICIENCY: 88%

POWER FACTOR: 0.9

INPUT REQUIREMENTS: less than 20A RMS at 240VAC nominal RMS
single phase

INITIAL PROTOTYPE COST ESTIMATE: Less than \$400 each in small quantities (100-1000) units (1978 dollars).

RELIABILITY: Commensurate with automotive industry electrical equipment.

ELECTRICAL SAFETY: Battery load will be electrically isolated from utility line.

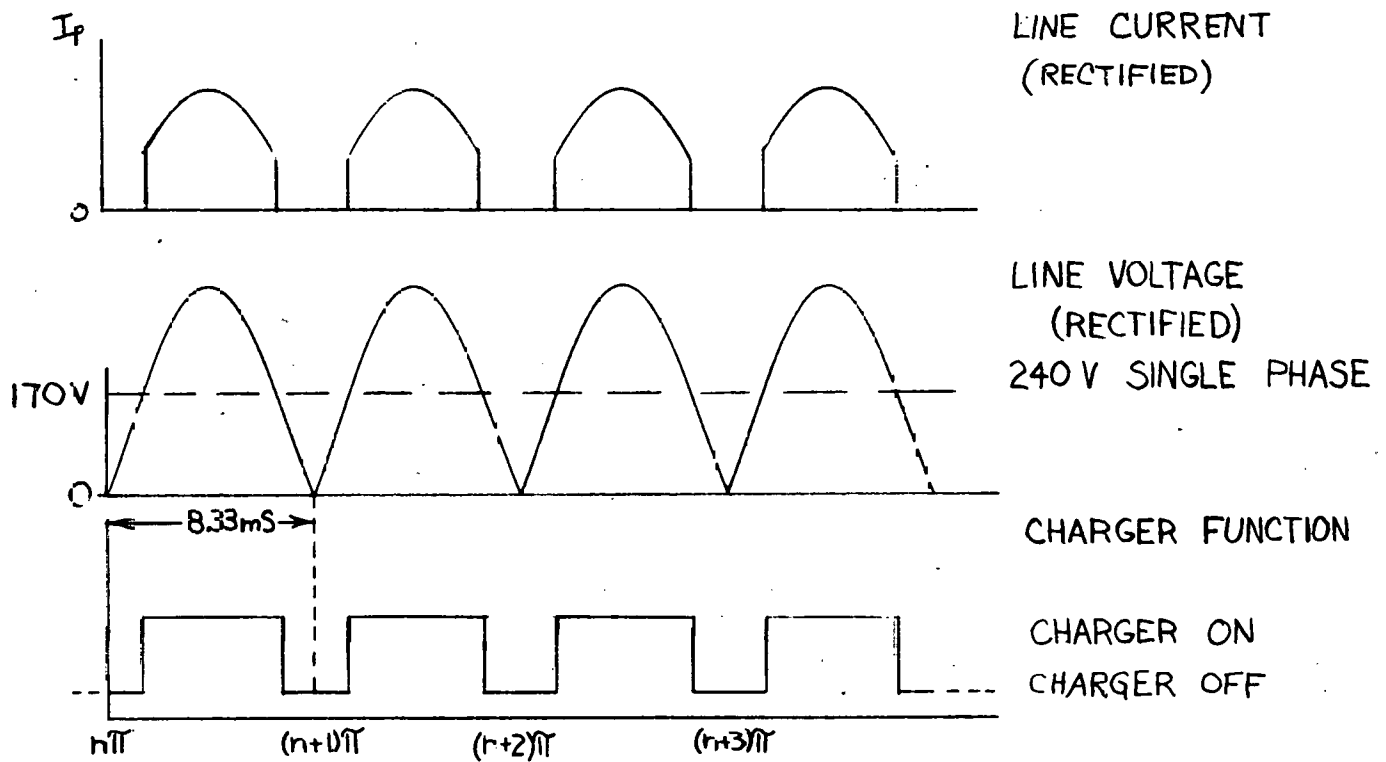
3.2 Conceptual Design

3.2.1 Power Factor

To fulfill the above goals, it became obvious that to achieve the required line power factor (0.9), the charger must draw a sinusoidal current that is in phase with the input voltage. This eliminates the possibility of extensive line filtering to establish a DC supply. The method chosen requires that the power module operate over the entire line voltage swing. However, the operation of the power module requires a minimum DC supply voltage. To obtain reasonable power factor (which would be measured by standard meters), the charger is prevented from operating until the instantaneous line voltage reaches 170V. The charger is then turned on, and the instantaneous line current is a function of the applied line voltage (see Figure 3-1).

3.2.2 Power Circuit Configuration

The selection of a half bridge configuration was made for several reasons. First, the reduced voltage stresses on the resonant capacitors permit the use of standard components; second, the number of switching elements is half that of a full bridge configuration. The penalty paid for the half bridge is that the current in each switching element is double that for the full bridge. In conversation with SCR Manufacturers, we have



Note: Timing shown for 60 Hz.

FIGURE 3-1
TYPICAL CHARGER OPERATION

learned that, although SCR's capable of operating in the charger are presently limited to 40A RMS, higher rated devices are in the laboratories and should be available in the near future. Half-bridge operation would then be economically achieved with a single device in each switching element.

At present, the resonant current required is greater than a single SCR can handle, so two SCR's configured in parallel are fired simultaneously. The alternate switch is constructed similarly. To divide the current equally in each SCR leg, we have split the resonant inductor and placed a portion in each leg. The current that flows in each switch leg is controlled by this dominant impedance, minimizing current imbalances caused by different SCR conduction characteristics. This inductor will also provide the small but necessary snubbing inductance to limit the rate of change of reapplied forward voltage (dv/dt) on the SCR's.

The output transformer is basically a current fed device. The principal drive current is the 20 KHZ inverter current. In addition, the current will be modulated at a 120Hz rate. Control of the flux in the core is of prime importance. The only fixed voltage available in the power circuit is the battery. Therefore, the secondary (battery side) of the transformer is placed closest to the core and stabilizes the core flux. The mismatches of the diodes and other contributors to a DC imbalance are compensated by a small air gap between core halves. The primary is spaced off the secondary winding to provide a leakage inductance between the primary and secondary windings, and in addition, to provide increased cooling of both windings.

3.2.3 Control Circuit

Although the basic control of the inverter is straightforward, it is necessary to monitor such functions as line voltage, battery voltage, charger current and instantaneous resonant current, to maintain semiconductor operation within their ratings.

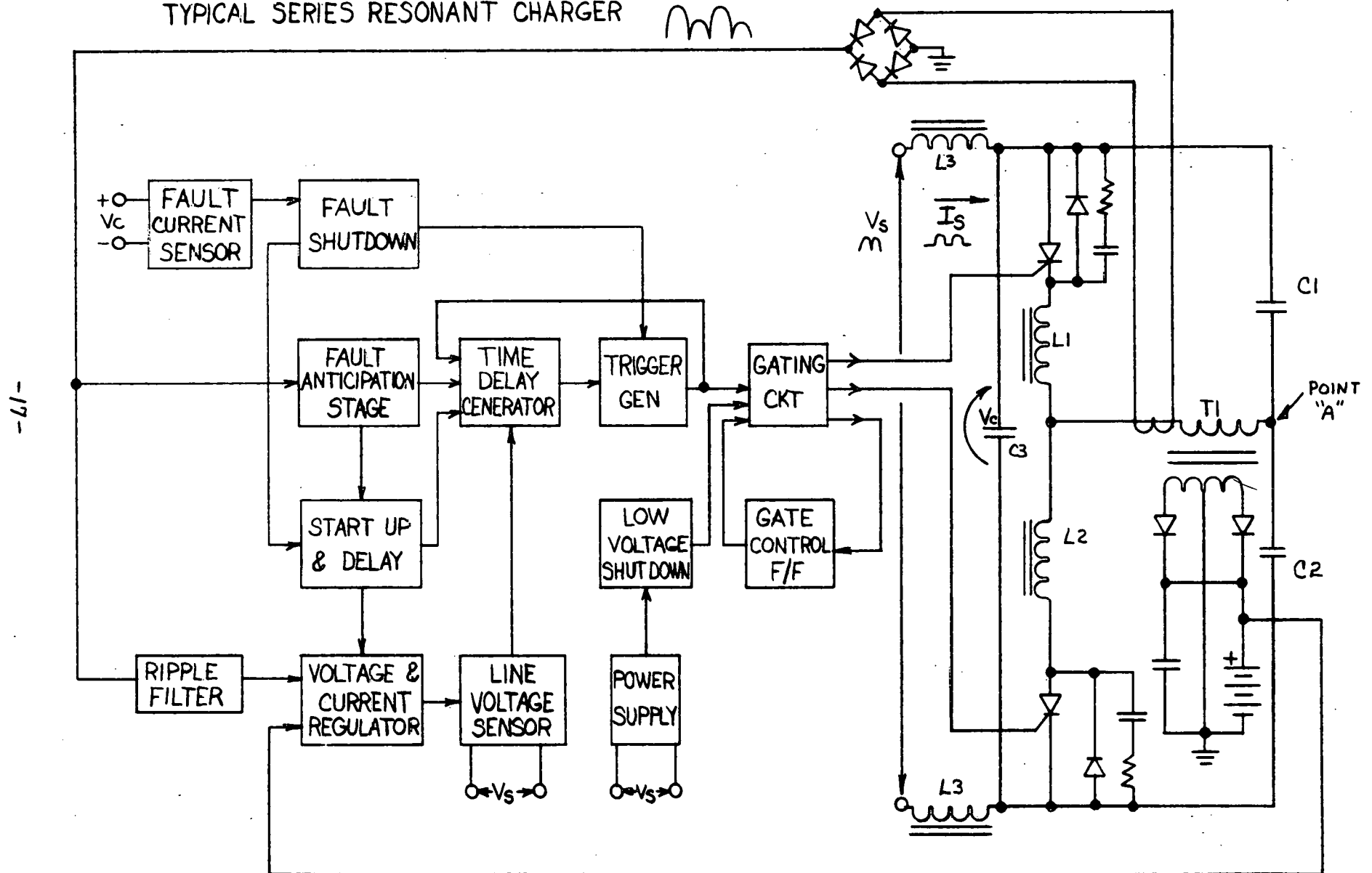
The control circuit block diagram shown in figure 3-2 helps illustrate the interdependence of the above conditions.

The Power Supply provides power to all the logic control elements and is advantageously operated from the utility line. This power supply is constantly monitored by the Low Voltage Shutdown so that the trigger signals to the main SCR's are stopped whenever the supply voltage drops below that required for reliable operation. Also, during the first application of the power supply, a Start-Up and Delay Circuit inhibits the triggering of the SCR's and allows the circuit to stabilize before starting the charger.

The Start-Up and Delay circuit is basically a retriggerable multi-vibrator. When the charger is not operating, this circuit gives a command allowing the charger to deliver one trigger signal to an SCR if and only if all other criteria are satisfied. When the charger is operating, each triggering of the SCR's must give rise to a corresponding current pulse.

The Voltage and Current Regulator circuit continually monitors the battery voltage and charger and output current. These then determine the amount of current required from the charger to maintain the required parameters. The Line Voltage Sensor monitors the line voltage and inhibits any triggering of the SCR's until the minimum line voltage has been achieved. This inhibit signal and the output signal from the Voltage and Current Regulator are combined and fed to the Time Delay Generator. It is important to note that the inhibit signal is operating at twice the power line frequency.

FIGURE 3-2
TYPICAL SERIES RESONANT CHARGER



The Time Delay Generator is the means by which the power module output power is controlled. It controls the time between SCR triggers. The control is responsive to the magnitude of the output current required. Demand for more output current requires that the time between the end of one main current pulse and the triggering of the next SCR decrease. This decrease in time results in the alternate SCR starting to conduct before completion of the ringback pulse of the previous SCR. The triggering of the second SCR during the ringback pulse of the first increases the apparent supply voltage and current of each resonant pulse as described in Section 2.1. In addition, the time is completely controllable except for the restrictions noted in Section 2.1.

After the desired time delay has elapsed, the Time Delay Generator sends a signal to the Trigger Generator circuit. This circuit in cooperation with the Gating Circuit and the Gate Control Flip-Flop (F/F) delivers a pulse of fixed width alternately to each SCR.

Once the SCR is triggered, the Fault Anticipation Stage monitors the result of the power circuit stimulation. The next firing of the power module is completely dependent on the magnitude and duration of the main current pulse produced, if all other requirements are maintained. This main current must reach a minimum current level before the circuit is capable of transmitting a trigger signal to the Time Delay Generator. However, the signal is not sent until the main current pulse is complete (current goes to zero). This establishes an easily recognizable time mark so the Time Delay Generator can use it to accurately determine the next SCR trigger. This time mark is also used to reset the Start-Up and Delay circuit, so it remains inactive as long as successive firings are obtained at some low repetition rate.

In the event the main current pulse does not reach sufficient amplitude, no pulse is given to the Time Delay Generator and the triggering of the SCR's will not be sustained. The Start-Up and Delay circuit will try to restart the charger after a programmed delay (approximately 3 seconds).

The last major control block is the Fault Current Sensor. In the event both SCR's are turned on, the power module automatically goes into a fault clearing process discussed in Section 3.2.4. The function of the Fault Current Sensor is to prevent charger operation from continuing until the SCR junctions have cooled sufficiently. This is accomplished by aborting any triggering sequence already started and waiting for the delay of approximately 3 seconds provided by the Start-Up and Delay circuit.

3.2.4 Circuit Protection

The series resonant inverter is inherently immune to short circuit or open circuit conditions on the output terminals. However, circuit protection is needed for misapplication or abnormal fault conditions.

Output circuit protection is provided by a DC fuse. Input protection is provided by a circuit breaker on the AC input leads; any unusual fault conditions, such as a component failure in the resonant circuit, will clear the input breaker.

The most difficult aspect of circuit protection is a functional fault -- an apparent fault caused by noise, utility line disturbances, or abnormal conditions on the output terminals.

A functional fault can occur during power module operation when any signal causes both SCR's to conduct simultaneously. This will result in a short across the DC supply. The ability to survive a fault condition and automatically to resume normal operation is desirable in all equipment.

With the addition of the input inductor (L3), such survival is ensured for this inverter. The input inductor will hold the input current constant or limit its rate of rise to a reasonable value while the fault clearing action takes place. The fault clearing action is initiated automatically whenever both SCR's conduct simultaneously. A separate series resonant circuit is established with L1, L2 and the Input Capacitor (C3). The Input Capacitor is discharged, and by resonant action achieves a reverse voltage. At this time, the current through both SCR's is reduced to zero. As in normal operation, a ringback current pulse occurs and discharges the negatively charged Input Capacitor. While the ringback current flows, both SCR's are being commutated. During this fault clearing process, high peak currents flow for a significant period of time and therefore we must allow the junctions of the SCR's to cool to normal levels before proceeding with normal operation (see Section 3.2.3). The addition of the Input Inductor to permit automatic recovery from a fault condition complicates the input circuit. During normal operation, the inductor limits the rate of rise of current from the utility line. If the di/dt is too large, the input capacitor voltage will drop below the minimum input voltage required for circuit operation. If the charger continues to operate through the voltage dip, the stored energy in the inductor when the charger switches off (each half cycle) must be removed. Therefore, the smaller the input inductance, the better the normal operation. But in a fault condition, the inductor must limit the rate of rise of line current to allow the L1/L2/C3 resonant circuit to clear the fault condition before destructive currents are obtained in the SCR's. Thus, the design of L1 must be a compromise.

3.3 Implementation of the Development Goals

Referring to the control circuit schematic SC6041022, let's assume the SCR's are being alternately triggered and normal operation has been achieved. The main current pulse produced by the first SCR is coupled to the control circuit by a current sense transformer. The current from the secondary of this current transformer is first full wave rectified and then converted into a usable voltage for processing. Since the last fired SCR is always known, no information is lost in the rectification and simple processing is facilitated. There is a very small time delay between the actual current zero crossing and the voltage zero as seen by the control circuit. The comparator (U203C) has a reference voltage equal to the minimum current level which must be obtained by the main current pulse, so successful commutation of the SCR will occur. Once the current has reached this current minimum, the comparator's reference is changed to some arbitrary low value (i.e., 2A). This will approximate the new current crossing without complicated detectors. When the current reaches this level, the pulse produced by the comparator sets a flip-flop. When the flip-flop (U211A) is in the set position, we assume that the last stimulus produced a main current pulse and ringback pulse that commutated the SCR.

To assure proper operation, a minimum line voltage must be present at the input terminals of the charger. When the instantaneous line voltage exceeds 170V, the comparator (U212D) provides a digital signal indicating this condition. This signal and the signal from the flip-flop (U211A) are applied to a logical AND gate. When both signals are present, the flip-flop (U211B) is set. This activates the Time Delay Generator. A constant current source is produced by Transistor Q209 in conjunction with R287, R288, R282, and R281. The current flows into the capacitor C229, forming a

voltage ramp. This signal is then applied to the input of two comparators, U209A and U209D. The outputs of the two comparators are combined in a logical AND gate that will produce the firing signal to the trigger generator. One of the comparators establishes a minimum delay required to guarantee successful commutation of the SCR's. The second comparator U209A is used to vary the time between SCR triggers. This is accomplished by a variable reference voltage applied to the inverting input of U209A.

The combined signal is inverted by U214A and its output triggers a monostable, U204B. The purpose of the monostable is to provide a pulse of fixed duration required to assure reliable triggering of the SCR's. This pulse passes through an inverter and is applied simultaneously to the OR gates U201A, U201C and the clock input of flip-flop U202B. This pulse causes the flip-flop to change state on the trailing edge and assures alternate digital 1's and 0's to OR gates U201A and U201C. A third (normally) constant digital "0" is also applied to the OR gates from the low voltage shut-down circuit which will be discussed later.

The toggling action of the gating circuit causes positive-going pulses to be produced by alternate 1's of inverter U205A and 205B. Depending upon which of the inverters is actuated, pairs of transistors Q207 and Q204, or Q205 and Q206, are biased into conduction. This causes triggering current to flow in the pulse transformer windings for triggering SCR's alternately. It is important to note that where one SCR is being fired, the alternate SCR is being subjected to a negative gate voltage that will utilize the high dv/dt capability of the device in its Gate-Assisted Turn-Off operation.

The time delay between the conduction of alternate SCR's is controlled by the output current and battery voltage. The current signal extracted

from the resonant power circuit by the current transformer is applied through a calibrating divider network to a ripple filter, including resistors R236, R237 and a capacitor C219 to the negative input of the current regulating operational amplifier U208D. The positive input of the amplifier is coupled to a point of biasing potential V_{CC} through an appropriate voltage divider and the output of the amplifier coupled to subsequent circuitry by way of isolating diode CR225. The battery voltage signal is applied to the negative input terminal of the voltage regulator amplifier U208C through a calibrating divider network. The voltage reference signal is also derived from the bias voltage V_{CC} through a voltage divider. The output of the amplifier is coupled to subsequent circuitry by way of isolating diode CR228. The purpose of the isolating diodes is to permit the lowest current demand to dominate, thus producing a constant current-constant voltage control with automatic current crossover.

The combined signal now represents the current required by the load. This signal is fed into an inverting amplifier, U208, and scaled to obtain a usable signal for the Line Voltage Sensor.

The Line Voltage Sensor separates the current requirement signal into two signals. This separation of signals, although not required for the charger's function, minimizes the characteristic acoustic noise of a high frequency charger when operated at reduced current levels. The separation is based on the required current level and the period of the resonant circuit. The first requirement is that the maximum delay between alternate main switching elements firing is limited to about 25 microseconds. This will maintain the charger above the audible range except for the 10KHz noise components due to the difference in amplitudes of main current pulses and ringback current pulses. This is accomplished by directly controlling the

voltage applied to the inverting input of comparator U209A. The diode CR234 isolates this voltage from the line voltage comparator U212. When the current is reduced, the voltage applied rises to the maximum allowed as determined by the reference source. As less and less current is required, the current requirement signal rises above this reference voltage and diode CR237 now isolates the inverting input of comparator U209A from the current requirement signal. The diode CR234 now connects the signal to the line voltage comparator's reference. As the required current decreases, the signal at the non-inverting inputs of comparators U212D and U212A increases. This causes the charger to operate during smaller and smaller intervals during each half of the 60Hz waveform by raising the minimum line voltage for charger operation, as shown in figure 3-3.

As charger output power is increased, finite utility line impedance can cause the line voltage comparators to "chatter" resulting in erratic operation. To prevent this from occurring, a variable lock-out pulse width is derived from the current requirement signal using comparator U212B and the comparators U212A for the rising edge of the 60Hz waveform. The comparator U212D is activated when the line voltage is greater than that required by the charger. At this time, the output of comparator U212D goes low and indicates charger operation can continue. This output signal is processed through a logical AND gate with the signal from flip-flop (U211A). The comparator will remain at a logical zero until the sine wave falls below the reference signal.

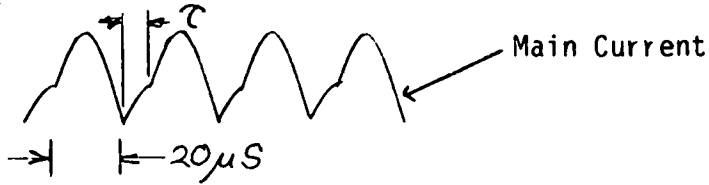
The above process takes place as long as no abnormal condition occurs. The following circuits protect the charger from these conditions.

FIGURE 3-3

1 ϕ Series Resonant Charger Current Control

Examples of Main Resonant Current, Line Voltage and Line Current
(All shown Full Wave Rectified) for Particular Output Current Levels

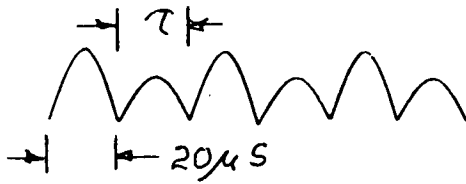
NOTE: Timing shown for 60 Hz.



HIGH CURRENT

$\tau = < \pi$

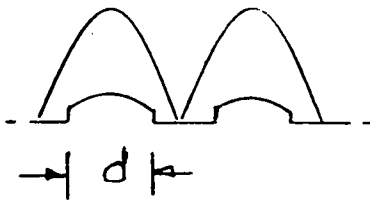
$d = 5.5ms = \text{maximum}$



MEDIUM CURRENT

$\tau = \text{maximum} \sim \pi$

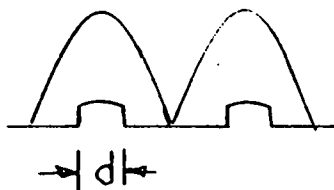
$d = \text{maximum}$



LOW CURRENT

$\tau = \text{maximum} \sim \pi$

$d < \text{maximum}$



The low voltage shutdown circuit monitors the power supply voltage by guaranteeing there is always sufficient voltage across the voltage regulator Q203. This is accomplished by comparator U203A and the value of zener diode CR208 providing the required voltage difference. In addition to the voltage requirements across the regulator Q203, a thermal switch has been included to protect the charger against fan failure or air blockage.

The Fault Shutdown circuit is responsive to a signal from the Fault Current Sensor and causes an inhibit, through comparator U203B and flip-flop U202A, of trigger signals to the SCR's in the event of a power circuit failure of a type which tends to draw excessive current. This condition usually exists as a result of both SCR's conducting simultaneously. The fault condition is sensed by reversal of the voltage on the input capacitor.

The Start-Up and Delay circuit is utilized whenever the natural control loop stimulus-response sequence is broken. This stage actually performs two functions. First, it introduces a restart firing signal into the Time Delay Generator at some time subsequent to the sensing of a thyristor commutation failure sensed by the Fault Shutdown circuit. Second, it functions to energize, in proper sequence, the various elements of the control circuit so that upon start or restart of the charger, all elements will function properly.

3.4 Major Characteristics of Power Components

3.4.1 Input Capacitor (C3)

The purpose of the input capacitor is to filter the high frequency inverter ripple on the power supply bus. Half of the current of each resonant pulse and each ringback pulse flows through this capacitor. The capacitor is not sized to filter the power line frequency ripple. In fact,

the capacitor voltage will track the line voltage when the charger is operational. The RMS ripple current capability at the series resonant frequency is the most stringent requirement on this component.

3.4.2 Series Resonant Capacitors

The series resonant capacitor, along with the snubber inductors and the primary leakage inductance of the main transformer, form the basic resonant circuit which controls the transfer of current into the main transformer (and thus to the battery). It serves, due to the resonant current reversal, to naturally commute the SCR's. Once the values of these components are fixed, the resonant frequency has been chosen. If the driving voltage across the resonant circuit is known, and the resonant current amplitude is known, two parallel capacitors can be used instead of one to halve the amplitude and double the frequency of the high frequency ripple current into the input capacitor. As with the input capacitor, the RMS current capability at the operating frequency is one of the most stringent requirements for this component.

3.4.3 Current Sense Transformer

The purpose of the current sense transformer is to transmit information about the series resonant current to the control circuit. Since it is important to know the instant of the current reversal, there must be very little delay in the signal transfer between actual primary current and secondary current in the sense transformer. To minimize the primary to secondary capacitance, a single well-insulated primary turn is used.

3.4.4 Anti-Parallel (Ringback) Diode

The purpose of the ringback diodes is two-fold. First, they limit the peak reverse voltage seen by the SCR's and second, they improve the primary current form factor while facilitating control of the current magnitude.

Without the diodes, the peak resonant capacitor voltage would appear across one SCR until the alternate SCR is fired. If this were the case, a larger initial driving voltage would appear across the resonant inductor and capacitor with each successive half-cycle, causing an increasing peak resonant current limited only by the Q of the circuit. The requirements for these diodes include fast reverse recovery and a current rating commensurate with the power rating of the charger.

3.4.5 Snubber Components

The purpose of the snubber is to limit the reapplied dv/dt to the SCR's. It is necessary to do this without imposing high peak forward voltage on the SCR's as a result. The snubber begins with a classical underdamped RLC. The L is made as large as possible, and in this case serves as one of the main resonant inductors. The C is made as large as necessary to limit the dv/dt . The R is chosen to limit discharge current when the SCR is turned on, and to damp and limit voltage overshoot.

3.4.6 Fault Survival Configuration

A suitable input choke placed between the line and the input capacitor provides short term line isolation when the main SCR's are both conducting simultaneously (functional fault). This condition shorts the input capacitor, and without the input inductor will cause sufficient current to flow from the line causing the input protector (breaker) to open, with attendant risk of damage to the SCR's. The current that flows in this inductor must have an alternate path when the charger is turned off, or destructive voltages will exist as the inductor tries to dissipate the stored energy. This energy dump occurs 120 times a second or every time the power circuit is stopped. An additional winding is placed on the inductor as an alternate path, and is diode coupled so that when current is flowing

into the charger, the diode isolates this circuit. When the line current stops flowing into the charger, the diode becomes forward biased and circulates the current until the charger restarts. This diode must have a surge current rating equal to the peak fault current.

3.4.7 Main Power Transformer

The purpose of the main transformer is two-fold. First, it provides isolation between the primary, which is common to the utility line, and the secondary, which is common to the battery. This isolation allows safe operation. Second, it provides optimum impedance matching to facilitate the power transfer from the inverter to the battery. The secondary of this transformer is center tapped to produce full wave rectified power. It is bifilar wound to improve mutual coupling, reducing peak reverse voltage on the diodes. Litz wire should be used in both primary and secondary windings to reduce skin effect losses.

3.4.8 Output Filter Capacitors

The purpose of the output filter capacitor is to limit the high frequency output voltage ripple, and filter output ripple current so that the battery and battery cables do not have to carry any significant high frequency components of the inverter output current. This reduces the peak reverse voltage on the output diode and allows lower form factor for the battery current. The most stringent requirement for this component is ripple current rating and low impedance at the 20KHz ripple frequency.

3.4.9 SCR's (Silicon Controlled Rectifiers)

Series resonant inverters have been built using a variety of fast switching SCR's. The primary requirement of SCR's for 20-25KHz operation are fast turn-off time (T_q), high reapplied dv/dt rating (to reduce snubber losses) and fast turn-on (T_{on}). The characteristic of the RCA ASCR (asymmetric SCR) used in the construction of the model are:

T_q	$7\mu S$
dv/dt	$2000V/\mu S^*$
T_{on}	$<1\mu S$ to $7V_{ak}^{**}$

*with negative gate bias applied.

** V_{ak} = Instantaneous Anode-Cathode Voltage

4.0 RESULTS

4.1 Performance Evaluation

The power module was evaluated using 20 Exide EV106 lead acid batteries provided by the Contractor for this evaluation. The batteries were physically located 12 ft. from the charger output terminals. The charger was connected through a variable autotransformer to the utility line. The current, voltage, and power supplied by the line was monitored using conventional AC meters and methods. The output of the power module was monitored by average responding voltage and current meters.

In the following figures, waveforms were photographed using a Tektronics 7623A High Speed Storage Oscilloscope. A Tektronics P6303 current probe was used to obtain instantaneous current waveforms.

The data presented is as follows:

Figure 4-1 Closed Loop V-I Response

Figure 4-2 Efficiency (η) vs. Battery Voltage

Figure 4-3 Efficiency (η) vs. Line Voltage

Figure 4-4 Output Power Data Reduction

Figure 4-5 Power Factor vs. Battery Voltage

Figure 4-6 Power Factor vs. Line Voltage

Figure 4-7 Power Factor vs. Input Watts

Figure 4-8 Line Current vs. Battery Voltage

Figure 4-9 Power Module Front View

Figure 4-10 Power Module Rear View

Figure 4-11 Photograph of Typical Line Current

Figure 4-12 Photograph of Typical Resonant Current
envelope, High

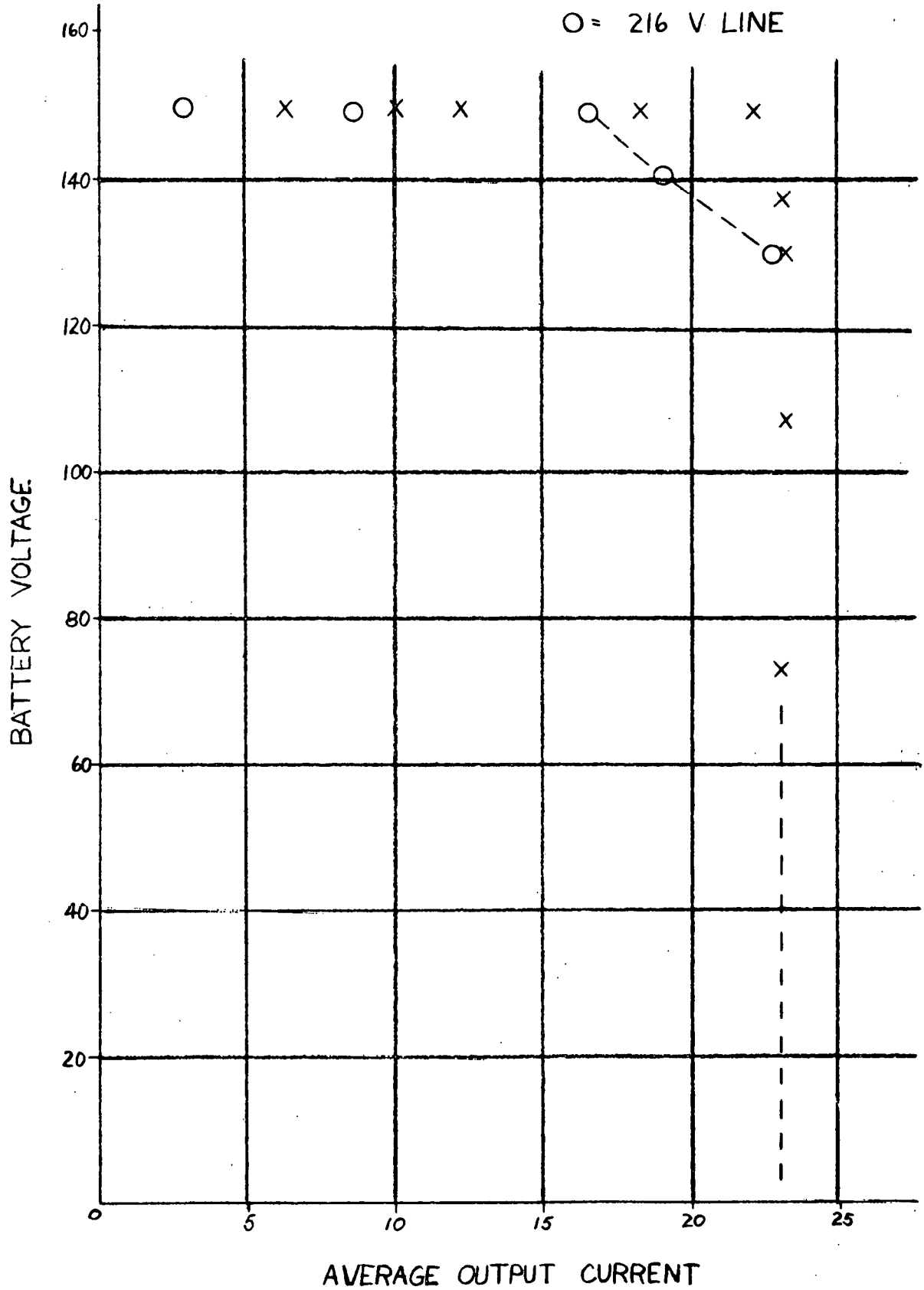
- Figure 4-13 Photograph of Typical Resonant Envelope, Med.
- Figure 4-14 Photograph of Typical Resonant Envelope, Low
- Figure 4-15 Photograph of Typical Resonant Current Cycle, High
- Figure 4-16 Photograph of Typical Resonant Current Cycles,
Med. & Low
- Figure 4-17 Photograph of Typical Input Capacitor Voltage
- Figure 4-18 Photograph of Typical Resonant Capacitor Voltage
(at point "A" in the Schematic Diagram, fig. 2-1)
at Medium and Low Current
- Figure 4-19 Photograph of Typical Resonant Capacitor Voltage
(at point "A" in the Schematic Diagram, fig. 2-1)
at High Current
- Figure 4-20 Component Weights.

4.2 Achievements Against Goals

4.2.1 The Output: Goal 3300 W max. (23A @ 145V)

The power module developed under this contract has a continuously variable output, that is defined to be a constant voltage-constant current type with automatic crossover. The maximum output terminal voltage is 145VDC and the maximum output current is 23 amperes DC (optimized for 20 Exide EV-106 batteries). The actual closed loop VI characteristic is found in figure 4-1. The output current of the power module is constant until the terminal voltage reaches 144.2V. From 144.2V to 145V, the control circuit for the power module can no longer provide full output current due to the voltage control being at the threshold of operation. When the output voltage reaches 145V, the current will be reduced to maintain a constant voltage output. This profile will charge the batteries in 6-8 hours (to 80 percent in 4-6 hours).

FIGURE 4-1
 CLOSED LOOP V-I RESPONSE
 X = 240 V LINE
 O = 216 V LINE



When operating at low line (216VAC), the charger is prevented from increasing the line current beyond the 20A limit. This limiting causes the output power, at low line, to be limited to approximately 3000W (delivered to the battery load). This is illustrated graphically in figure 4-1.

4.2.2 Efficiency: Goal 88%

The efficiency curves of the power module are shown in figure 4-2 and 4-3. Because of the non-linear characteristics of the output voltage and current, the efficiency at each point must be calculated from measurements of instantaneous voltage and current. The general expression for power is:

$$P_{out} = \frac{1}{T} \int_0^T V(t) I(t) dt \quad (4.1)$$

In the well-known case of AC sinusoidal voltage and current, the above equation reduces to

$$P_{out} = VI \cos \theta$$

where θ is the phase angle between voltage and current, and $\cos \theta$ is the power factor. In DC battery charging equipment, where the battery voltage does not vary during a half cycle of line voltage, equation 4.1 would reduce to

$$P_{out} = V_{bat} \frac{1}{T} \int_0^T I(t) dt$$

or the product of battery voltage and average output current.

FIGURE 4-2
EFFICIENCY (η) VS BATTERY VOLTAGE
at NOMINAL LINE VOLTAGE

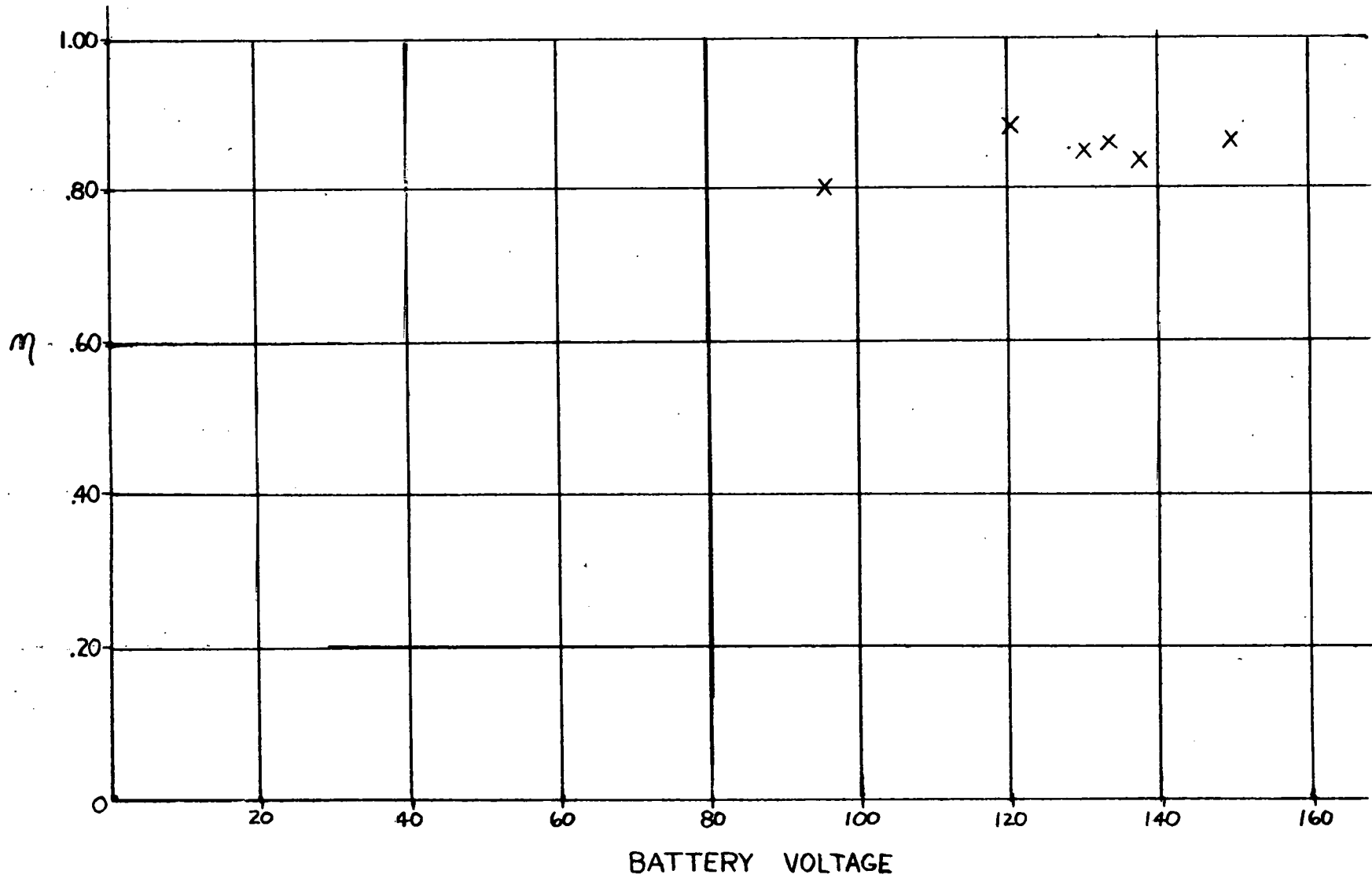
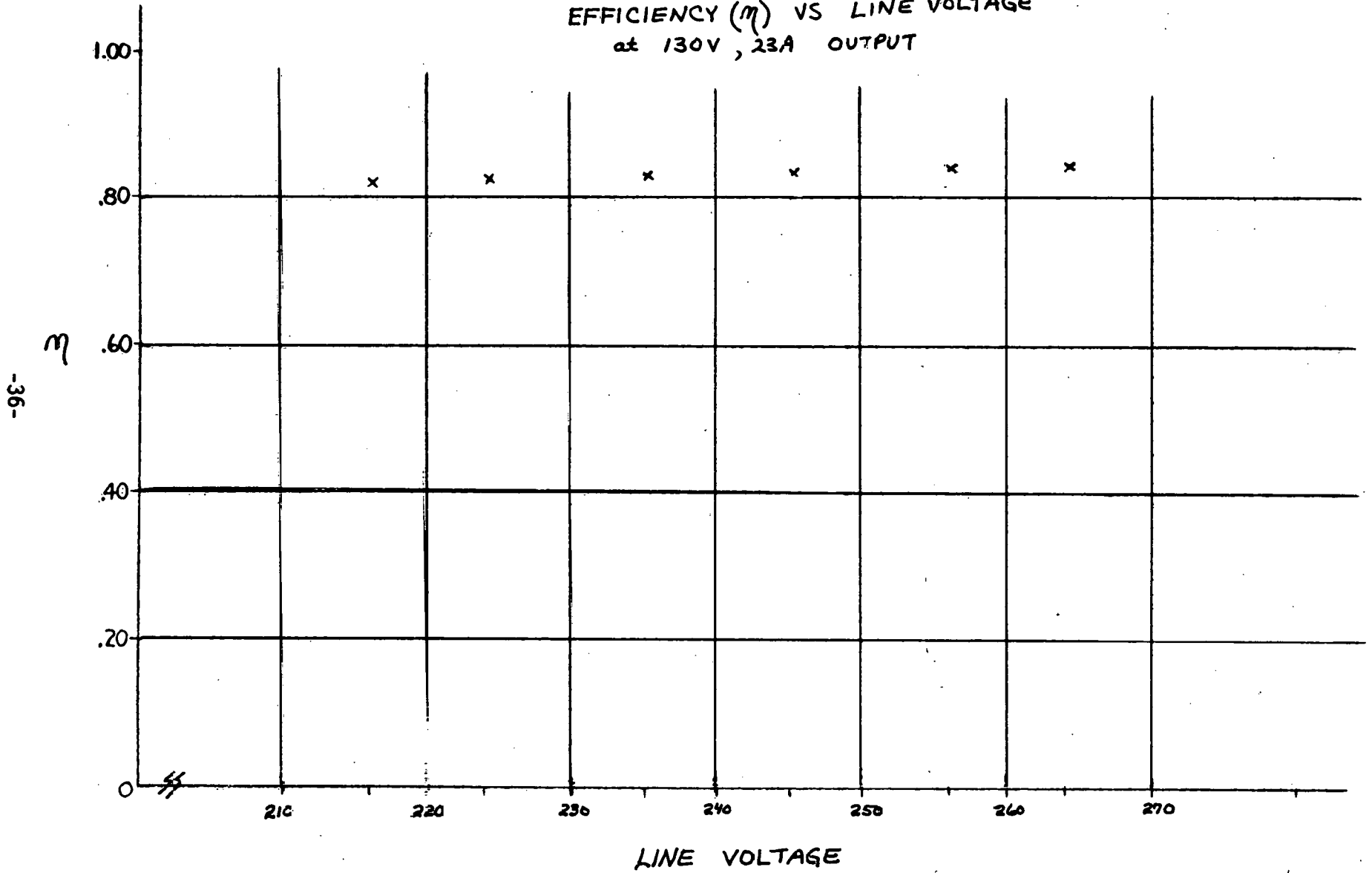


FIGURE 4-3
EFFICIENCY (η) VS LINE VOLTAGE
at 130V, 23A OUTPUT



Like other charging equipment whose outputs are substantially unfiltered (e.g., ferroresonant charger), the power module developed under this contract does not display either sinusoidal or constant DC voltage characteristics. In this power module, the current is delivered only during a fraction of the line cycle, and it causes the battery voltage to be modulated. For this reason, output power at 60Hz either must be measured with sophisticated instrumentation, or calculated.

Since neither the terminal voltage nor line current can be represented by a constant, we must calculate the instantaneous voltage-current product, then integrate the product over a period of one-half cycle. To illustrate the difference between the apparent power delivered (average battery voltage times average output current) and the actual power delivered, we present the comparison shown in figure 4-4. The efficiency curves of figures 4-2 and 4-3 are based on sets of data reductions, which are found in Appendix E. Based on these output power calculations, the efficiency of the power module between nominal battery voltage (120V) and maximum battery voltage (at one-third maximum output power) varies from 84.2 to 90.4 percent.

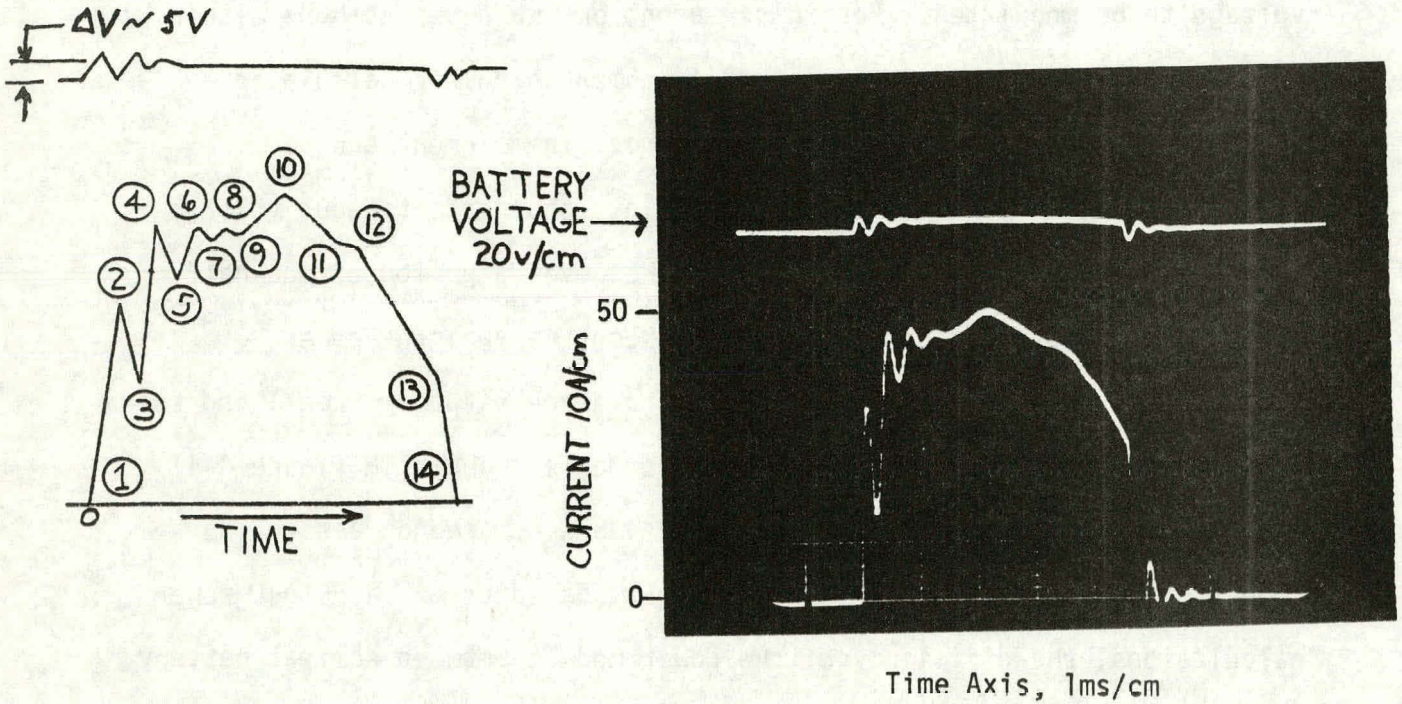
4.2.3 Power Factor: Goal 0.9

The power factor of the power module vs. battery voltage is shown in figure 4-5 and power factor vs. line voltage in figure 4-6. The power factor is maintained greater than 0.9 until 135VDC, then decreases as battery voltage increases from 135VDC to the charge maintenance point (145VDC at approximately 3A). The relationship of power factor to input power is shown in figure 4-7.

FIGURE 4 - 4

COMPARISON BETWEEN MANUAL INTEGRATION AND METER READINGS

OUTPUT POWER DATA REDUCTION



	<u>Meter Readings</u>	<u>Manual Integration</u>
Average Current	23.0	22.76
Average Power, metered (Average current x average voltage)	2990	
Average Power, calculated (Integrated Instantaneous products)		3038

See Appendix E for additional data and data reductions.

FIGURE 4-5
POWER FACTOR VS BATTERY VOLTAGE

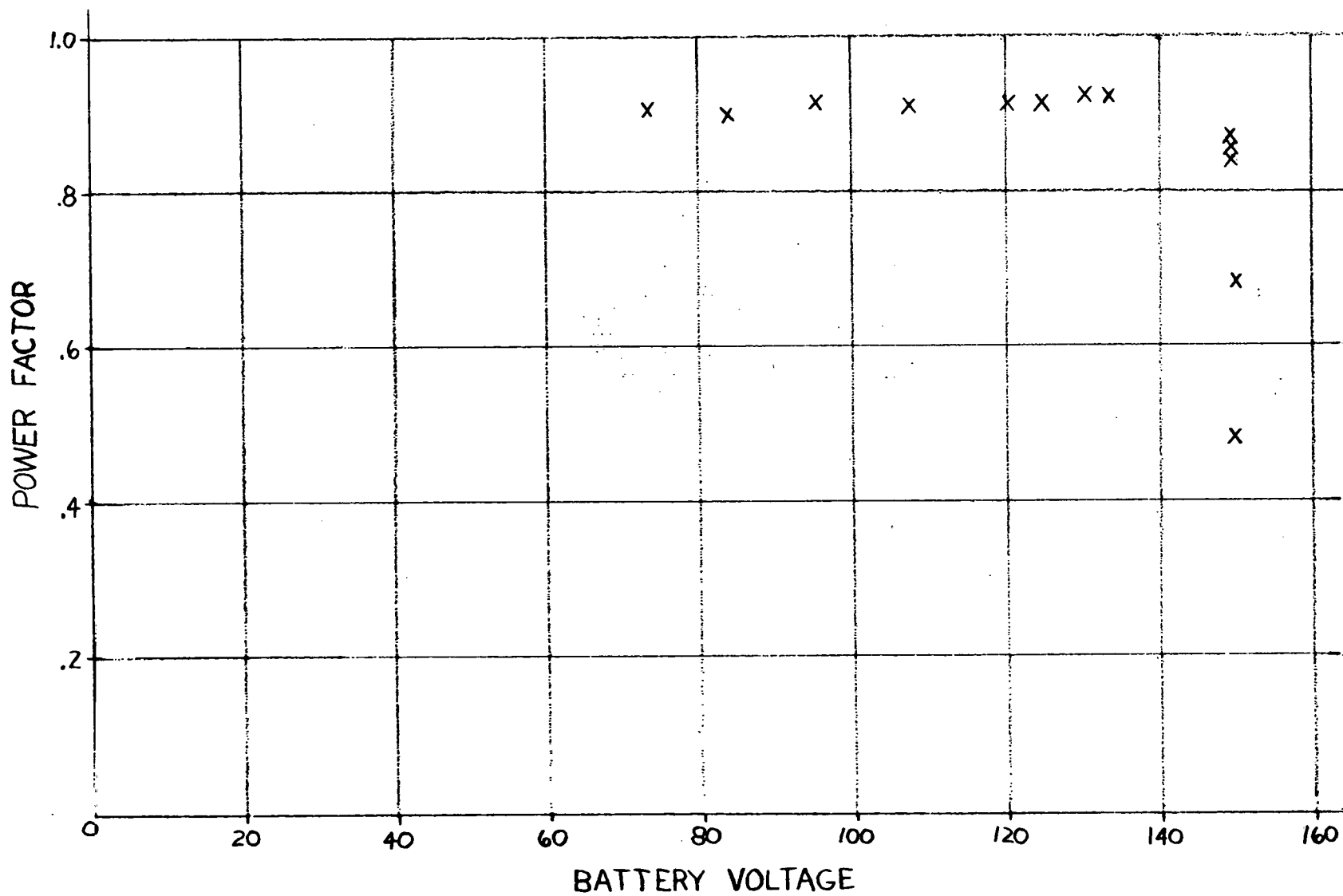
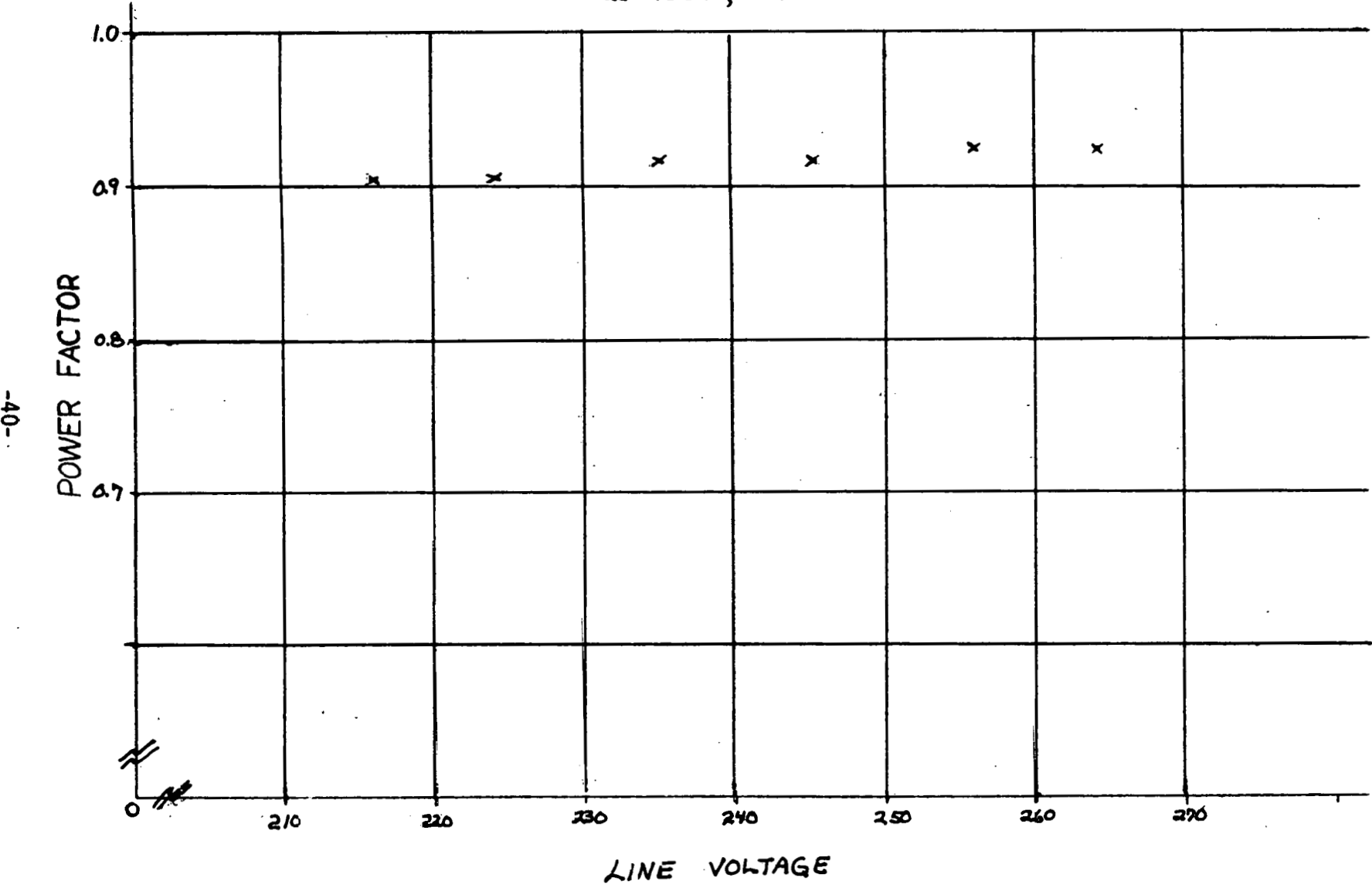


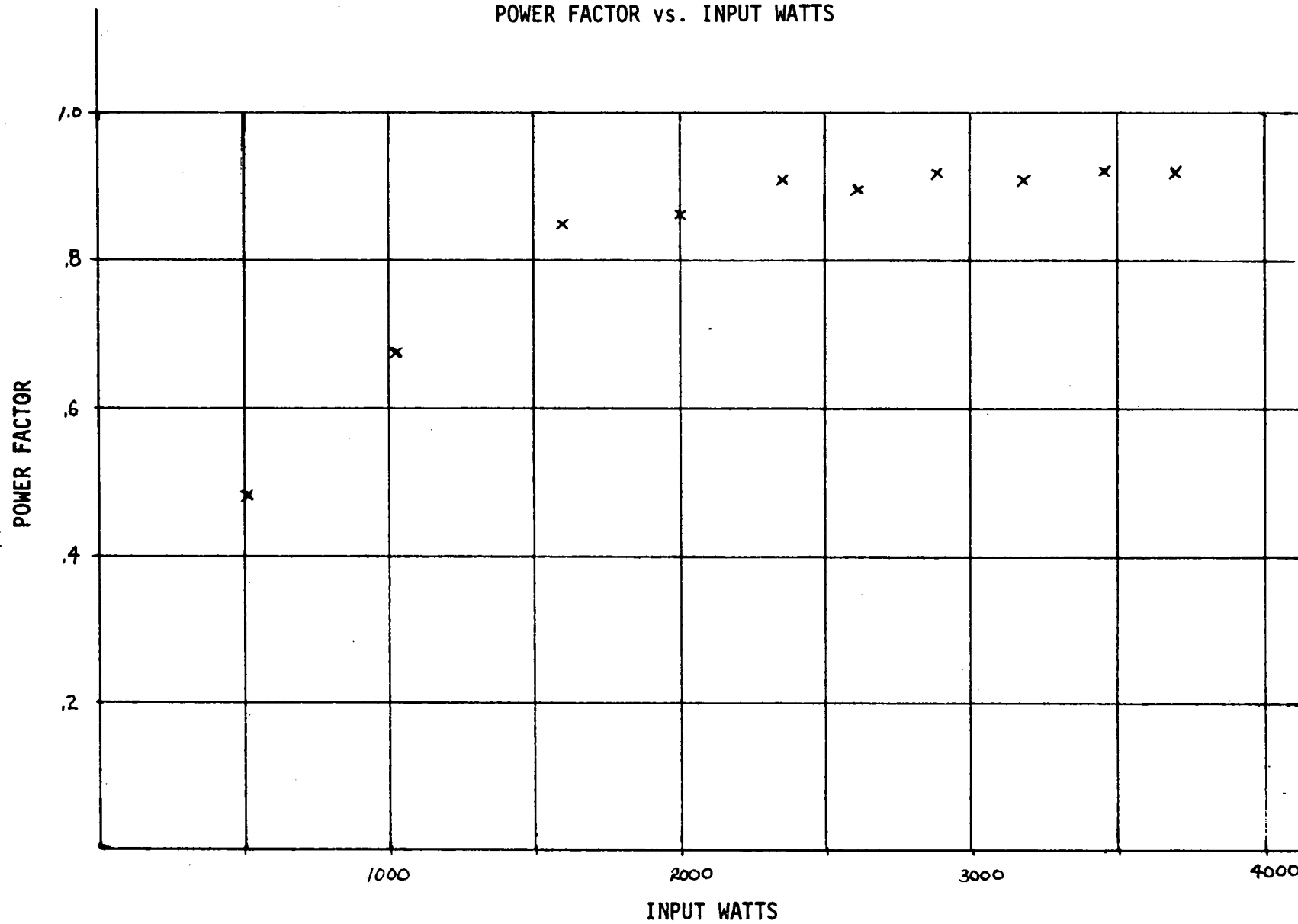
FIGURE 4-6
POWER FACTOR VS LINE VOLTAGE
at 130V, 23A OUTPUT



-40-

FIGURE 4-7

POWER FACTOR vs. INPUT WATTS



The power factor was computed as $(\text{input watts}) \div (\text{input VA})$. Because the input V-I characteristic of the module is non-linear, the power factor does not give a true indication of the phase between input (line) voltage and input current. In this equipment, the input voltage and input current are actually in phase.

4.2.4 Input Requirements: Goal 240V, 1 ϕ , 20A max.

The power module was designed to operate from a 240V single phase line. In addition, the power module will operate over a line voltage range of 264V to 216V. The line current is monitored by the control circuit and is prevented from exceeding 20A. This limiting of line current results in a limit of the power output of the charger at a low line voltage (see figure 4-8).

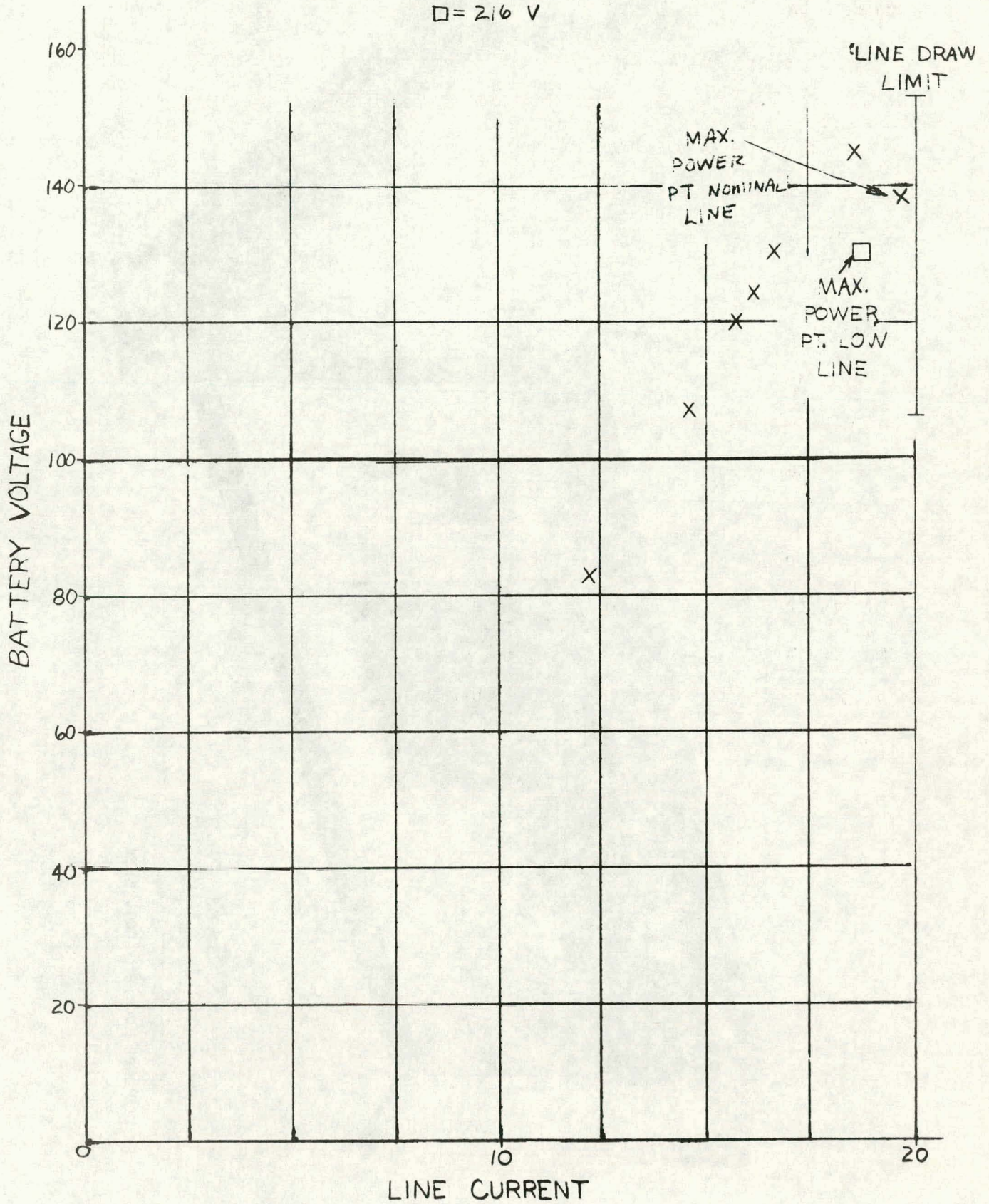
4.2.5 Size and Weight: Goal 20,000-26,000 cm³, 16-20 Kg

The power module is completely self-contained in an aluminum chassis that is 44 x 31 x 18 cm. The volume of this package is 24,552 cm³, and weight is approximately 17 Kg. Figure 4-9 is a photograph of the power module front view, and Figure 4-10 is a photograph of the power module rear view.

FIGURE 4-8
LINE CURRENT VS BATTERY VOLTAGE

X = 240 V

□ = 216 V



-44-

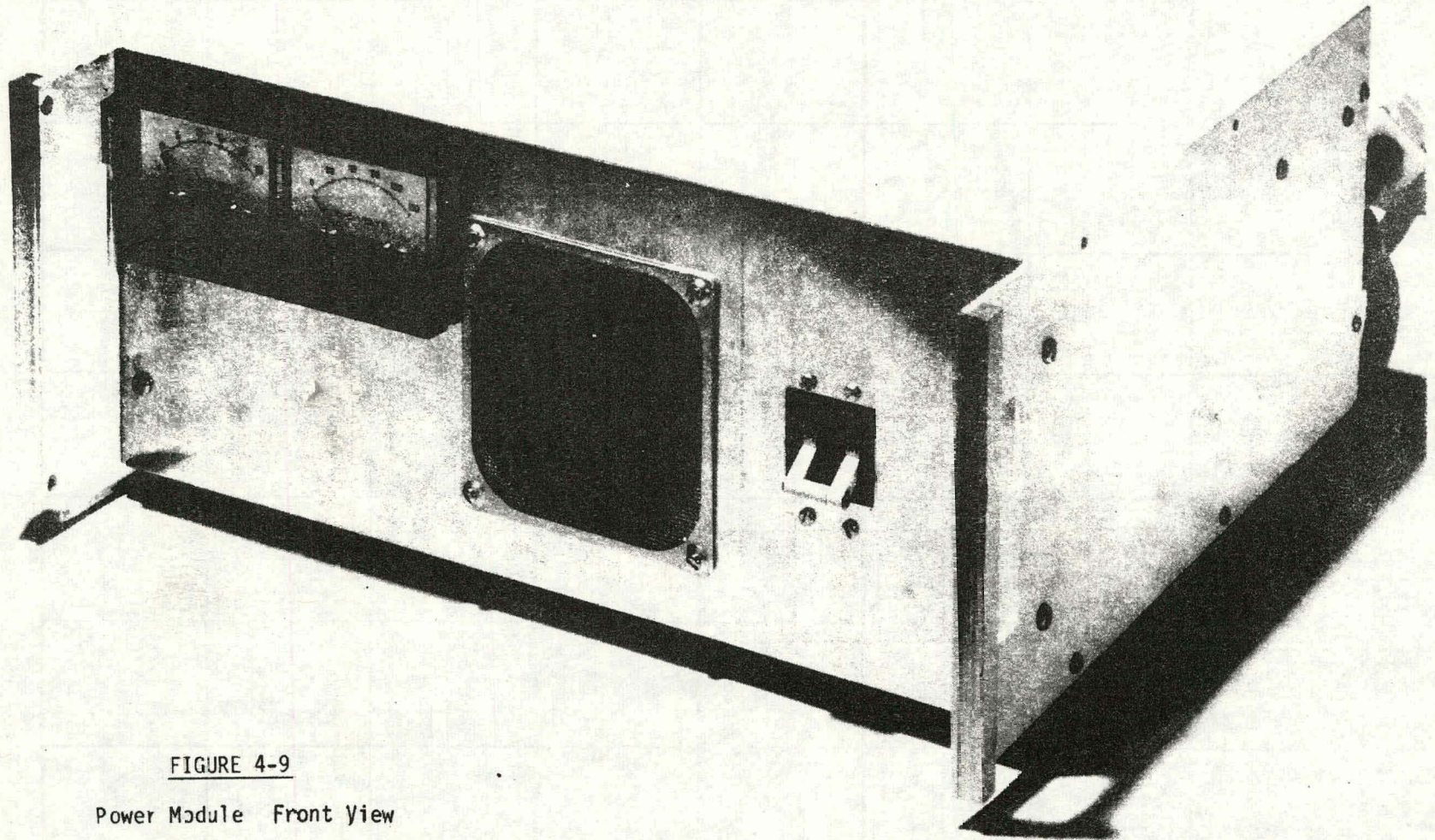
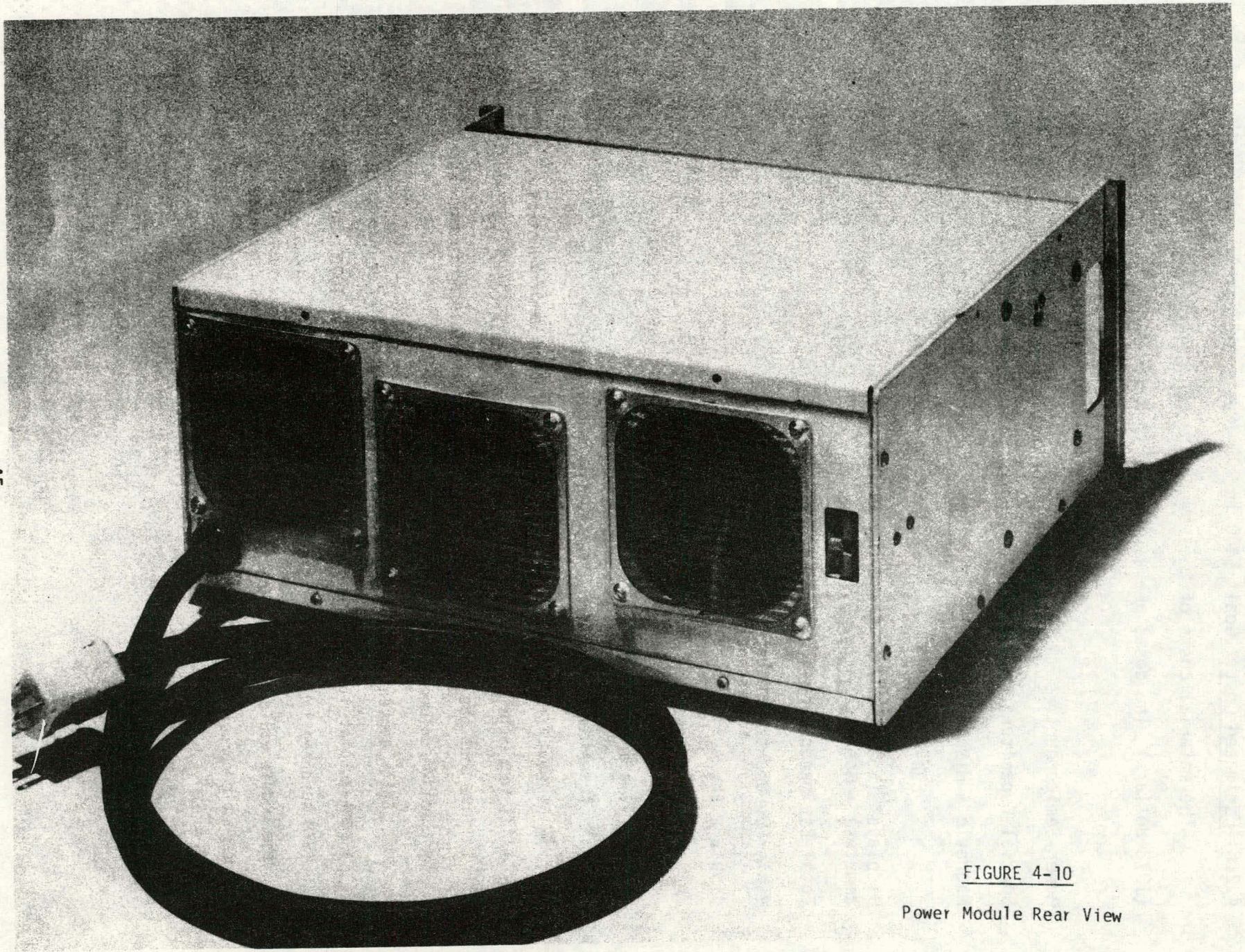


FIGURE 4-9

Power Module Front View



-45-

FIGURE 4-10

Power Module Rear View

4.2.6 Estimated Cost: Goal \$400 in 100-1000's (1978 Dollars)

The material costs of the power module have been estimated (1978 dollars) The costs are as follows:

	<u>100</u>	<u>1000</u>	<u>10,000</u>
Power Semiconductors	165	144	117
Special Capacitors	72	61	
Magnetic & Miscellaneous	<u>189</u>	<u>157</u>	<u>139</u>
Sub-Total	426	362	315
Displays* (voltmeter, ammeter) - Non-essential	<u>42</u>	<u>38</u>	<u>34</u>
Total Estimated Material Costs	\$468	\$400	\$349

*This represents actual parts purchased; however, less expensive displays are available.

The material cost for a "no-frills" power module is \$426 for 100's; \$362 for 1000's; \$315 for 10,000. The power semiconductors still represent a significant part of the power module cost. We believe that the costs of power semiconductors should drop further as production volume and demand increase.

Labor content for the module has been estimated at 2.0 hours, in a semi-automated production facility, for quantities of 1000. At a 1978 burdened labor cost of \$16.00/hr, the total manufacturing cost of the module would be \$394 each in thousands. This assumes purchased magnetic components.

4.2.7 Circuit Protection Features

The charger is designed to be self-protected against misapplication and random line and load disturbances.

- 4.2.7.1 If charger is operated into an open circuit, a fast responding voltage control will inhibit charger operation.
- 4.2.7.2 The charger is protected by a double-pole AC circuit breaker in the utility line input circuit.
- 4.2.7.3 A line transient protector has been incorporated to prevent false triggering due to utility line surges and noise.
- 4.2.7.4 The output circuit has been fused internally to guard against catastrophic failures of the charger output diodes or reverse connection of charger leads. If these fuses should clear, the difficulty should be determined and corrected before the charger is returned to service.

4.2.8 Additional Data

Additional information on the power module performance has been included. Figures 4-11 through 4-19 show voltage and current waveforms of actual power module operation. Figure 4-20 shows major component weights in tabular form.

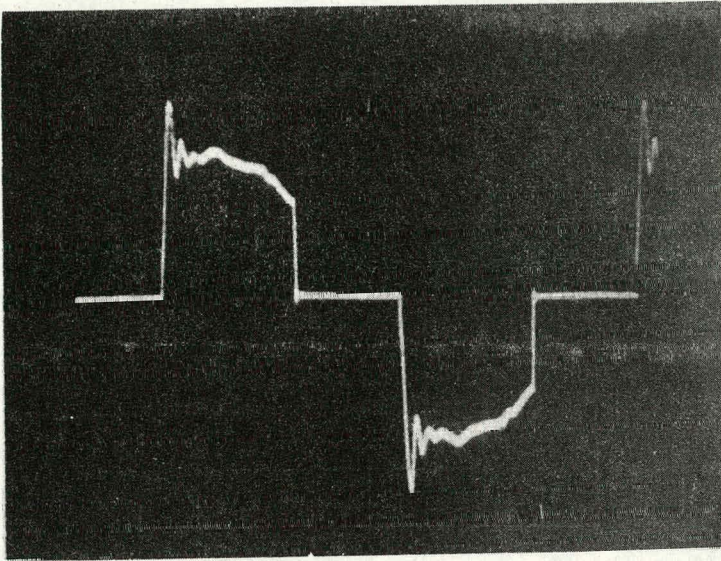


FIGURE 4-11

Typical Line Current

10A/DIV

Taken at 23A, 132VDC Output

Vertical:

Horizontal: 1 ms/cm

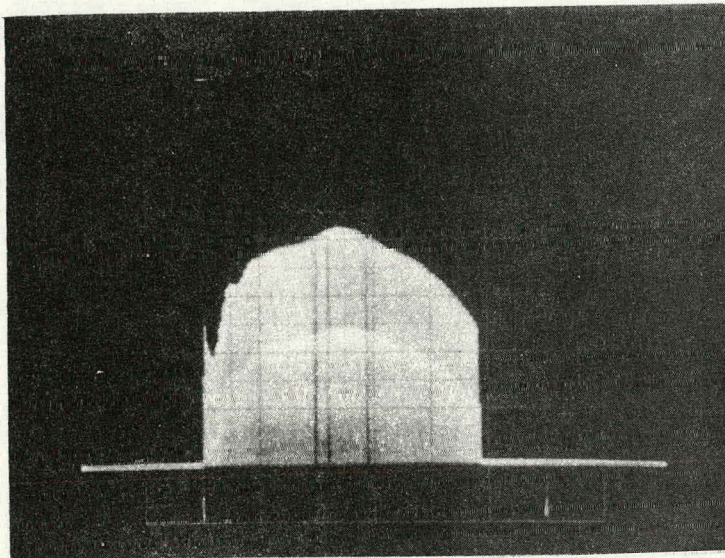


FIGURE 4-12

Typical Resonant Current
(envelope)
at 23A, 130VDC Output

Vertical:

Horizontal: 1 ms/cm

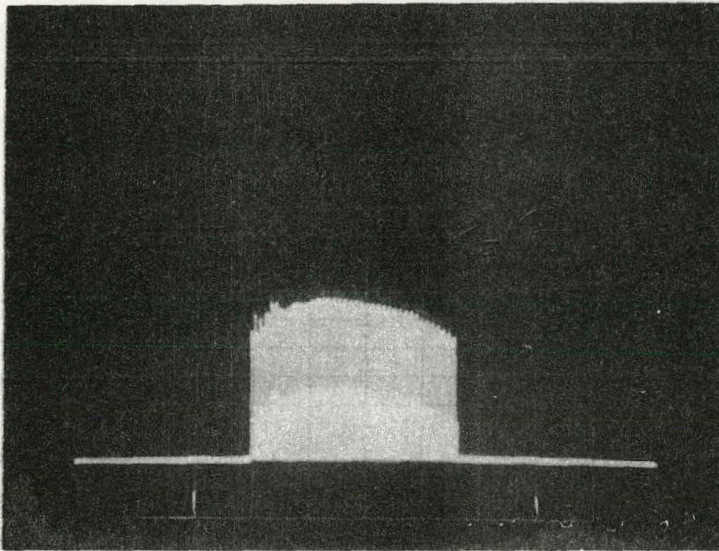


FIGURE 4-13

Typical Resonant Current
(envelope)
@ 10A 144VDC Output

Vertical:

Horizontal: 1 ms/cm

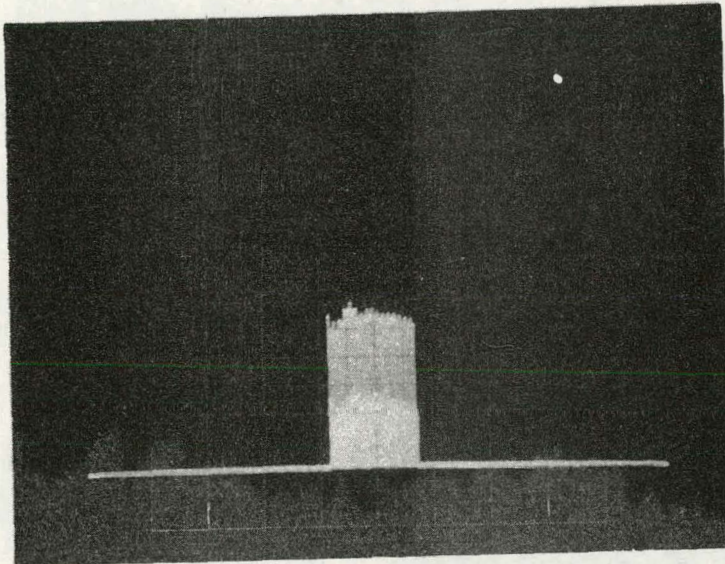


FIGURE 4-14

Typical Resonant Current
(envelope)
@ 4A 145VDC Output

Vertical:

Horizontal: 1 ms/cm

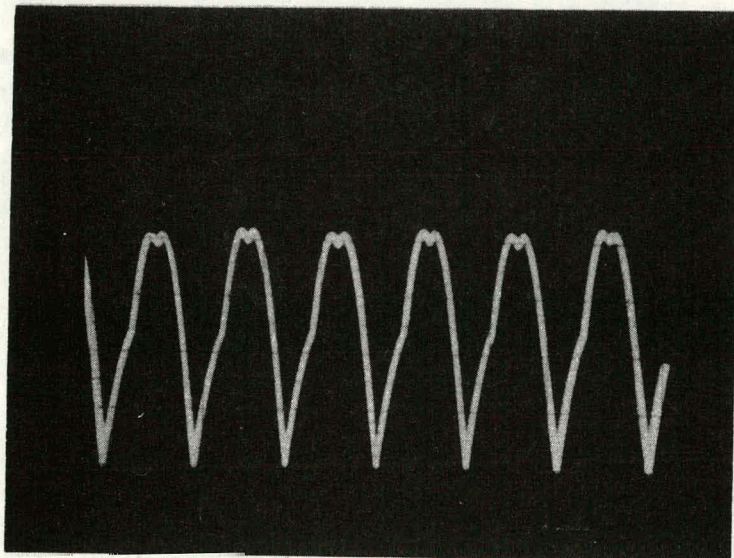


FIGURE 4-15

Typical Resonant Current
@ 23A, 130VDC Output

Vertical:

Horizontal: 20 μ s/cm

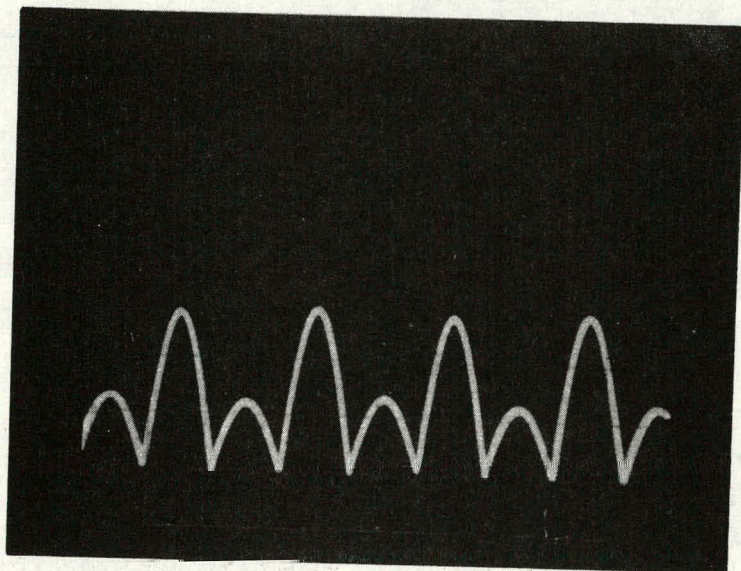


FIGURE 4-16

Typical Resonant Current
less than 10A

Vertical:

Horizontal: 20 μ s/cm

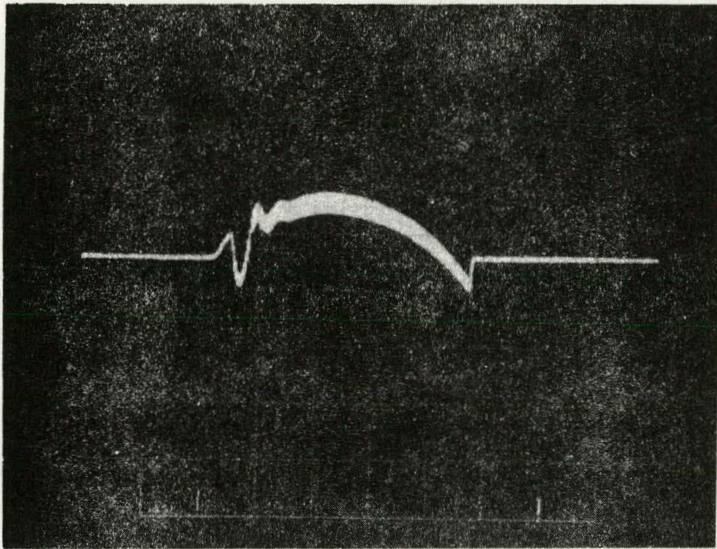


FIGURE 17

Typical Input Capacitor
Voltage
@ 23A, 130V Output

Vertical: 100V/cm

Horizontal: 1 ms/cm

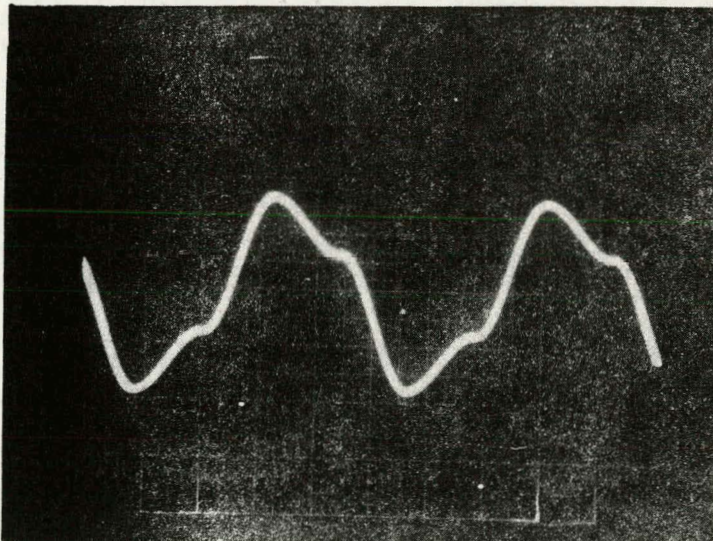


FIGURE 18

Typical Resonant Capacitor
Voltage
(at point A on Schematic Diagram,
fig. 2-1, at less than 10A)

Vertical: 200 V/cm

Horizontal: 20 μ s/cm

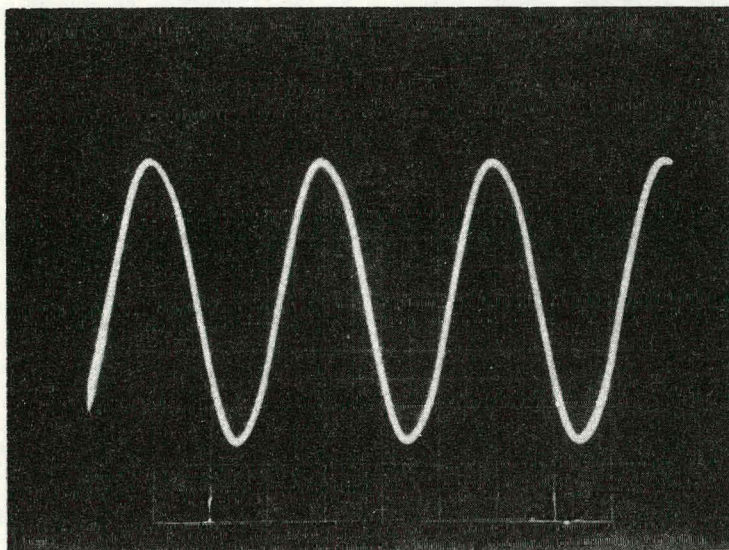


FIGURE 19

Typical Resonant Capacitor
Voltage

(at point A on Schematic Diagram
fig. 2-1 @ 23A, 130VDC Output)

Vertical: 200 V/cm

Horizontal: 20 μ s/cm

Figure 4-20 - Weights of Major Components (Typical)

<u>Component or Assembly</u>	<u>Weight, Kg</u>
SCR Heat Sink Assy.	0.370
Output Capacitor	0.460
Input Capacitor	0.930
Input Choke	1.400
Resonant Capacitor	0.220
Fan	0.688
Main Transformer	2.840
Output Diodes w/Heat Sink	0.147
Current Transformer	0.392

THIS PAGE
WAS INTENTIONALLY
LEFT BLANK

APPENDIX A: PROJECT CHRONOLOGY

Month 1 - The first month was directed to an investigation of various inverter and power line input configurations. A variety of approaches were considered to determine the most promising configuration to meet the specification goals. A half bridge configuration was used to minimize component voltage stress on the series resonant capacitors. This stress occurs during inverter operation at full power output, when the switching elements are turned on during the period of ringback current flow. It is clear that the inverter can be configured in a full bridge circuit also. Such a configuration would not present any change in the basic operation of the power circuit and in addition would reduce voltage stresses on switching elements. The characteristics of the DC bus voltage as seen by the inverter power circuit was examined to insure that the equipment presents a high power factor to the utility line. In addition, the fault mechanism that occurs with both main switching elements turned on simultaneously was examined. The resulting requirements for the input filter are 1) a sufficiently high series inductance to permit the operation of the Fault Survival circuit, and 2) the filter components must not significantly attenuate the higher order harmonics of the power line generated by the rectifier circuit.

Month 2 - The actual topology of the power circuit was investigated. The selection of two pairs of main switching elements was a result of the resonant current being greater than the single SCR capability. The current was divided in each main switching element by the use of a resonant inductor placed in each switch leg. The current that flows in the leg will be controlled by this dominant impedance

element. This will minimize the current imbalances caused by the different SCR conducting characteristics. Snubber components were selected based on computer-generated curves for an underdamped second order response. The selection was based on allowable dv/dt , inductor and capacitor values, overshoot in terms of natural frequency, damping coefficient and critical resistance. The major magnetic components were designed. These include the power transformer and input filter inductor. All magnetic components were designed to minimize conducted RFI.

Month 3 - The construction of the breadboard was started. The main magnetic components were fabricated. These main magnetic components are small, lightweight and cost effective. Forced air cooling is required to maintain these components within their specified temperature limits. Heat sink assemblies were fabricated. Each of these assemblies contained the snubber components and pulse transformer. A simple control circuit was designed to drive the switching elements, provide fault current detection, main current measurements and start up sequences as required to operate the power stage.

Month 4 - The control circuit was assembled and tested separately from the power circuit to insure proper operation. The power stage was then energized and operated to examine waveforms. At this time, some difficulty was experienced when the charger automatically shut down without any apparent reason and then restarted after the appropriate delays, as designed into the charger.

Month 5 - The difficulty in which the charger automatically shut down without any apparent reason, then restarted after the appropriate delays, was solved. As a result of this, the fault detection circuit

was redesigned to permit operation even with large noise pulses on the AC line. The input inductor began to oscillate with the input capacitors each time the charger shut off or turned on. The oscillations proved to be unpredictable in amplitude. Steps were taken to control the oscillations by the use of a freewheeling diode which circulated current in the input inductor when the power stage turned off.

Month 6 - During the month some difficulty was experienced when the charger was operated at the lower voltage limits (170V). It was undesirable to increase the circulating VA. A more direct approach was taken. Investigation revealed that the magnetizing current of the main transformer began to dominate the resonant current and caused an apparent lowering of the natural frequency of the power circuit. The approach that was taken was to reduce the transformer air gap and double the core cross-section. By using this approach we obtained approximately one-quarter of the magnetizing current of the original transformer.

Month 7 - The input inductor remained a source of concern. It caused a dip in the supply voltage at the start of conduction on each half cycle of the utility line. The dip results from the inability of the inductor to carry load current instantaneously so that the severity of the dip increased with increasing output power. The solution to this problem was not as straightforward as we had hoped. The decrease in the value of this inductor will increase the rate of rise of line current during a fault. Using computer modelling, we have chosen the inductor so that reasonable line fault currents exist but the dip will be minimized to acceptable levels.

Month 8 - During this month the design of an automatic closed-loop

control circuit was completed. This control circuit alleviates one of the disadvantages of a series resonant inverter. This objection is due to the generation of acoustic noise when the output power is reduced. The conventional means of reducing output current is to reduce the pulse repetition frequency, leading to operating frequencies in the audible range. The new control circuit reduces this effect.

The control loop was also designed for constant-voltage and constant-current with automatic crossover. This type of control circuit cannot be overloaded.

Month 9 - The automatic control circuit designed during the previous month was placed in operation. The circuit operated as intended with the exception of the line voltage monitor. The difficulty experienced was due to local line voltage changes as the power stage switched on and off at the 120Hz rate. The small local line voltage changes sensed during the power stage switching caused the line voltage monitor circuit to oscillate near 170V. The on/off oscillation of the power stage is not desirable, especially when approaching the off interval. If the power stage is allowed to oscillate during this period, there will be insufficient ringback current to commutate the SCR's causing a fault when the alternate main SCR is fired. The circuit was modified to prevent the power module from oscillating regardless of the severity of the line voltage disturbances. This lockout interval is a dynamic one that prevents the on/off oscillation of the power module at high power but allows very small on intervals when the output power is low.

Month 10 - During the month of July assembly of the demonstration

model of the power module was completed, and engineering documentation started. Current imbalance occurred between the two main switching elements. As output power was increased, the current imbalance became more severe. Investigation revealed that the problem was caused, at least partly, by the coupling between snubber inductors.

Month 11 - During the month documentation of the power module continued. Engineering sketches of the mechanical assembly were forwarded to the documentation group to prepare formal drawings of the power module. The design of the fixed control circuit on a standard printed circuit board for the demonstration model has been completed. The assembly drawings that define the power module will reflect only the major mounting locations and component layout. The drawings may vary from the model, primarily in the location and size of fasteners but will not alter the operational characteristics of the charger. The difficulty experienced last month when the power circuit was placed in the tight confines of the enclosure continued. This has been linked to the close magnetic coupling between the snubber inductors. It was possible, by physical rearrangement of some components, to reduce the effects of the inductance coupling but not completely eliminate it.

Month 12 - During the month documentation of the power module continued. The formal drawings that will define the electrical and mechanical configuration of the power module were started and were 20% complete by the end of the month. The circuit performance problem caused by the coupling between snubber inductors is partly alleviated by the repositioning of the inductors as described last month. The final control circuit printed circuit board was etched, assembled,

and successfully bench tested. The printed circuit board differs from the handmade prototype board in that it incorporates components that were previously off the board, e. g., fault survival circuitry. This circuit board also differs from the prototype in the input and output pins assignments. This difference was required to satisfy the board layout criteria. The testing of the control circuit board assembly and the power module was not so successful. The board failed on turn-on of the utility line resulting in destruction of several components and some printed wiring runs. The cause was traced to an error in rewiring of the harness to the new input/output pins of the connector.

Month 13 - The documentation of the power module continued. Formal drawings of both the mechanical and electrical configurations of the power module are 70% complete. The circuit performance problems reported last month continued to give difficulty. The coupling of the snubber inductors to each other and to the printed circuit board has caused erratic operation. The problems are the result of the tight packaging concept selected and have also delayed the final testing of the completed charger package. Present steps are directed toward minimizing coupling by providing a shield or barrier between the circuit board and the magnetic components. If this does not solve the problem, the charger must be reconfigured.

Month 14 - Most of the documentation for the charger power module was completed during November. Work on the module itself was limited to investigation of the current imbalance and shielding problems previously reported. We have had moderate success in understanding and controlling both problems. The two circuit problems reported last

month are related to the high-density packaging concept for the power module. The presence of high amplitude, high-frequency currents generates noise fields that couple between parts of the power circuit and from the power circuit to the control circuit assembly.

We have determined that current imbalance problems can be minimized, but not eliminated, by careful redesign and construction of the SCR snubber inductors to provide close matching of inductance. To solve the circuit noise problems in the control circuit, a shield was installed between the power circuit and control circuit assembly, electrically connected to the chassis (earth ground). However, the disadvantage of this solution is that circuit energy coupled into the shield heats the shield and reduces the overall efficiency. For this reason we will also investigate noise decoupling methods without the use of a shield.

**THIS PAGE
WAS INTENTIONALLY
LEFT BLANK**

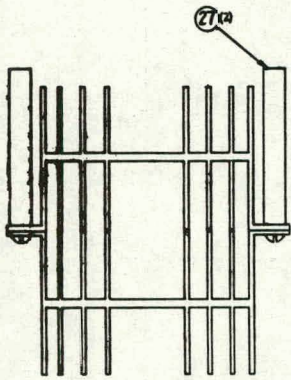
APPENDIX B
DOCUMENTATION LIST

APPENDIX B: DOCUMENTATION LIST

<u>No.</u>	<u>Title</u>
6041000	Single Phase High Frequency Charger Assembly
SC6041000	Single Phase High Frequency Charger Assembly Schematic
PL6041000	Single Phase High Frequency Charger Assembly Parts List
6041001	Baffle Sub-Assembly
PL6041001	Baffle Sub-Assembly Parts List
6041002	Baffle Assembly
PL6041002	Baffle Assembly Parts List
6041003	Heat Sink, Main
6041004	Baffle, Left Hand
6041005	Baffle, Right Hand
6041006	SCR Gate Trigger Pulse Transformer
6041007	Support Rods - Main Heat Sink
6041008	Support Clip Printed Circuit Board
6041009	Spacer Rod, Main Heat Sink
6041010	Detail, Back Panel
6041011	Panel, Left Side
6041012	Panel, Right Side
6041013	Base Plate
6041014	Snubber Inductor
6041015	Front Panel
6041016	Main Transformer
6041017	Main Transformer Assembly
6041018	Input Choke
6041019	Current Transformer

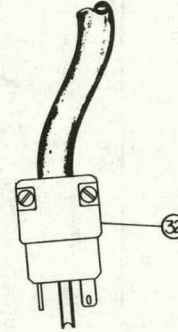
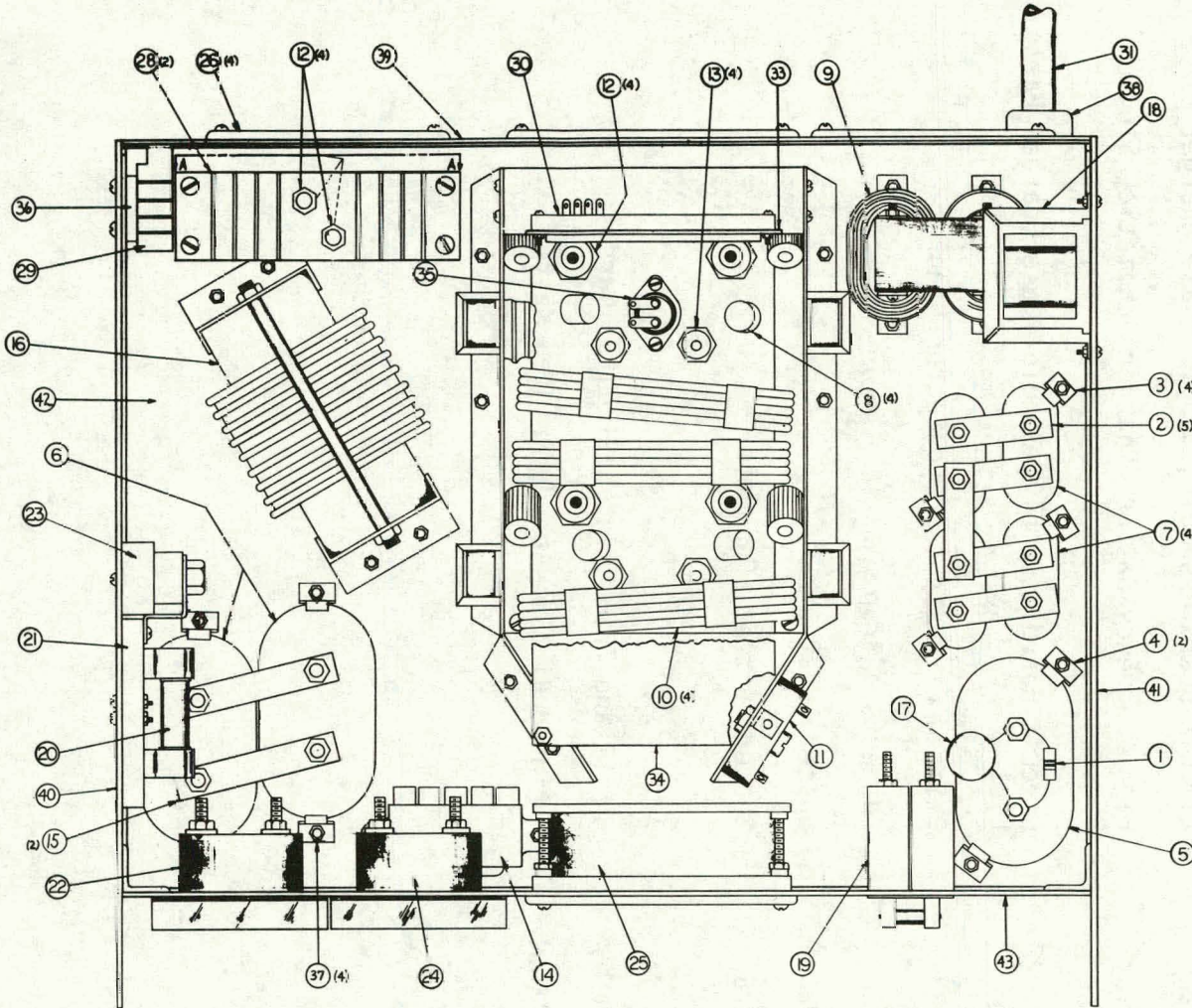
APPENDIX B: DOCUMENTATION LIST (cont'd)

<u>No.</u>	<u>Title</u>
6041020	Bracket - Main Transformer
6041021	Extrusion-Hole Layout - Heat Sink
6041022	Circuit Board Assembly, Single Phase Charger
SC6041022	High Frequency Battery Charger Schematic, Single Phase
PL6041022	Circuit Board Assembly, Single Phase Charger Parts List
6041023	Printed Circuit Board Connector Bracket
6041024	Connector Strap
6041025	Spacer, Heat Sink
6041026	Spacer, Battery Connector
6041027	P.C. Board Baffle
6042001	Drill and Trim Printed Circuit Board
PM6042001	Printed Circuit Board, Printed Master



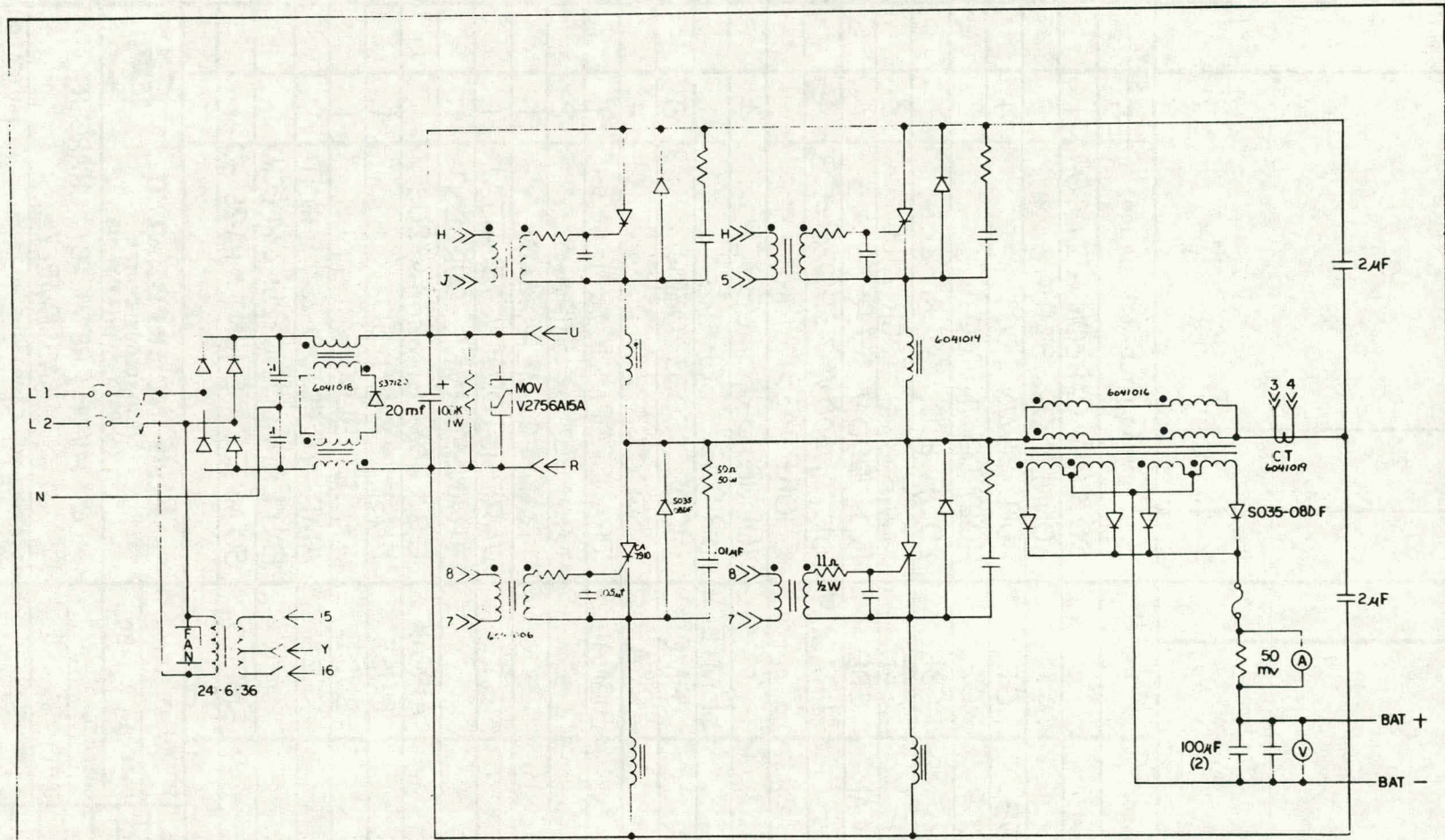
VIEW AA

99



NOTE:
 1. SHOWN WITH TOP COVER NOT INSTALLED
 2. BUD. CO. PART NO. HC14100* COVER
 3. NO ASSEMBLY HARDWARE CALLED OUT
 FOR DRAWING SIMPLICITY.
 * FOR POWER MODULE SCHEMATIC
 SEE DWG. SC041000.

DESIGN/RELEASE APPROVAL	DATE	BY	DATE	BY
DO NOT SCALE DRAWING		ESB INCORPORATED		
		TECHNOLOGY CENTER		
		VALLEY, PENNSYLVANIA		
		10 HIGH FREQUENCY CHARGER		
		ASSEMBLY		
PRODUCTION	DATE	BY	DATE	BY
		6041000 D		



- NOTES:
 1. CT. (CURRENT TRANSFORMER)
 2. PIN NUMBERS REFER TO CORRESPONDING PIN NUMBERS ON P.C. CARD SCHEMATIC NO. SC6041022

DESIGN/RELEASE APPROVALS		DRN BY	DATE	CHECKED BY	DATE	
NAME	DATE	Att	Oct 1, 1979			
TOLERANCES UNLESS OTHERWISE SPECIFIED FRACTIONS DECIMALS ANGLES 1/16" .001" .001" 1/16°						SCALE: DRAWING NO. SC 6041000

1 Ø HIGH FREQUENCY POWER MODULE


REV.	REVISION RECORD	DR.	REV.	DATE	REVISION RECORD	DR.

ITEM NO.	IDENTIFICATION NO.	MFR	DRAWING TITLE / DESCRIPTION	QTY.	
				-1	-2
1			100K, 1W CARBON RESISTOR	1	
2	6041024-1		CONNECTOR STRAPS	5	
3	302C920P198	GE	HOLD DOWN FOOT	4	
4	302C920P209	GE	HOLD DOWN FOOT	2	
5	INPUT CAP	CDE	20 μ F, 600V * SCR N 227	1	
6	OUTPUT CAP	CDE	100 μ F, * SCR 2100	2	
7	RESONATING CAP	CDE	1 μ F, 1000V * SCR 213	4	
8		SPRAGUE	.01 μ F, 1600V * 715P103516LD3	4	
9	6041018		CHOKE ASSY, INPUT		
10	6041014		INDUCTOR, SNUBBER	4	
11		SEMTECH	BRIDGE * SCBAR8	1	
12		FMC	DIODE * S035-08DF	8	
13		RCA	ASCR * CA7910	4	
14		SIGNAL	TRANSFORMER * 241-6-36	1	
15	6041024 2		CONNECTOR STRAPS	2	
16	6041017		TRANSFORMER, MAIN	1	
17		G.E.	VARESISTOR * V275LA15A	1	
18	6041019		TRANSFORMER, CURRENT	1	
19		AIRPAX	C.B. * 205-11-1-62-4A-203	1	
20		BUSS	FUSE * KWN-30	1	
21		BUSS	FUSE BLOCK	1	
22		G.E.	AMP METER 0-25A SHUNT	1	
			EXTERNAL * 50-251-224 ECNJ		
23		EMPRO	50 MV, 25A SHUNT * HA-25-50	1	

DRAWING NO.

DRAWING NO.

SHEET NO.

DESIGN/RELEASE APPROVALS		DRAWN MT		ESB INCORPORATED TECHNOLOGY CENTER YARDLEY, PENNSYLVANIA 		
APPROVED BY	DATE	DATE	Jan. 4, 1980			
		CHECKED		NEXT ASSY NO. DRAWING NO. SHEET NO. PL 6041000 PL 6041000 1 of 2		
		DATE				
		APPROVED				
		DATE				

REV.	REVISION RECORD	DR.	REV.	DATE	REVISION RECORD	DR.

ITEM NO.	IDENTIFICATION NO.	MFR	DRAWING TITLE / DESCRIPTION	QTY.	
				-1	-2
24		G.E.	0-150 V METER #50-251220PZPZ	1	
25		BOXER	FAN #BS2107FL-6	1	
26			SCREEN, SLIM LINE #69-93-1(060000)	4	
27	6041025		HEAT SINK SPACER	2	
28	6041021		HEAT SINK	2	
29		ANDERSON	CONNECTOR #6319	1	
30		CINCH	CONNECTOR #251-2230-160	1	
31			5' 12-3 TYPE "S" SERVICE CORD	1	
32		HUBBELL	"T" PLUG #5464	1	
33	6041023		P.C. CONNECTOR BRACKET		
34	6041022		P.C. BOARD ASSY.	1	
35		AIRPAX	THERMOSTAT 5003-07 OPEN 105°C, CLOSE 80°C	1	
36	6041026		SPACER, CONNECTOR	1	
37	3020920P201	GE	HOLD DOWN FOOT	4	
38		HEYCO	STRAIN RELIEF #1284	1	
39	6041010		BACK PANEL	1	
40	6041011		LEFT SIDE	1	
41	6041012		RIGHT SIDE	1	
42	6041013		BASE	1	
43	6041015		FRONT PANEL	1	
44		BUD	CHAB515 HC14104, COVER	1	


DRAWING NO.

DRAWING NO.

SHEET NO.

DESIGN/RELEASE APPROVALS		DRAWN	MT
APPROVED BY	DATE	DATE	JAN. 4, 1980
		CHECKED	
		DATE	
		APPROVED	
		DATE	

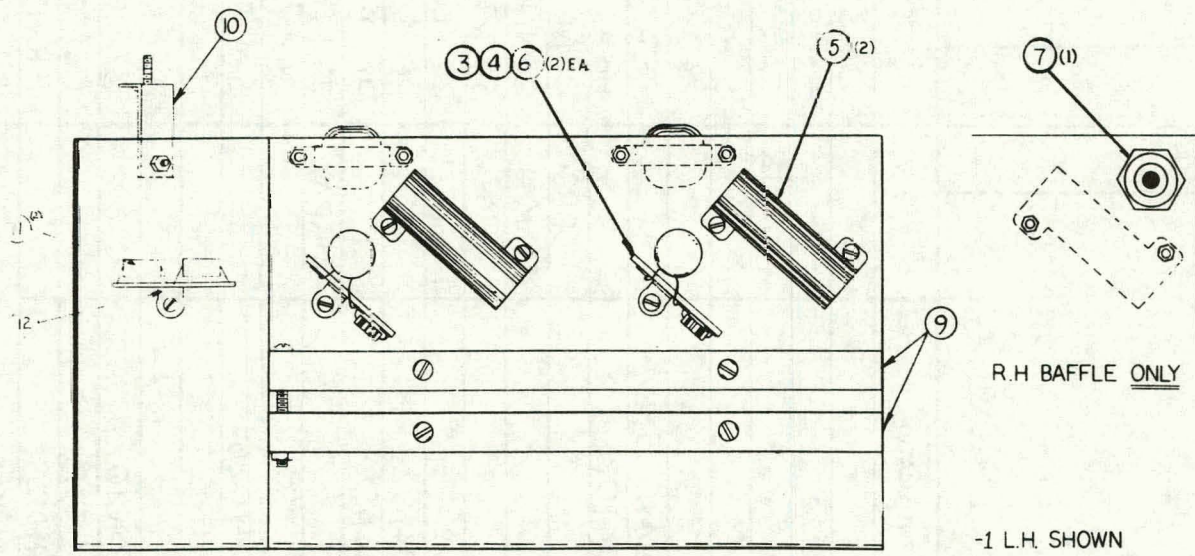
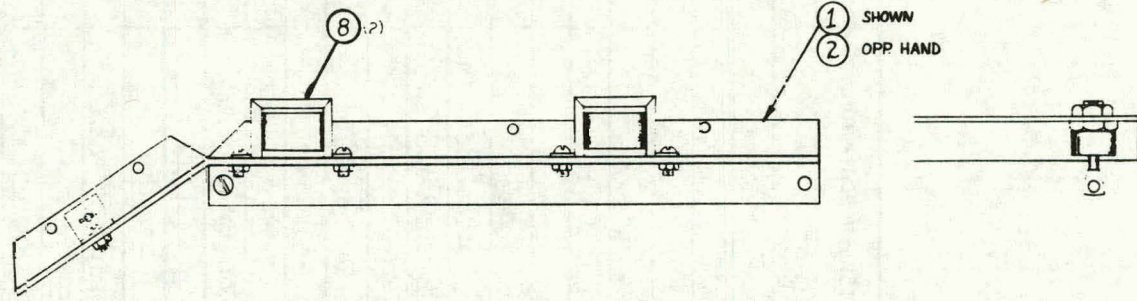
ESB INCORPORATED
TECHNOLOGY CENTER
YARDLEY, PENNSYLVANIA



1Ø HIGH FREQUENCY CHARGER
ASSEMBLY

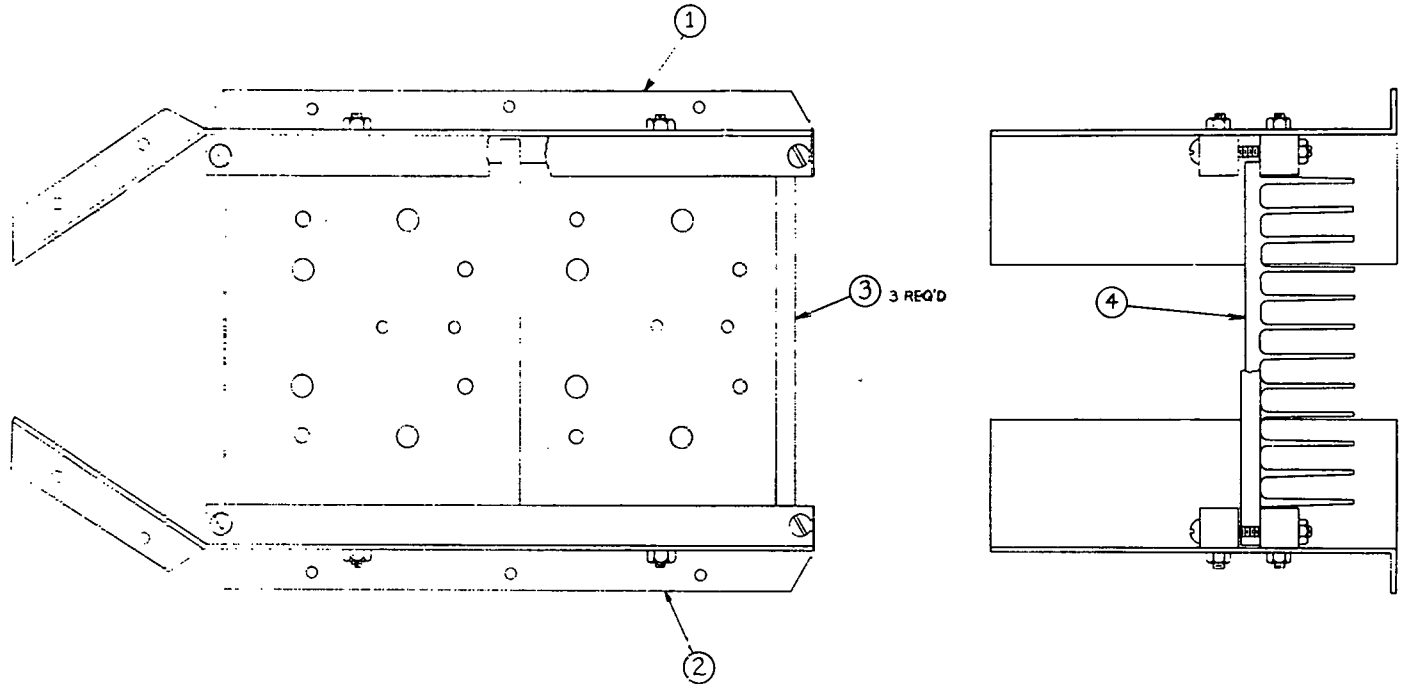
NEXT ASSY NO.	DRAWING NO. PL 6041000	SHEET NO. 2 of 2
---------------	---------------------------	---------------------

70



-1 L.H. SHOWN
-2 R.H. OPP

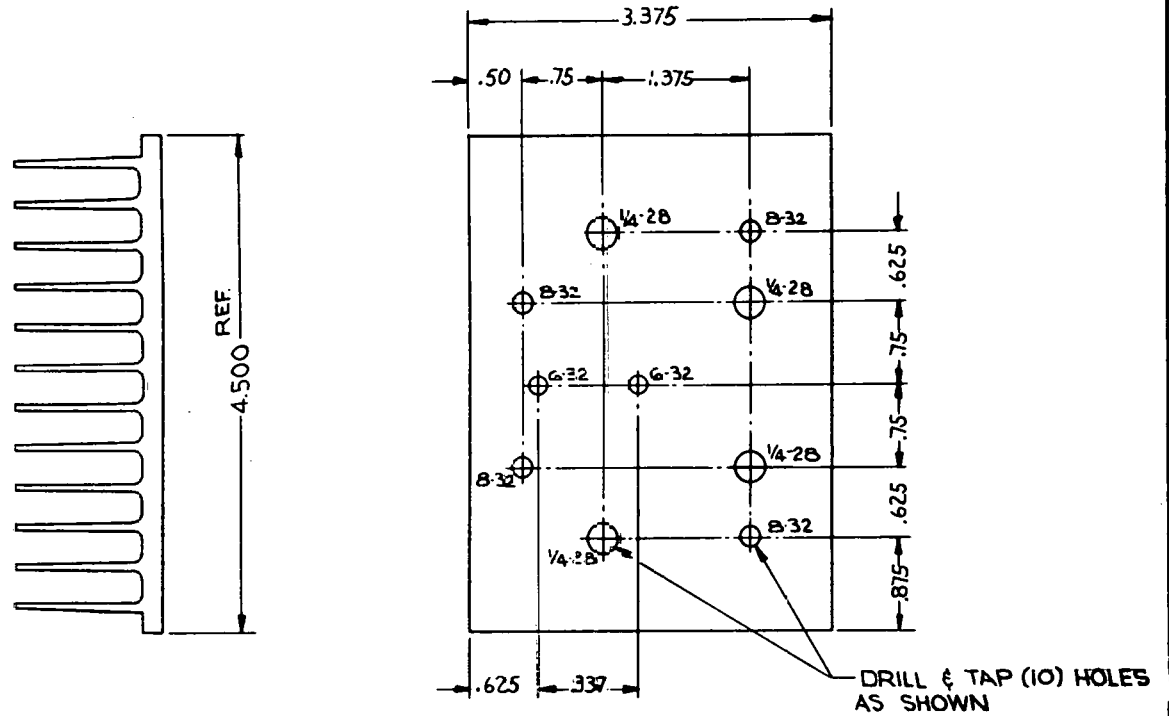
DESIGN/RELEASE APPROVALS		DRAWN BY	DATE	CHECKED BY	DATE	
NAME	DATE	Attwell	OCT 16 1979			
		MATERIAL				
		FINISH				
		TOLERANCES UNLESS OTHERWISE SPECIFIED				SCALE
NEXT LIST NO.	FRACTIONS	DECIMALS	ANGLES	SIZE	DRAWING NO.	DO NOT SCALE DRAWING
	1/16"	.001" - .005"	.001" - .005"	1/16" 9	C	6041001
						DRY
						OP



DESIGN/RELEASE APPROVALS		DESIGN BY: ATTWELL	DATE: OCT 19, 1972	CHECKED BY:	DATE:
NAME:	DATE:	MATERIAL:			
		FINISH:			
TOLERANCES UNLESS OTHERWISE SPECIFIED					
KEY: 1/16" = 1"	FRACTIONS	DECIMALS	ANGLES	SCALE:	DO NOT SCALE DRAWING
	1/16"	.001" - .010"	.005" - 1.000"	AS SHOWN	6041002

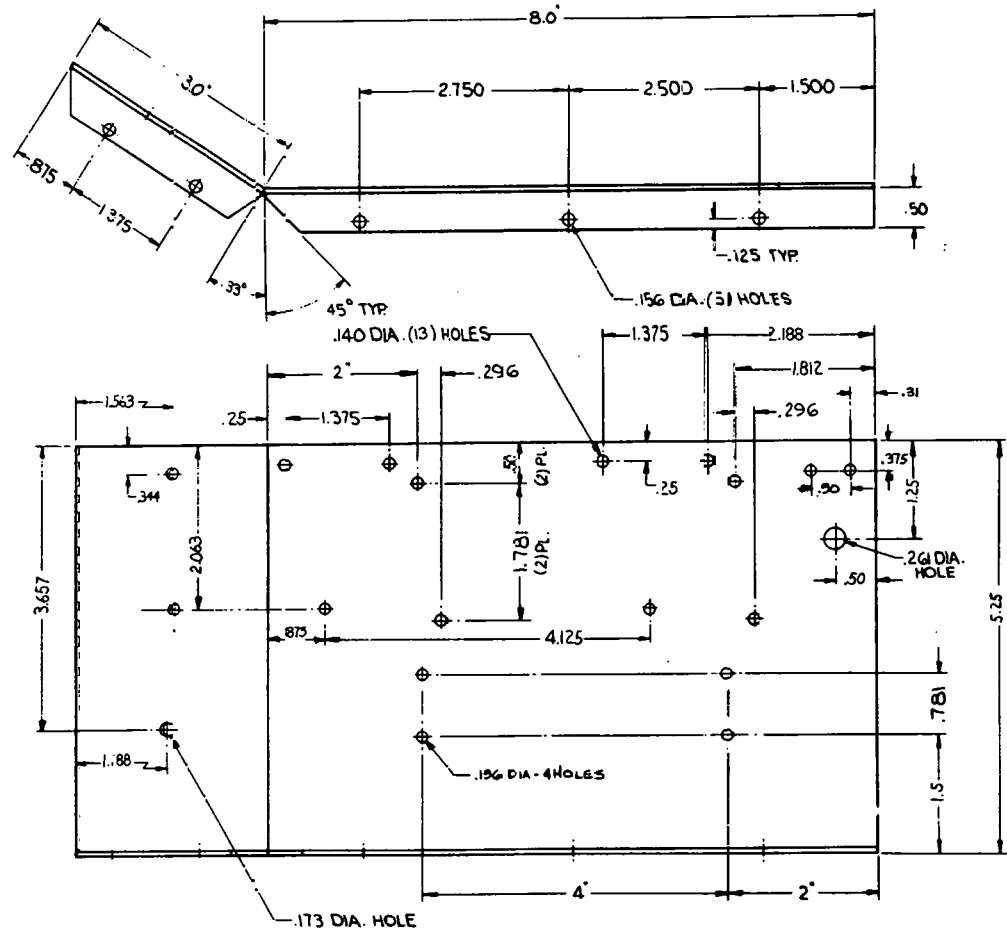
**SAFFLE ASSY.
1 φ CHARGER**

6041002

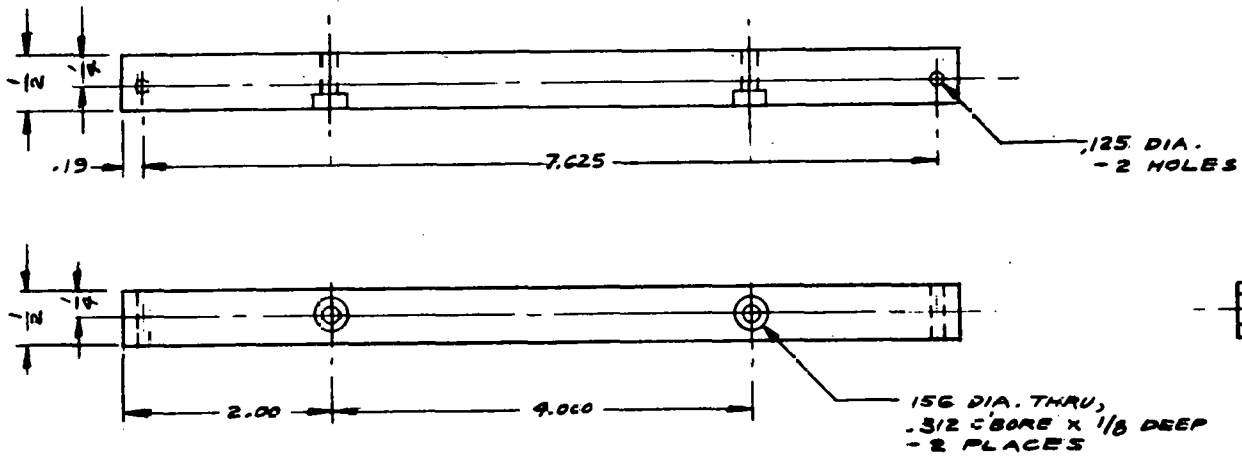


MAKE FROM AHAM EXTRUSION 2003

DESIGN/RELEASE APPROVALS		DRAWN BY: <i>Ry</i>	DATE: <i>Oct 6, 1979</i>	ENGINEER: <i>ST</i>	DATE:	 HEAT SINK, MAIN 1 Ø CHARGER
NAME	DATE	MATERIAL				
		FINISH				TOLERANCES (UNLESS OTHERWISE SPECIFIED) DEC: B DO NOT SCALE DRAWING
		TOLERANCES (UNLESS OTHERWISE SPECIFIED)				
NAVY ARMY NO.		FRAC"IONS	DECIMALS	ANGLES	DEC	DRAWING NO. 6041003
		± .1750"	.00 ± .010"	.000 ± .000"	± 1/4°	

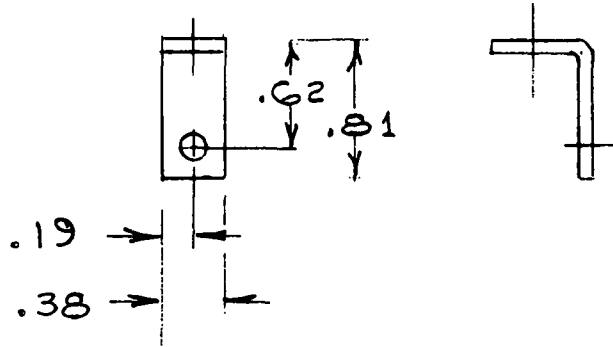
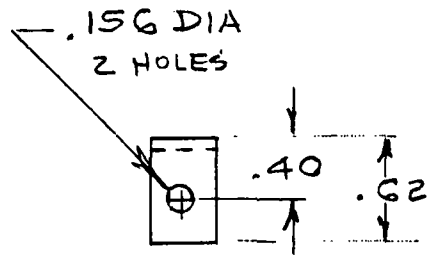


DESIGN/RELEASE APPROVALS		DATE: OCT 12 1979	CHECKED BY:	DATE:
NAME:	DATE:	APPROVAL:		
		JOB NO. TPK AWM 5052-NS2		
		VOL. CHANGED NUMBER OTHERWISE SPECIFIED		
DATE: 12/12/79	REVISIONS:	QUANTITY:	BY:	DATE:
		SCALE: FULL	DO NOT SCALE DRAWING	
		C	604005	



DESIGN/RELEASE APPROVALS		DESIGN BY:	DATE:	CHECKED BY:	DATE:	VIEW NO.	IDENTIFICATION	DESCRIPTION	REV.
NAME	DATE	MFL	6-4-84					GENERAL TOLERANCES	
		MATERIAL		FINISH		TOLERANCES UNLESS OTHERWISE SPECIFIED		SCALE:	DO NOT SCALE DRAWING
		1/2 SR-ROD, ELASTIC REINFORCED FIBERGLASS OR EQUIV.		-				SEE DRAWING NO.	
REV	DATE	FRACTIONS	DECIMALS	ANGLES	SEE	DRAWING NO.			
		1/100"	.001"	1/16°	B	6041007			

79



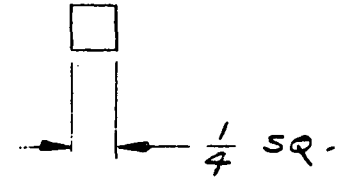
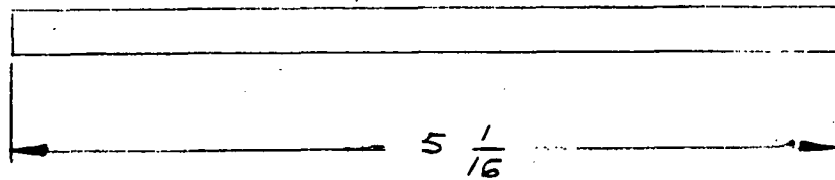
DESIGN/RELEASE APPROVALS		ITEM NO.	IDENTIFICATION	DESCRIPTION	QTY.
NAME	DATE	DRAWN BY:	DATE	CHECKED BY:	DATE
		JT.	1/4/80		
		MATERIAL	06 THICK ALUM 5052-H32		
		FINISH	CLEAR IRIDITE		
		TOLERANCES (UNLESS OTHERWISE SPECIFIED)		SCALE:	DO NOT SCALE DRAWING
NEXT ASSY NO.		FRACTIONS	DECIMALS	ANGLES	SIZE
		± 1/64"	.XX = ± .010"	.XXX = ± .005"	± 1/4" 0
				DRAWING NO.	SHEET
				A	6041008
				1 OF 1	


ESB INCORPORATED
TECHNOLOGY CENTER
YARDLEY, PA. 19067

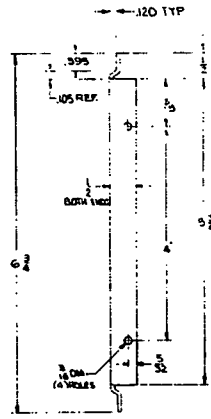
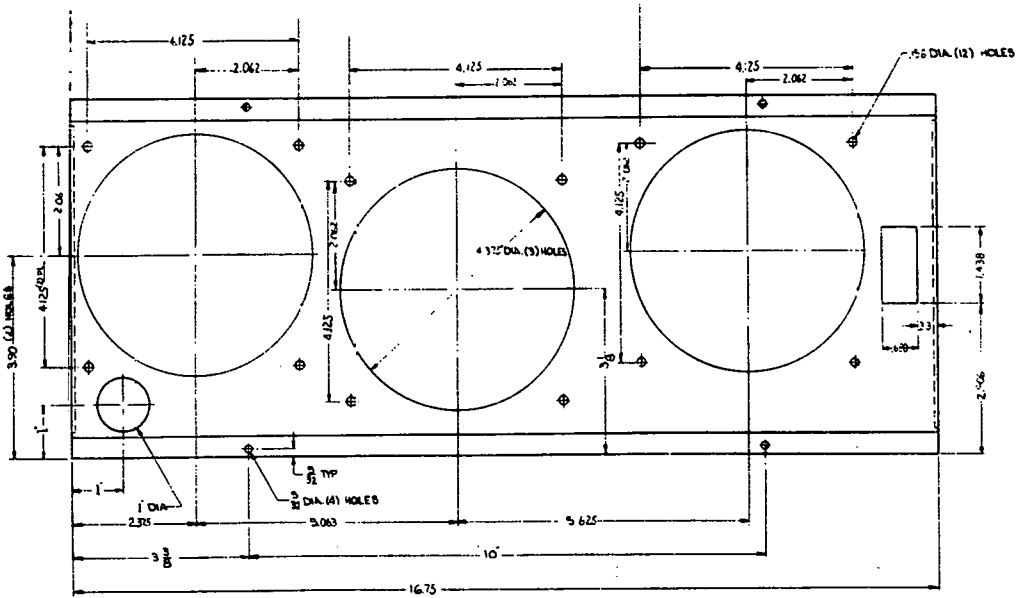


SUPPORT CLIP P.C. BOARD
1 Ø CHARGER

80

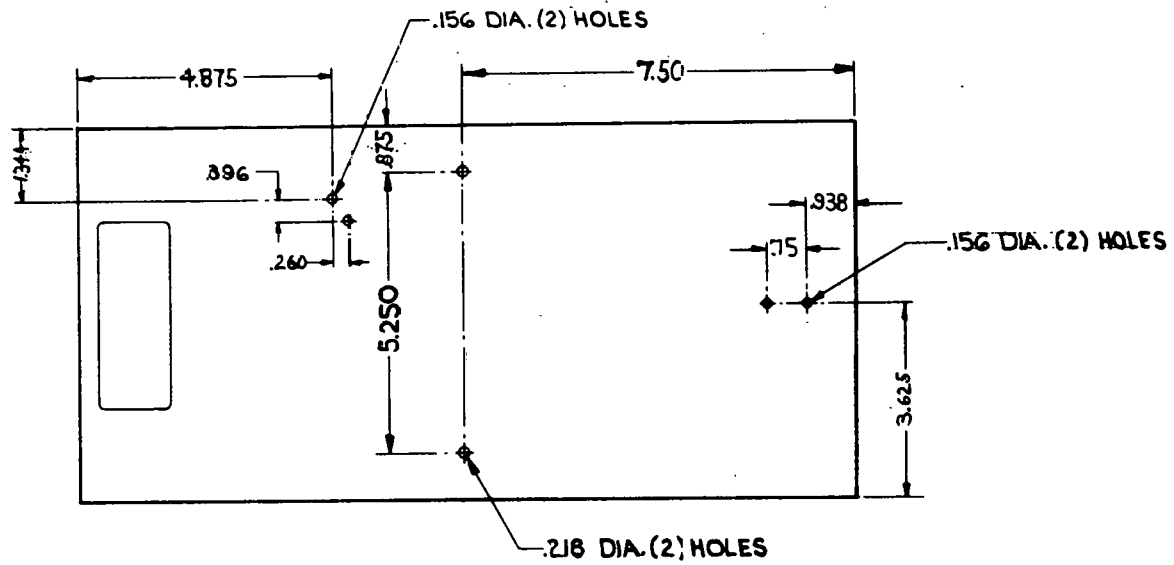


DESIGN/RELEASE APPROVALS		DRAWN BY: K I.	DATE 1-7-80	CHECKED BY:	DATE	ESB INCORPORATED  TECHNOLOGY CENTER YARDLEY, PA. 19067	
NAME	DATE	MATERIAL "GLASTIC" REINFORCED FIBERGLASS ROD OR EQUIV.			SPACER ROD - MAIN HEAT SINK 1" CHARGER		
		FINISH			TOLERANCES (UNLESS OTHERWISE SPECIFIED)		
NEXT ASSY NO.		FRACTIONS ± 1/64"			DECIMALS .XX = ± .010" .XXX = ± .005"	ANGLES ± 1/4°	SCALE: DO NOT SCALE DRAWING
		SIZE A			DRAWING NO. 6041009		SHEET OF



MAKE FROM BUD CH6515 HC M104, BACK PANEL

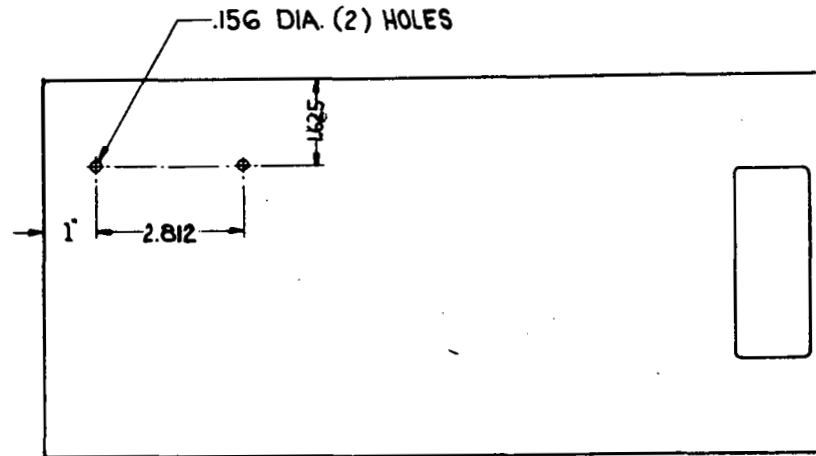
APPROVED FOR	DATE	BY	DESIGNED BY	DATE	BY	DRW. NO.	REV. NO.	REV. DATE	REV. BY	REV. DESCRIPTION	ESB INCORPORATED TECHNOLOGY CENTER 10000 W. CENTRAL EXPRESS SUITE 100 DALLAS, TEXAS 75243-1000 TEL: (214) 343-1000 FAX: (214) 343-1001
			J. G. ALLEN								DETAIL - BACK PANEL 10 CHARGER CS-0010
								11/88			



INSIDE SHOWN

MAKE FROM BUD CHASSIS HC14104
LEFT SIDE PANEL

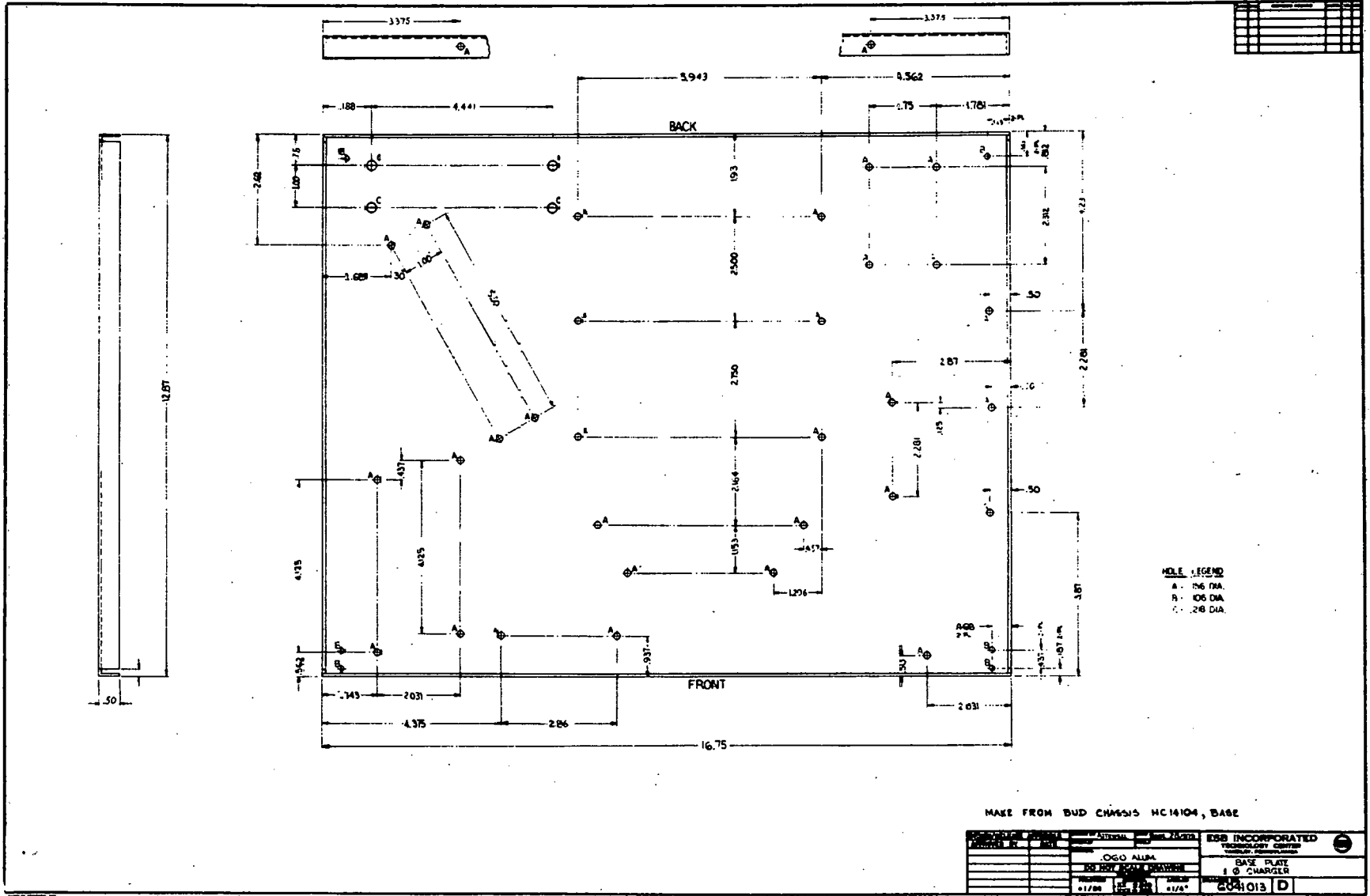
DESIGN/RELEASE APPROVALS		DRAWN BY	DATE	CHECKED BY	DATE	
NAME	DATE	ATTWELL	2-2-77			
		MATERIAL				1 Ø CHARGER LEFT SIDE
		FINISH				
		TOLERANCES (UNLESS OTHERWISE SPECIFIED)				SCALE: 1/2" = 1"
		FRACTIONS	DECIMALS	ANGLES	SEE	DO NOT SCALE DIMENSIONS
BEST COPY NO.		1/16"	.001" - .010"	.001" - .005"	1/16°	8
						6041011



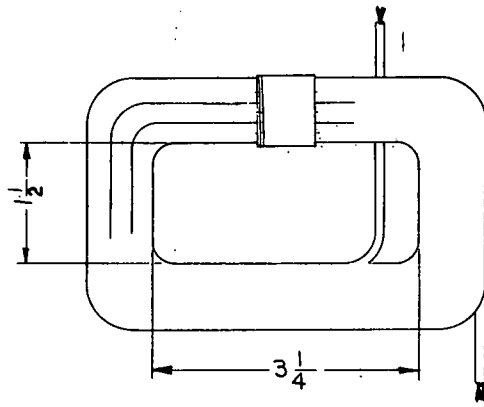
INSIDE SHOWN

MAKE FROM BUD CHASSIS HC14104
RIGHT SIDE PANEL

DESIGN/RELEASE APPROVALS		DRAWN BY: ROY	DATE	CHECKED BY:	DATE	
NAME	DATE	ATTORAL				
		MATERIAL				1 Ø CHARGER RIGHT SIDE
		FINISH				
		TOLERANCES (UNLESS OTHERWISE SPECIFIED)				SCALE: 1/8" = 1"
VERY AMY US.		FRACTIONS	DECIMALS	ANGLES	SIZE	DO NOT SCALE DRAWING
		± 1/64"	.001" - .010"	.005" - .0005"	B	DRAWING NO. 6041012



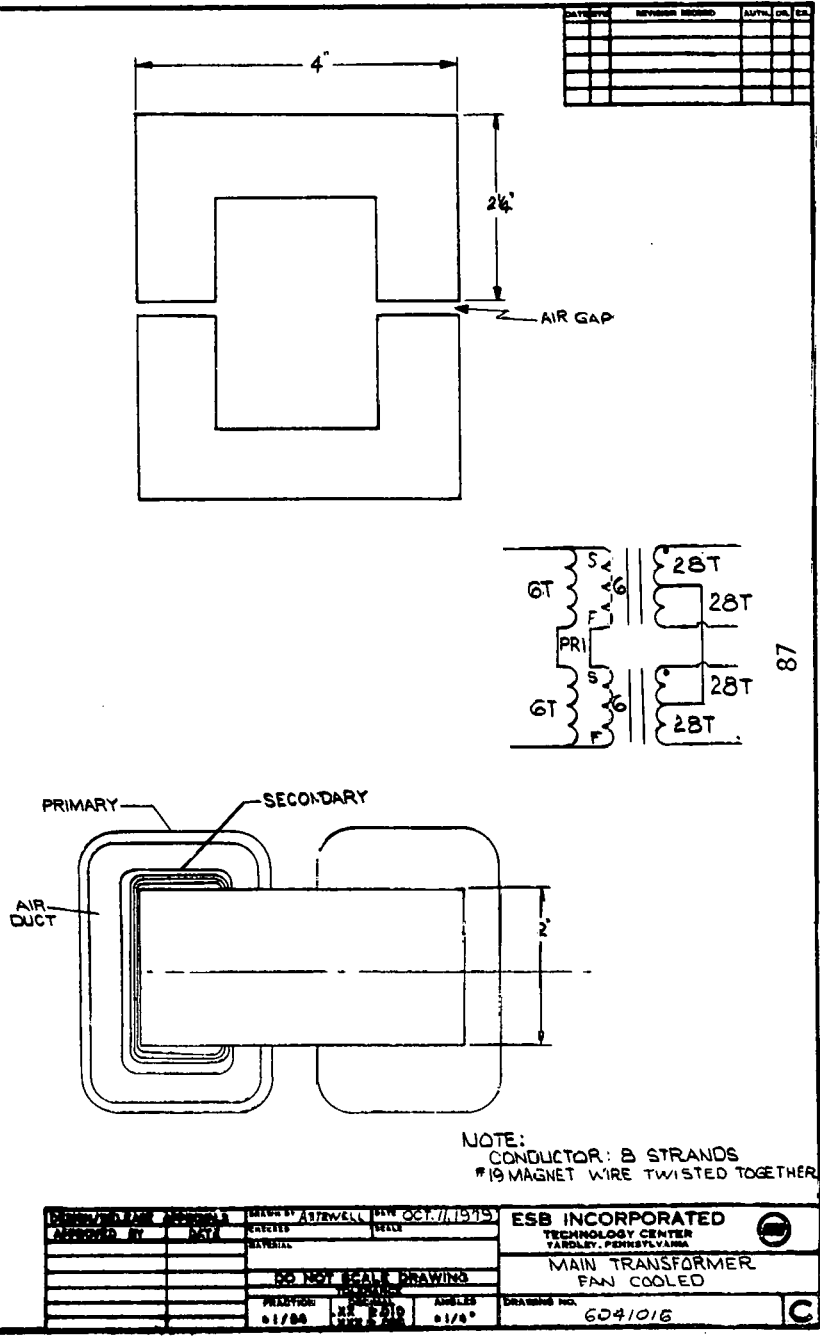
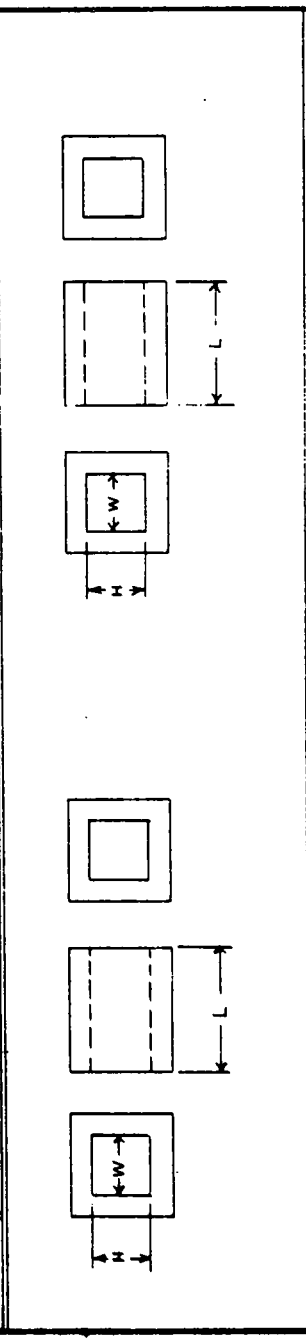
CORE MATERIAL		STACK		AIR CORE		SHUNT MAT'L		INSUL CLASS		UL-	°C	
CORE DIMENSIONS W=		D=	H=	CORE WGT.		lbs	SHUNT DIM: W=	10.002 L=	90.00	AMBIENT-		°C
COIL FORM DIMENSIONS	COIL #1- W=	3/4" H=	1/2"	MAT'L-			SHUNT STACK-	EACH MIN.		TEMP RISE - AC-PR		°C
	COIL #2- W=	H=	L=	MAT'L-			SHUNT GAP	EACH LEG		TEMP RISE - CAP WDG.		°C
COIL #	1											
WINDING												
PAPER WIDTH												
WDG. WIDTH												
WIRING												
WIRE	#10 LITZ											
URNS/LAYER	4											
LAYERS	3											
LAYER INSUL												
TOTAL TURNS	12											
TAPS												
WRAPPER												
LEADS TERMINALS	1-2											
BUILD	54"											
BCA @ 25° C												
CU. WEIGHT												



DESIGNED BY	DATE	SCALE	NO.
APPROVED BY	DATE	SCALE	NO.
DO NOT SCALE DRAWING			
FRAC. 1/8"	1/4"	3/8"	1/2"
1/8"	1/4"	3/8"	1/2"
ESE INCORPORATED			
TECHNOLOGY CENTER			
1400 N. 17TH ST. W.			
MINNETONKA, MN 55345			
DRAWING NO. 604/D14			
SNUBBER INDUCTOR			

NO.	REV.	DATE	BY	CHKD.

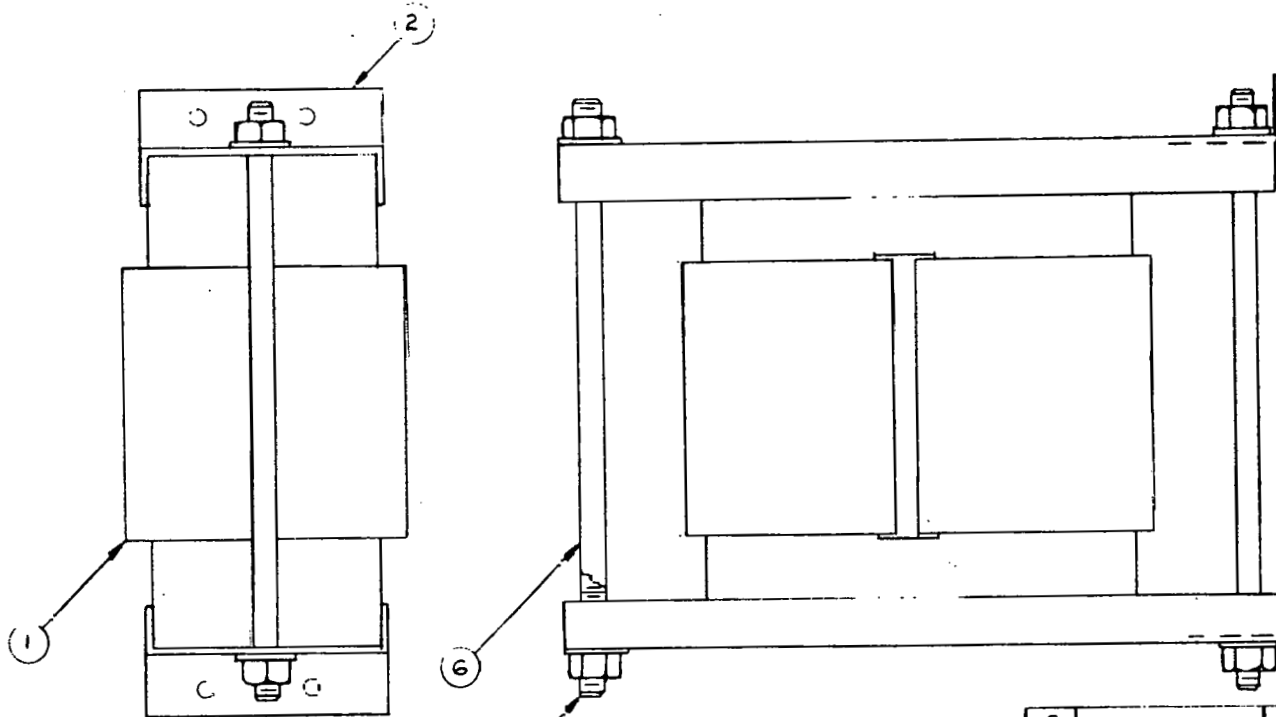
CORE MATERIAL: 05 FERRITE (F2141105)		STACK: 2" x 2" GAP: 2 x .005"	SHUNT MAT'L:	INSUL CLASS:	UL:
CORE DIMENSIONS: W: D: H: L:		CORE MAT: 5 lbs	SHUNT DIM: W: L:	AMBIENT:	°C
CORE TUBE DIMENSIONS: W: H: L:		MAT'L: 05 NOMEX	SHUNT STACK:	TEMP RISE - AC-PRI:	°C
COIL #1: W: H: L:		SILICONE BONDED	SHUNT GAP:	TEMP RISE - CAP WIND:	°C
COIL #2: W: H: L:			SHUNT WGT:	VARNISH:	
COIL #:		2 COILS/UNIT			
WINDING:		SEC. A & B	NOTES:		
PAPER WIDTH:			FRI		
WIND. WIDTH:					
MARGINS:					
WIRE:		(2) #18			
TURNS/LAYER:		28 BIFILAR			
LAYER INSUL:		1/4" AIR DUCT			
TOTAL TURNS:		BETWEEN SEC. & FRI			
TAPS:		28 + 28			
WRAPPEL:		BIFILAR WOUND			
LEADS TERMINALS:		ALL AROUND			
BUILD:		DUCTS MUST BE			
DCR @ 25° C:		CONNECT AS CT			
CUL WEIGHT:		NONE			



DATE	REVISION	BY	CHK	CR

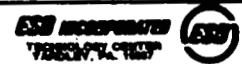
DESIGNED BY: [REDACTED]	CHECKED BY: ASTERWELL	DATE: OCT. 11, 1975	ESB INCORPORATED TECHNOLOGY CENTER YARDLEY, PENNSYLVANIA
APPROVED BY: [REDACTED]	MATERIAL:		
DO NOT SEAL DRAWING			MAIN TRANSFORMER FAN COOLED
PRICE: \$1784	QUANTITY: 200	ANGLE: 01/0°	Drawing No. 6041016

87



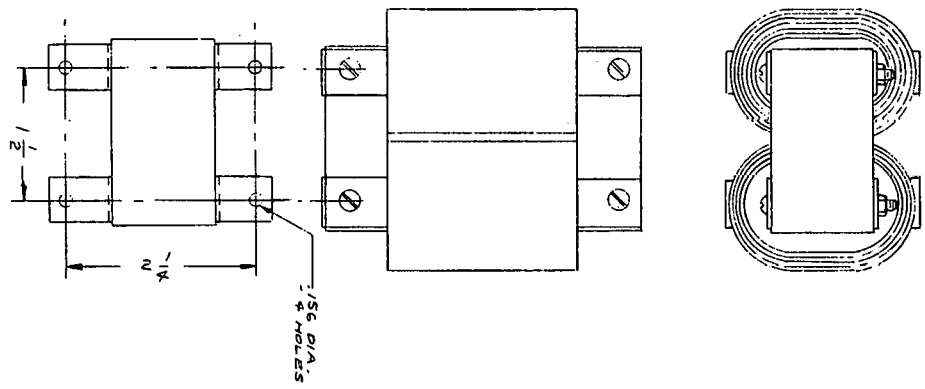
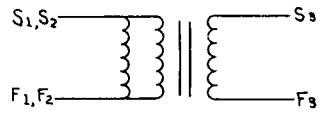
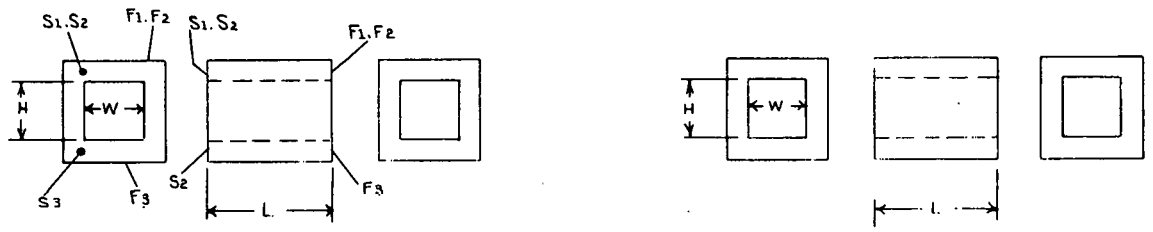
ITEM NO.	IDENTIFICATION	DESCRIPTION	QTY.
6		SHRINKABLE TUBING	AR
5	1/4-20	HEX NUT	4
4	1/4	FLAT WASHER	4
3	1/4-20 X 5 1/2 LG	THREADED STOCK	2
2	5C41020	BRACKET-MAIN TRANSFORMER	2
1	6041016	MAIN TRANSFORMER	1

DESIGN/RELEASE APPROVALS		DRAWN BY:	DATE	CHECKED BY:	DATE
NAME	DATE	K.L.	1-9-80		
		MATERIAL SEE PL			
		FINISH			
		TOLERANCES (UNLESS OTHERWISE SPECIFIED)			
		FRACTIONS	DECIMALS	ANGLES	SCALE: 1:1
		± 1/64"	.001" ± .010"	± .005" ± .0001"	DO NOT SCALE DRAWING
NEXT ASSY NO.		DRAWING NO. 6041017		REV D	



MAIN TRANSFORMER ASSY.

CORE TUBE DIMENSIONS		CORE WGT. 2.28 lbs		SHUNT MAT'L.		INDUCTION CLASS. 1L °C	
COIL # 1 - W = 25/32" H = 1 3/8" L = 2 3/16"		CORE WGT. 2.28 lbs		SHUNT DIM. - W		AMBIENT °C	
COIL # 2 - W = H' L'		MAT'L - 0.040 NOMEX		SHUNT STACK		TEMP RISE - AC/DKI °C	
2 COILS / UNIT		MAT'L -		SHUNT GAP		TEMP RISE - CAP WDG. °C	
COIL #		1		SHUNT WGT.		VARNISH	
WINDING		MAIN ① MAIN ② SPILLOVER ③		EACH MIN.			
PAPER WIDTH		2 3/16		EACH LEG.			
WDG. WIDTH		1 7/8					
MARGINS							
WIRE		#12° #12° #16°					
TURNS/LAYER		20 20 20					
LAYERS		1 1 1					
LAYER INSUL		- - -					
TOTAL TURNS		20 20 20					
TAPS							
WRAPPER		0.010 MYLAR 0.010 MYLAR 0.005 MYLAR					
LEADS TERMINALS		PARALLEL CONNECT ① + ②					
BUILD		.086					
DCR @ 25° C		.007 Ω					
CU. WEIGHT		.35*					



DRAWING NO. 6041018
 INPUT CHOKE
 ESB INCORPORATED
 TECHNICAL CENTER
 11111 W. 11TH AVE.
 DENVER, CO 80233
 DATE: OCT. 1, 1979
 CHECKED BY: []
 DESIGNED BY: []
 DO NOT SCALE DRAWING
 FRACTION: 1/64
 DECIMAL: .001
 ANGLE: 1/4°
 DRAWING NO. 6041018

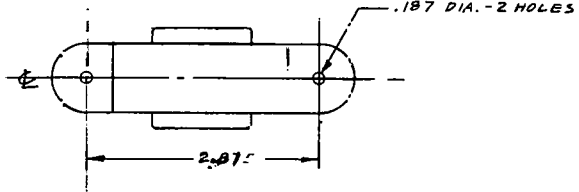
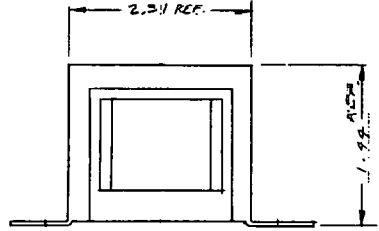
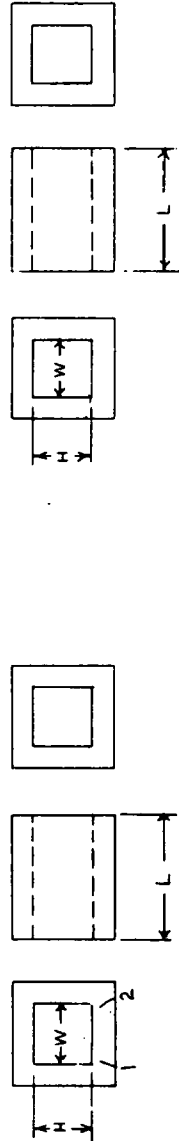
REV	DATE	BY	CHKD

8"

CORE MATERIAL .014 SUPERMULIO EI 75 STACK 3/4

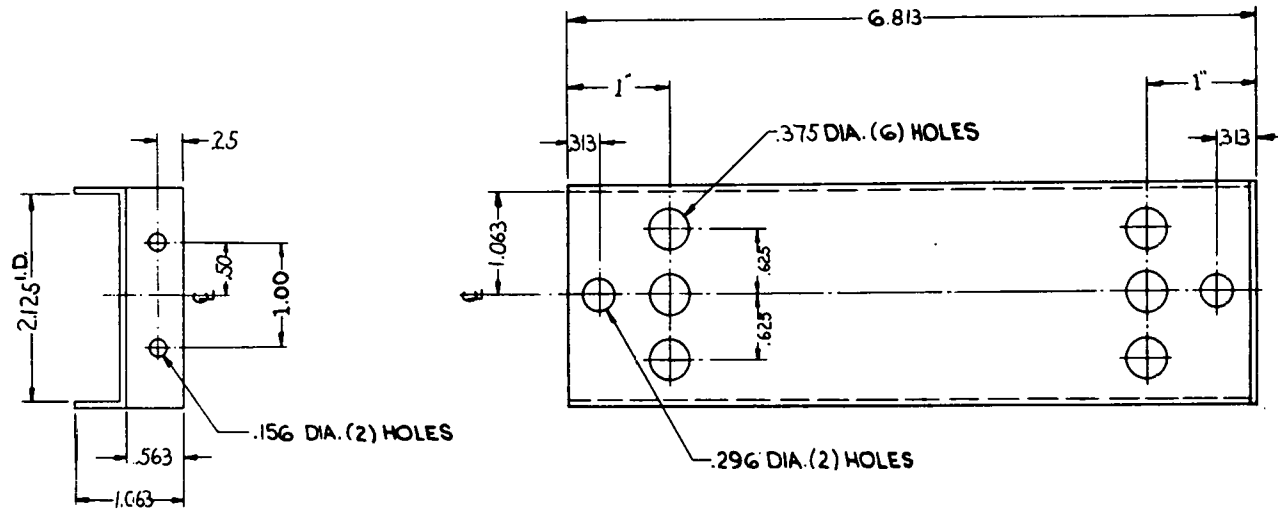
NYLON
S74 3/4
BOBBIN W/2 SOLDER LUGS

LINKING	SECONDARY
PAPER WIDTH	
Wdg. WIDTH	
MARKING	
WIRE	#30 NYLON
TURN/LAYER	1000
LAYER INSUL	.020 NOMEX
TOTAL TURNS	1000
TAPS	
WRAPPER	GLASS TAPE
LEADS	1-2
TERMINALS	SOLDER LUGS
BUILD	TOP SIDE
DCR @ 25°C	25 Ω
CU. WEIGHT	.08 US.



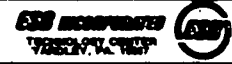
- NOTES:**
1. PART SHALL BE MANUFACTURED ACCORDING TO PROVISIONS OF ESS QC-STD: 302.
 2. TERMINAL #1 MAY BE IDENTIFIED BY A DOT IN LIEU OF TERMINAL NUMBERING.
 3. HORIZONTAL MOUNTING CHANNEL TO BE USED. CENTER TO CENTER.
 4. FREEBAKE FOR 30 MIN. @ VACUUM IMPREGNATE.

DESIGNED BY	DATE	APPROVED BY	DATE
W. PATRICK	MAY 12 1979		
CHECKED	SCALE	ESB INCORPORATED	
REVISION		TECHNOLOGY CENTER	
		YARDLEY, PENNSYLVANIA	
DO NOT SCALE DRAWING			
PLANNED BY	DATE	APPROVED BY	DATE
A. J. B.	JUN 28 1979	A. J. B.	A. J. B.
CURRENT TRANSFORMER			
6041019			

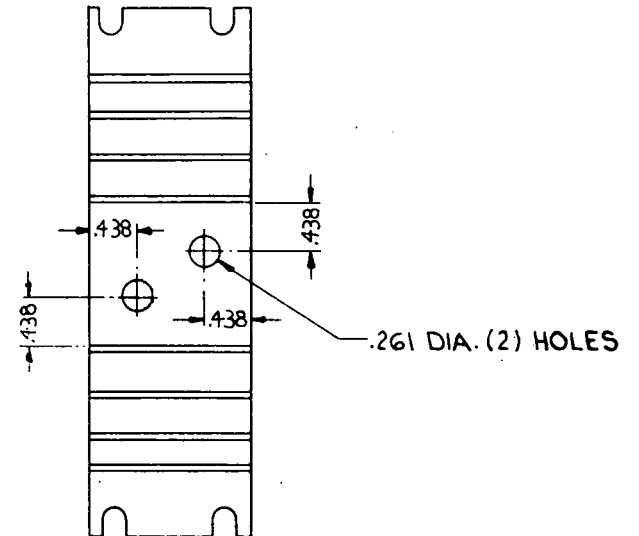
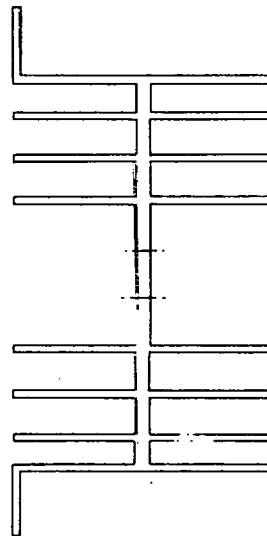


2 REQUIRED

DESIGN/RELEASE APPROVALS		DRAWN BY: <u>Atwell</u>	DATE: <u>SEP 28 1979</u>	CHECKED BY:	DATE:
NAME	DATE				
		MATERIAL: <u>.060 ALUM.</u>			
		FINISH:			
		TOLERANCES (UNLESS OTHERWISE SPECIFIED)			
REF: ASSY NO.		FRACTIONS	DECIMALS	ANGLES	SCALE: <u>B</u>
		<u>1/16"</u>	<u>.001 - .010"</u>	<u>1/4°</u>	DRAWING NO. <u>6041020</u>
					DO NOT SCALE DRAWING
					SHEET <u>1</u> OF <u>1</u>



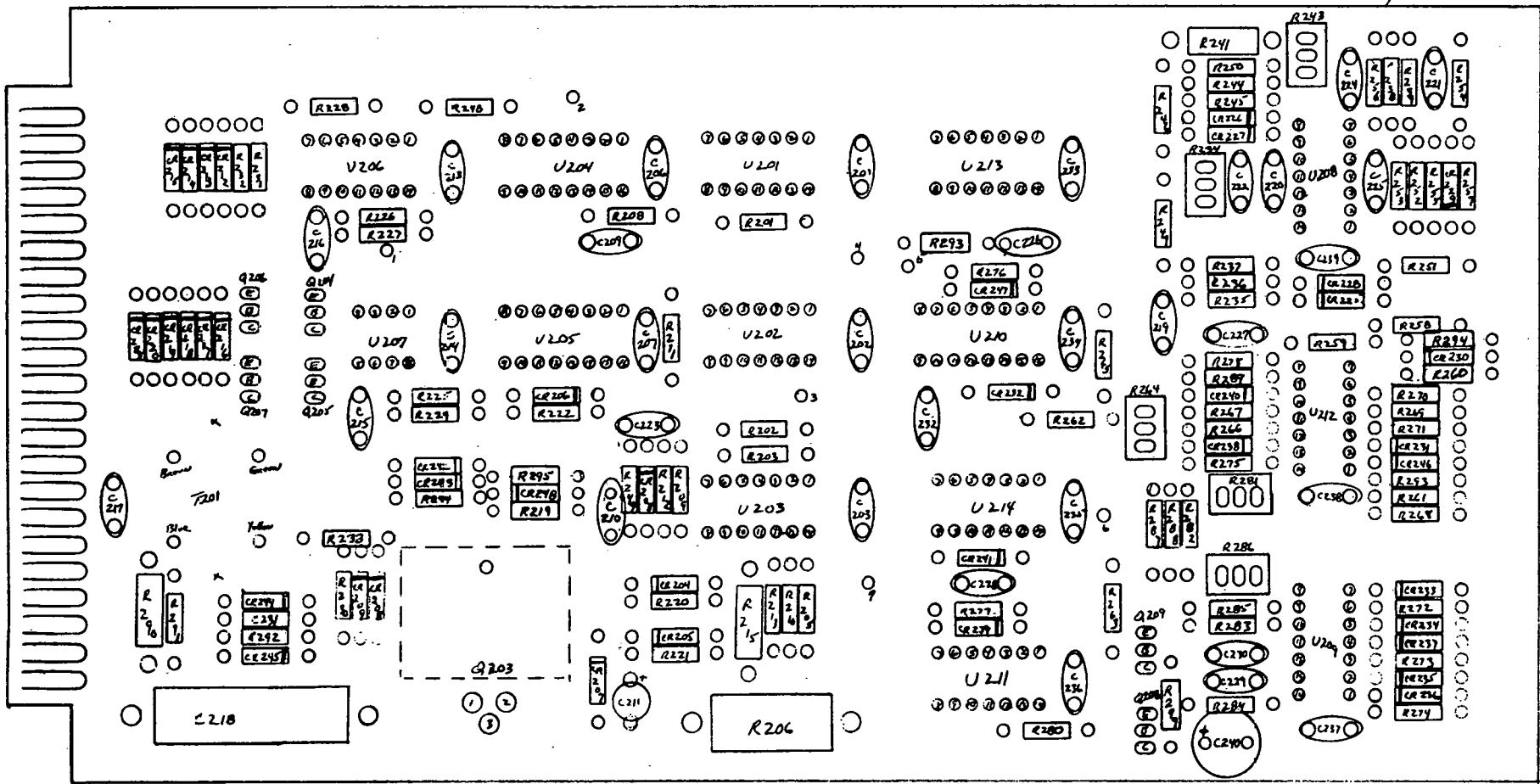
BRACKET - MAIN TRANSFORMER
1 Ø CHARGER




MAKE FROM AHAM EXTRUSION #6112 1 1/2 LONG

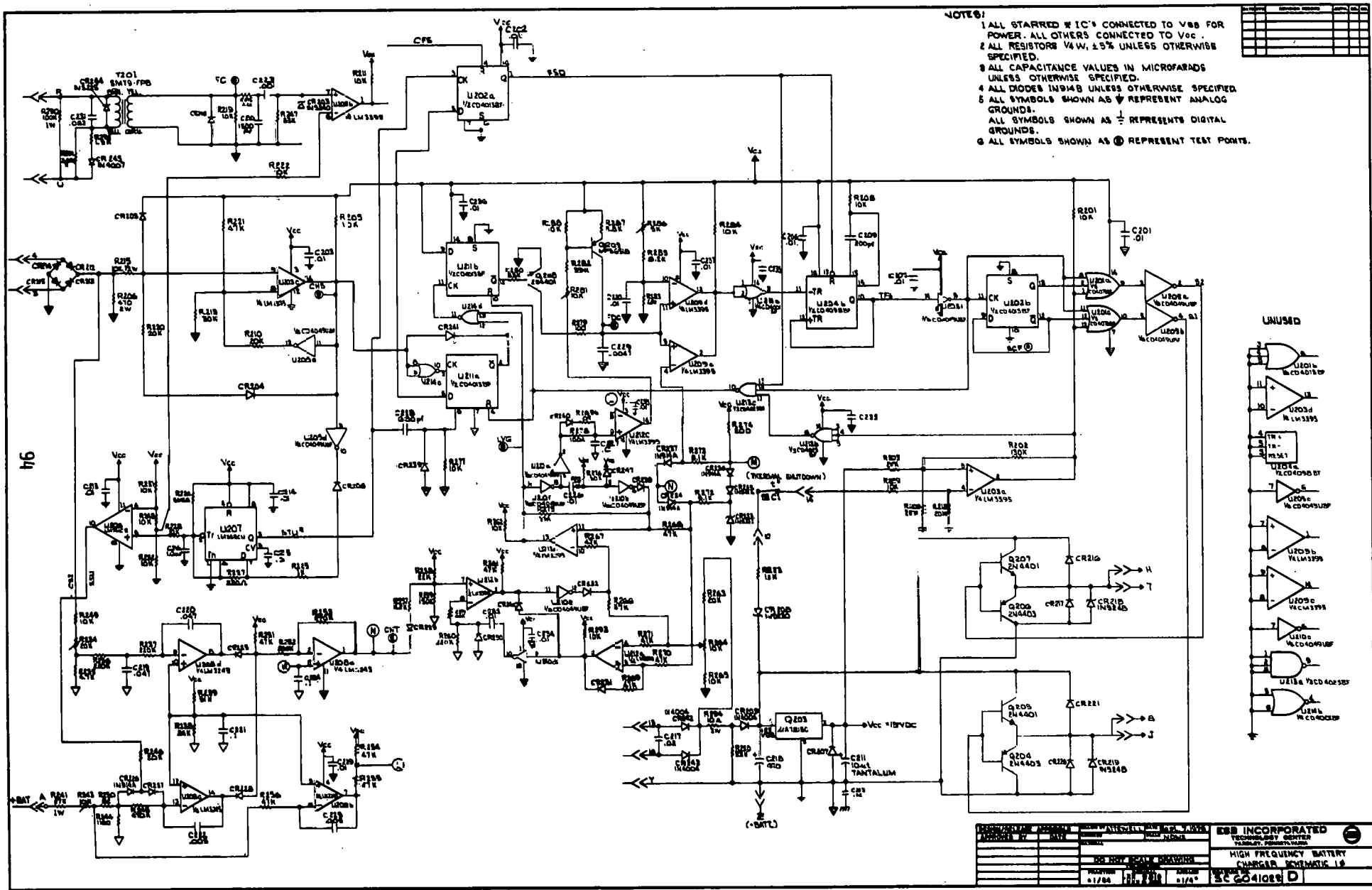
DESIGN/RELEASE APPROVALS		DRAWN BY: <i>R</i>	DATE: OCT 17, 1979	CHECKED BY:	DATE:	
NAME	DATE	Attewell				
		MATERIAL				
		FINISH				
		TOLERANCES UNLESS OTHERWISE SPECIFIED				
MILITARY ACRYL NO.		FRACTIONS		DECIMALS	ANGLES	SCALE: DO NOT SCALE DRAWING
		1/64"		.001"	.0005"	SEE DRAWING NO. 6041021
					1/16°	B

93



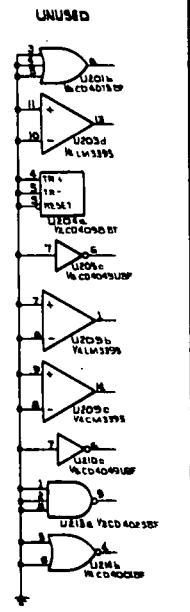
NOTE:
1. SEE DWG SC 6041022 FOR P.C. BOARD SCHEMATIC.

DESIGN/RELEASE APPROVALS		DESIGNED BY:	DATE	CHECKED BY:	DATE	ITEM NO.	IDENTIFICATION	DESCRIPTION	QTY.
NAME	DATE	MATERIAL		SEE PL 6041022		 ESB INCORPORATED 1000 W. 10TH ST. TULSA, OK 74104		CIRCUIT BOARD ASSY 1 Φ CHARGER	
		FINISH							
TOLERANCES (UNLESS OTHERWISE SPECIFIED)						SCALE:	DO NOT SCALE DRAWING		
NEXT ASSY NO.		FRACTIONS	DECIMALS	ANGLES		SIZE	DRAWING NO.		SHEET
		1/64"	.001"	1/4°		C	6041022		1 of 1



- NOTES:
- 1 ALL STARRED IC'S CONNECTED TO V_{BB} FOR POWER. ALL OTHERS CONNECTED TO V_{CC}.
 - 2 ALL RESISTORS 1/4 W, ±5% UNLESS OTHERWISE SPECIFIED.
 - 3 ALL CAPACITANCE VALUES IN MICROFARADS UNLESS OTHERWISE SPECIFIED.
 - 4 ALL DIODES IN 1N4148 UNLESS OTHERWISE SPECIFIED.
 - 5 ALL SYMBOLS SHOWN AS ▽ REPRESENT ANALOG GROUNDS. ALL SYMBOLS SHOWN AS ⊥ REPRESENTS DIGITAL GROUNDS. 6 ALL SYMBOLS SHOWN AS ⊙ REPRESENT TEST POINTS.

REV	DESCRIPTION	DATE	BY



DESIGNED BY	DATE	REV	DESCRIPTION

ESB INCORPORATED
 10000 JENNY STREET
 VAN NUYS, CALIFORNIA 91411
 (818) 708-1100
HIGH FREQUENCY BATTERY CHARGER SCHEMATIC 19
 PROJECT # 1174 DATE 11/74 19C 2041028 D

--	--	--	--	--	--

ITEM NO.	IDENTIFICATION NO.	MFR	DRAWING TITLE / DESCRIPTION	QTY.	
				-1	-2
19	R43, R44, R81		10K POT 329901-103		
20	R44		1.1K, 1/4W5% ϕ		
21	R45, R56		470K, 1/4W5% ϕ		
22	R48		5.1, 1/4W5% ϕ		
23	R50		82, 1/4W5% ϕ		
24	R53		270K, 1/4W5% ϕ		
25	R58		22K, 1/4W5% ϕ		
26	R59, R76		150K, 1/4W5% ϕ		
27	R72, R73		5.1K, 1/4W5% ϕ		
28	R74		200, 1/4W5% ϕ		
29	R75		1MEG, 1/4W5% ϕ		
30	R78		100K, 1/4W5% ϕ		
31	R79		100, 1/4W5% ϕ		
32	R82		39K, 1/4W5% ϕ		
33	R83		1.5K, 1/4W5% ϕ		
34	R85		8.2K, 1/4W5% ϕ		
35	R86		5K POT 3299W-1-502		
36	R87		1.8K, 1/4W5% ϕ		
37	R90		270K, 1/4W5% ϕ		
38	R91		560K, 1/4W5% ϕ		
39	R92		1.8K, 1/4W5% ϕ		
40	R93-R95		2.2K, 1/4W5% ϕ		


DRAWING NO.

DRAWING NO.

SHEET NO.

DESIGN/RELEASE APPROVALS		DRAWN	
APPROVED BY	DATE	DATE	
		CHECKED	
		DATE	
		APPROVED	
		DATE	

ESB INCORPORATED
 TECHNOLOGY CENTER
 YARDLEY, PENNSYLVANIA



NEXT ASSY NO.	DRAWING NO.	SHEET NO.
	PL6041022	2 of 5

REV.	REVISION RECORD	DR.	REV.	DATE	REVISION RECORD	DR.

ITEM NO.	IDENTIFICATION NO.	MFR	DRAWING TITLE / DESCRIPTION	QTY.	
				-1	-2
40	C9		10TS-T20, 200PT 1KV	1	
41	C10		5GA-D15, 1500PT	1	
42	C11		196D106Y9035PE4, 10MT	1	
43	C15		225P10291W03, 0.01MT	1	
44	C16		196D105X9035HA1, 1MT	1	
45	C17		225P22391W03, 0.022MT	1	
46	C18		5010477F035PS, 470MT	1	
47	C19, C20		HY-835, 0.047MT	2	
48	C21, C24		HY-750, 0.1MT	2	
49	C22, C25		5GA-050, 0.005MT	2	
50	C23		5GA-010, 0.001MT	1	
51	C26		HY-850, 0.1MT	1	
52	C27, C32		5GA-510, 0.01MT	2	
53	C28		5GA-T6B, 680PT	1	
54	C29		225P47291W03, 0.0092MT	1	
55	C30		HY-715, 0.01MT	1	
56	C31		225P02391W03, 0.002MT	1	
57			102MF 1000V	1	
58			HY-715, 0.01MT DE-COUPLE CAPS	15	
59	C40		100MT 20V 196D107X902TE4	1	

DRAWING NO.

DRAWING NO.

SHEET NO.

DESIGN / RELEASE APPROVALS		DRAWN	
APPROVED BY	DATE	DATE	
		CHECKED	
		DATE	
		APPROVED	

ESB INCORPORATED
 TECHNOLOGY CENTER
 YARDLEY, PENNSYLVANIA

NEXT ASSY NO.	DRAWING NO. 6041022	SHEET NO. 3
---------------	---------------------	-------------

REV.	REVISION RECORD	DR.	REV.	DATE	REVISION RECORD	DR.

ITEM NO.	IDENTIFICATION NO.	MFR	DRAWING TITLE / DESCRIPTION	QTY.	
				-1	-2
58	CR3		IN 5240	1	
59	CR4, CR5, CR6, CR7, CR10, CR11, CR12, CR13, CR14, CR15, CR16, CR17, CR20, CR21, CR22, CR23, CR25, CR26, CR27, CR28, CR29, CR30, CR31, CR32, CR34, CR35, CR36, CR37, CR38, CR39, CR40, CR41, CR46, CR47 CR48		IN 9149 IN 914B	25	
60	CR8		IN 5230	1	
61	CR9		IN 4004	1	
62	CR18, CR19		IN 5248	2	
63	CR33		IN 5231	1	
64	CR42, CR43		IN 4001	2	
65	CR44		IN 5235	1	
66	CR45		IN 4007	1	

DRAWING NO.

DRAWING NO.

SHEET NO.

DESIGN/RELEASE APPROVALS		DRAWN
APPROVED BY	DATE	DATE
		CHECKED
		DATE
		APPROVED
		DATE

ESB INCORPORATED
 TECHNOLOGY CENTER
 YARDLEY, PENNSYLVANIA

NEXT ASSY NO.	DRAWING NO. PL 6041022	SHEET NO. 4
---------------	---------------------------	----------------

REV.	REVISION RECORD	DR.	REV.	DATE	REVISION RECORD	DR.

ITEM NO.	IDENTIFICATION NO.	MFR	DRAWING TITLE / DESCRIPTION	QTY.	
				-1	-2
67	Q3		WA7B15C		
68	Q4, Q6		2N4403		
69	Q5, Q7, Q8		2N4401		
70	Q9		MPS 651B		
71	U1		CO4075BF		
72	U2, U4, U15		CO4013BF		
73	U3, U9, U12		LM339J		
74	U5, U10, U11		CO4049UBF		
75	U6		LM741CS		
76	U7		LM555CN		
77	U8		LM324J		
78	U13		CO4023BF		
79	U14		CO4001BF		
80	T201	MICROTRAN	SMT9-FPS		
81	6042001		PRINTED CIRCUIT BOARD		

DRAWING NO.

DRAWING NO.

SHEET NO.

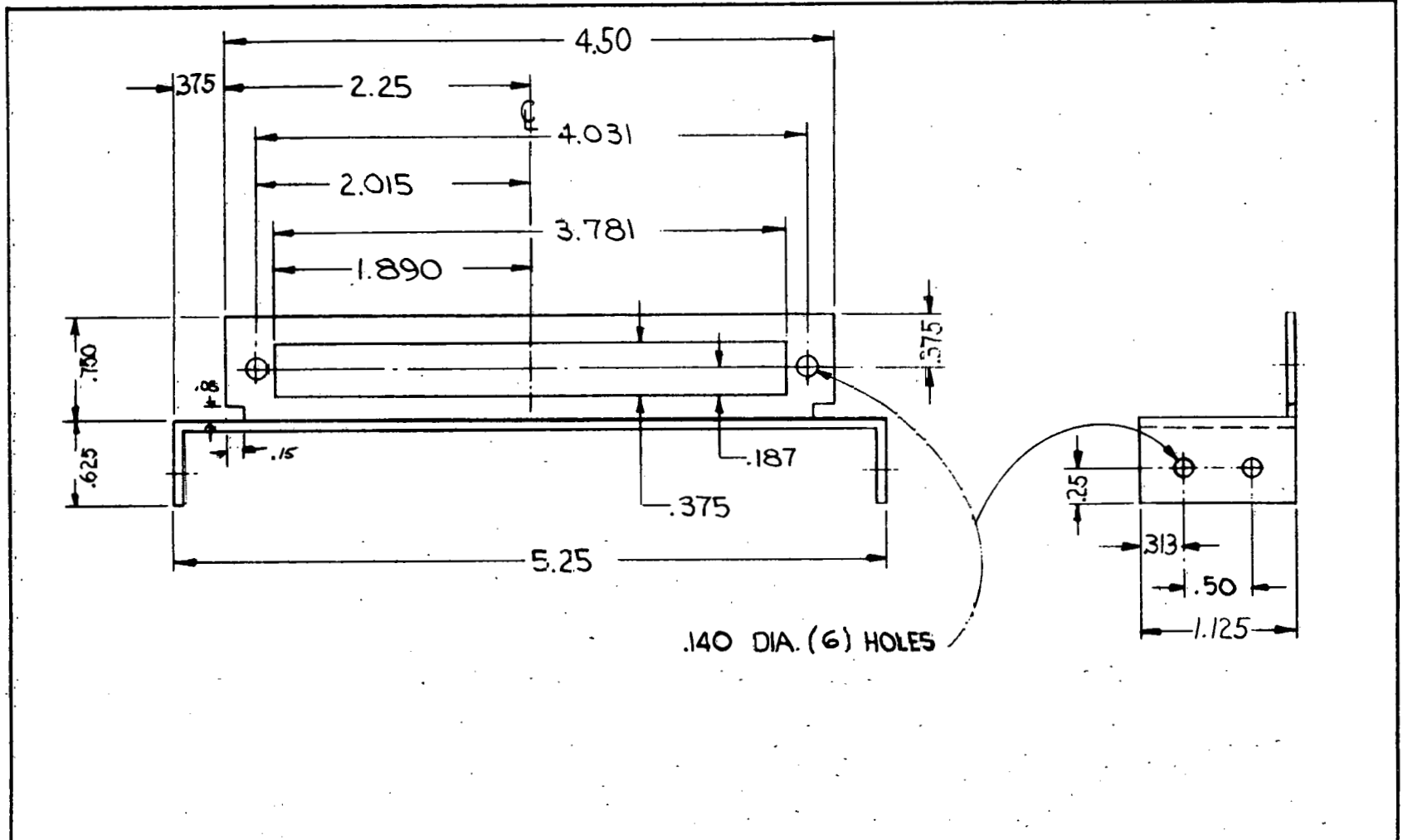
DESIGN/RELEASE APPROVALS		DRAWN	
APPROVED BY	DATE	DATE	
		CHECKED	
		DATE	
		APPROVED	
		DATE	

ESB INCORPORATED
 TECHNOLOGY CENTER
 YARDLEY, PENNSYLVANIA

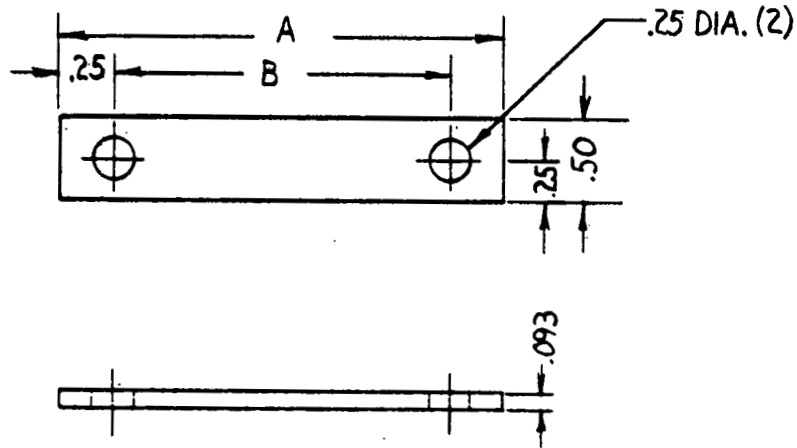


NEXT ASSY NO.	DRAWING NO.	SHEET NO.
	PI 6041022	5


100



DESIGN/RELEASE APPROVALS		DRAWN BY:	DATE	CHECKED BY:	DATE	ESB INCORPORATED TECHNOLOGY CENTER YARDLEY, PA. 19087 P.C. CONNECTOR BRACKET 1 Ø CHARGER
NAME	DATE	RAY ATTEWELL	9/21/79			
		MATERIAL: .060 ALUM.				
		FINISH:				
NEXT ASSY NO:		TOLERANCES - UNLESS OTHERWISE SPECIFIED:			SCALE: FULL	DO NOT SCALE DRAWING
		FRACTIONS	DECIMALS	ANGLES	SIZE	DRAWING NO.
		± 1/64"	.XX = ± .010"	.XXX = ± .005"	A	6041023
						SHEET 1 of 1

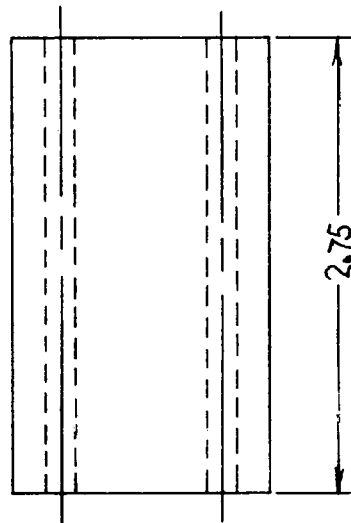
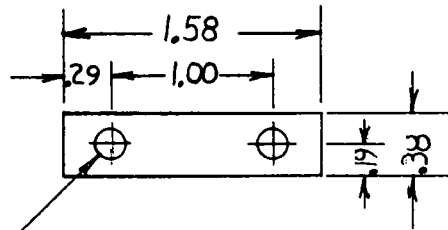



DASH N.	DIM."A"	DIM."B"
-1	2.00	1.50
-2	2.56	2.06

DESIGN/RELEASE APPROVALS		ITEM NO.	IDENTIFICATION		DESCRIPTION	QTY.
NAME	DATE	DRAWN BY:	DATE	CHECKED BY:	DATE	
		M.T.	11/4/80			
		MATERIAL				ESB INCORPORATED TECHNOLOGY CENTER YAROLEY, PA. 19067 
		.093 THICK COPPER				
		FINISH				
NEXT ASSY NO.		TOLERANCES (UNLESS OTHERWISE SPECIFIED)			SCALE:	DO NOT SCALE DRAWING
		FRACTIONS	DECIMALS	ANGLES	SIZE	DRAWING NO.
		± 1/64"	.XX = ± .010"	.XXX = ± .005"	A	6041024
						SHEET
						OF

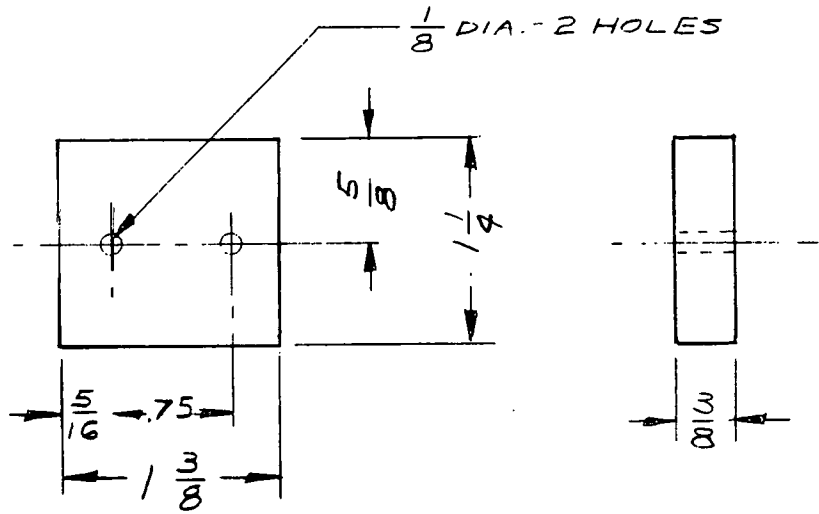
102


10-32 THD.
x .50 DEEP
- 2 HOLES



DESIGN/RELEASE APPROVALS		DRAWN BY:	DATE	CHECKED BY:	DATE	ESB INCORPORATED TECHNOLOGY CENTER YARDLEY, PA. 19067		
NAME	DATE	MT	1/4/80					SPACER-HEAT SINK 1 Ø HIGH FREQUENCY CHARGER
		MATERIAL				38 THICK NYLON		
		FINISH						
		TOLERANCES (UNLESS OTHERWISE SPECIFIED)				SCALE:	DO NOT SCALE DRAWING	
NEXT ASSY NO.		FRACTIONS	DECIMALS	ANGLES	SIZE	DRAWING NO.	SHEET	
		± 1/64"	.XX = ± .010"	.XXX = ± .005"	± 1/4"	A	6041025	
							OF	

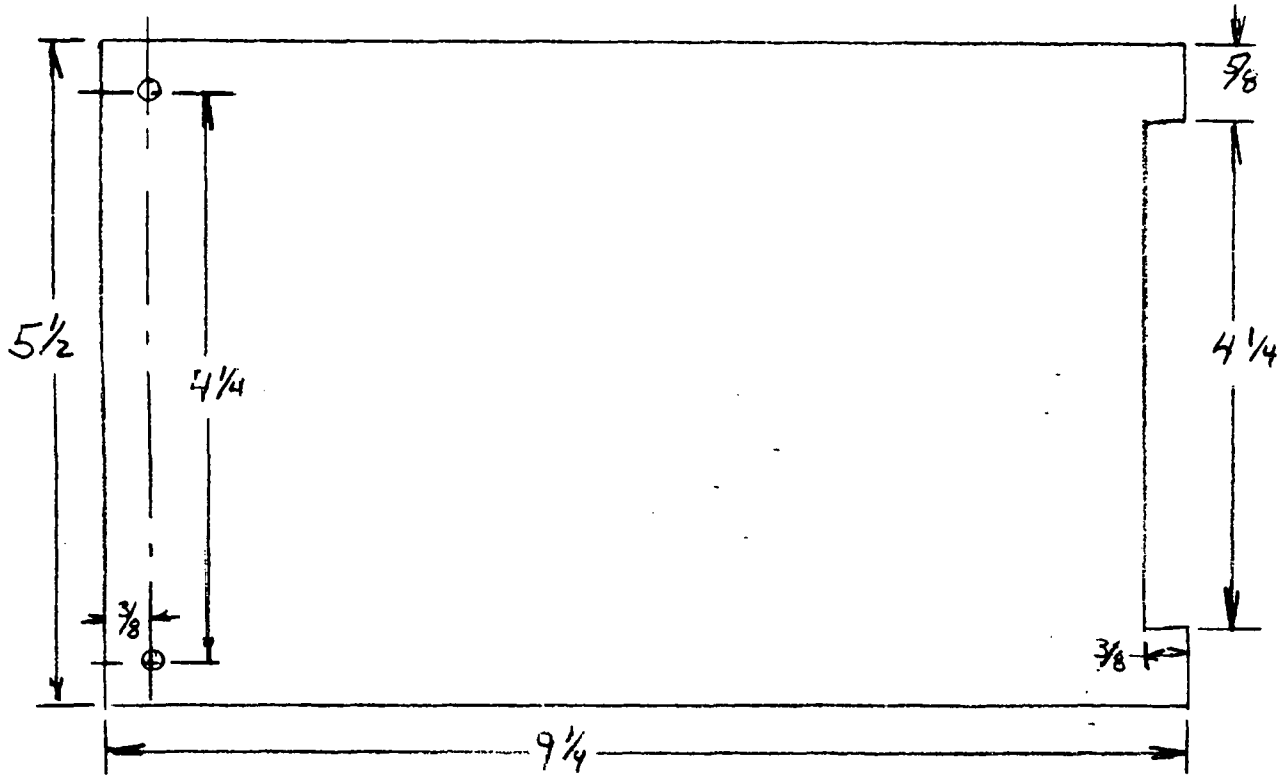
103




DESIGN/RELEASE APPROVALS		DRAWN BY:	DATE	CHECKED BY:	DATE	ESB INCORPORATED TECHNOLOGY CENTER YARDLEY, PA. 19087 
NAME	DATE	K.L.	1-4-80			
		MATERIAL				SPACER - BATTERY CONNECTOR 10 CHARGER
		NYLON				
		FINISH				TOLERANCES (UNLESS OTHERWISE SPECIFIED) SCALE: DO NOT SCALE DRAWING
NEXT ASSY NO.		FRACTIONS	DECIMALS	ANGLES	SIZE	DRAWING NO.
		± 1/64"	.XX = ± .010" .XXX = ± .008"	± 1/4°	A	6041026
						SHEET
						1 of 1

CUT HERE GUARANTEED 12-77

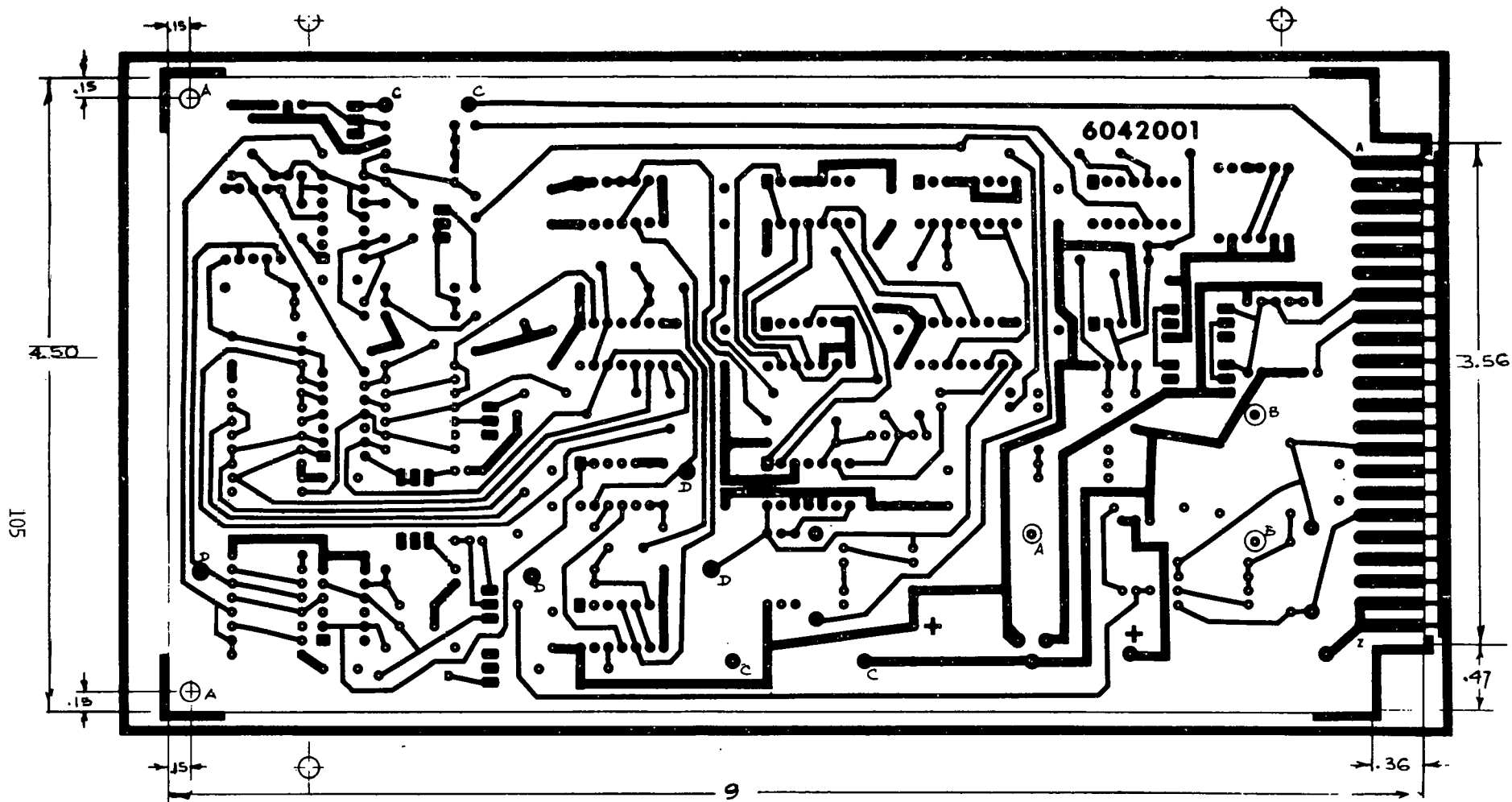
104



COVER BOTH SIDES
WITH .005 NOMEX
INSULATOR

DESIGN/RELEASE APPROVALS		ITEM NO.	IDENTIFICATION	DESCRIPTION	QTY.
NAME	DATE	DRAWN BY: <i>RWS</i>	DATE: <i>1/31</i>	CHECKED BY:	DATE:
		MATERIAL: <i>1/16" THICK ALUMINUM</i>			ESB INCORPORATED  TECHNOLOGY CENTER YARDLEY, PA. 19087
		FINISH:			
TOLERANCES UNLESS OTHERWISE SPECIFIED:				SCALE: <i>NONE</i>	DO NOT SCALE DRAWING
NEXT ASSY NO.		FRACTIONS	DECIMALS	ANGLES	SIZE
		$\pm .004"$	$.XX = \pm .010"$	$.XXX = \pm .008"$	$\pm 1/4^\circ$
				DRAWING NO. <i>6041.027</i>	SHEET OF

CUT HERE GUARANTEED 13.77

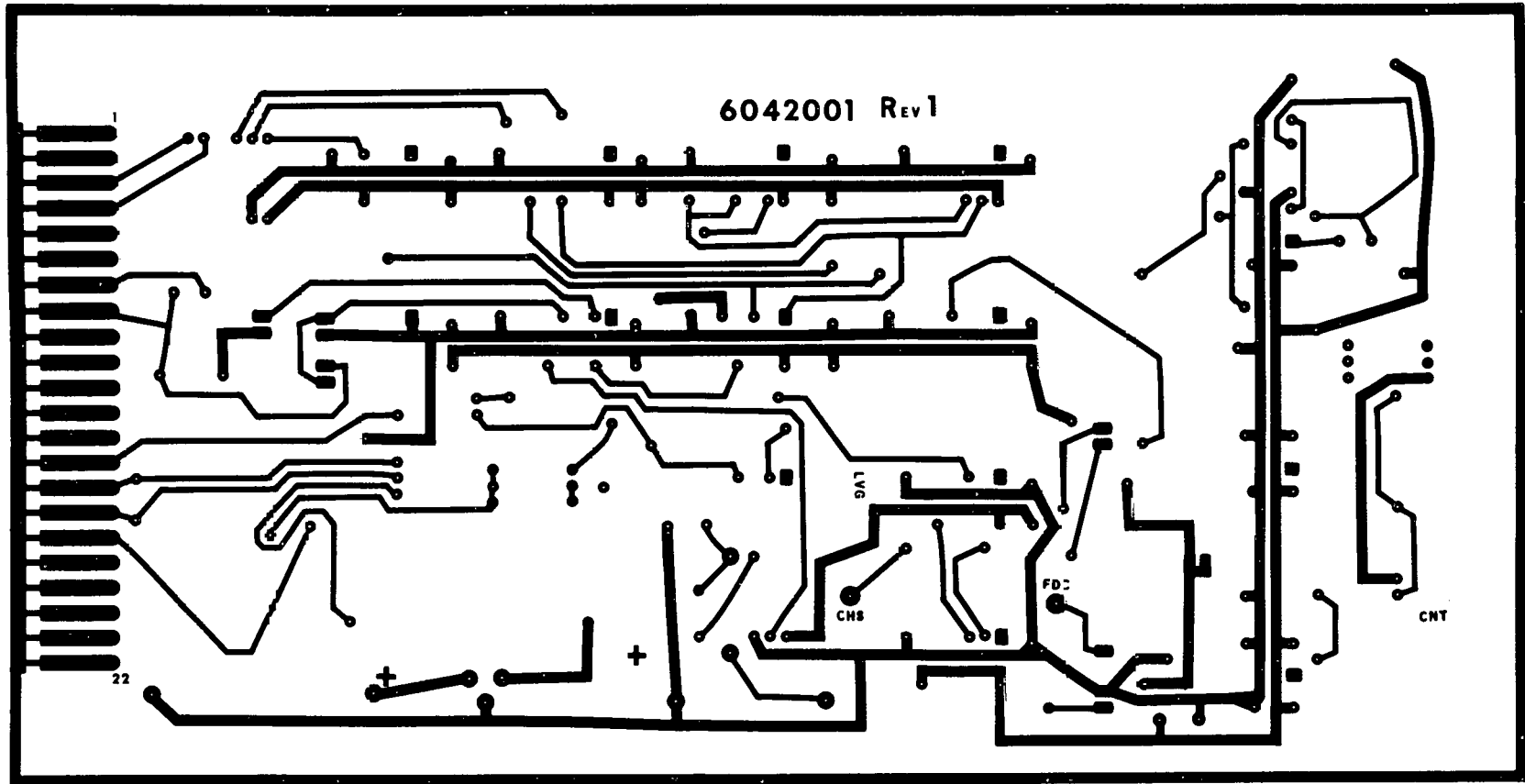


HOLE SCHEDULE		
SYM	SIZE	QTY
A	.141 ±.003 DIA	3
B	.156 ±.003 DIA	2
C	.046 ±.003 DIA	4
D	.062 ±.003 DIA	4
MINI	.037 ±.003 DIA	

NOTE:
 1. ALL HOLES PLATED THRU
 2. USE ARTWORK PM 6042001 (23H.)

DESIGN/RELEASE APPROVALS		DATE	CHECKED BY:	DATE	ITEM NO.	IDENTIFICATION	DESCRIPTION	QTY.
NAME	DATE							
MATERIAL:		1/8" THICK 2 OZ. COPPER FACED						
FINISH:		(2 SIDES) GLASS CLOTH LAMINATE, TYPE FR-4						
		SOLDER PLATE						
		TOLERANCES (UNLESS OTHERWISE SPECIFIED)						
KEY ART. NO.		FRACTIONS	DECIMALS	ANGLES	SCALE:	DO NOT SCALE DRAWING		
		1/16"	.005" - .010"	.001" - .002"	1/4" = 1"	DRILL & TRIM P.C. BOARD		
					C	G042001		1 of 1

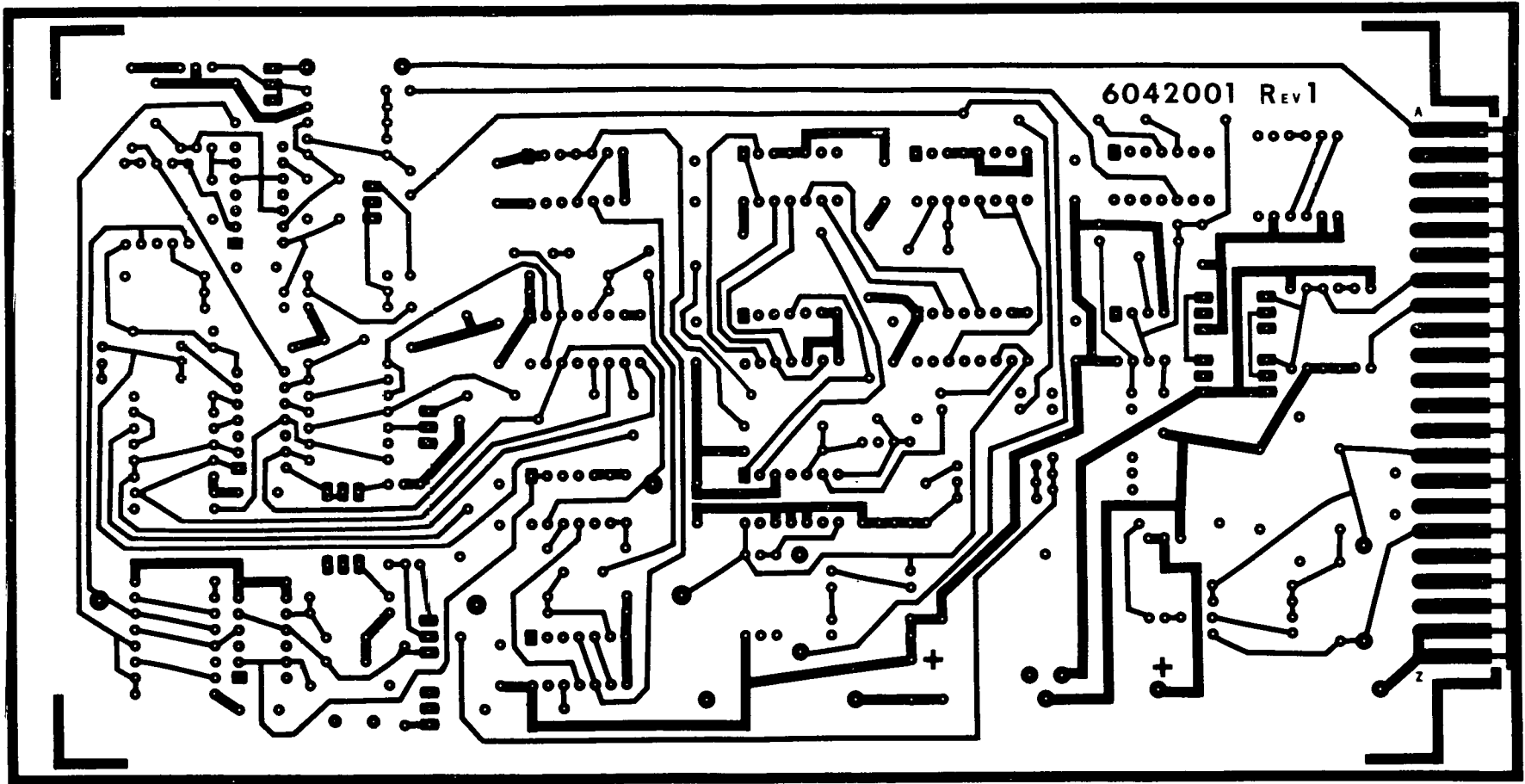
106



DESIGN/RELEASE APPROVALS		DRAWN BY	DATE	CHECKED BY	DATE	ITEM NO.	IDENTIFICATION	DESCRIPTION	QTY.	
NAME	DATE	MATERIAL			SEE DWG 6042001		ESB INCORPORATED TECHNOLOGY CENTER YANLEY, VA. 1987		CIRCUIT BOARD 1 φ CHARGER	
		FINISH								
NET ASBY NO		TOLERANCE* (UNLESS OTHERWISE SPECIFIED)				SCALE	DO NOT SCALE DRAWING			
		FRACTIONS	DECIMALS	ANGLES		SIZE	DRAWING NO.	SHEET		
		1/16"	.010"	1/4°		D	PM 6042001	1 of 2		

Reduce to 10.000 ± .005"

107



DESIGN RELEASE APPROVALS		ITEM NO.		IDENTIFICATION		DESCRIPTION		QTY.
NAME	DATE	DATE	PRECEDENT	DATE				
TOLERANCES (UNLESS OTHERWISE SPECIFIED)						SCALE:	DO NOT SCALE DRAWING	
						SEE	DRAWING NO.	SHEET
						D	PM 6042001	2 OF 2

ESB INCORPORATED
TECHNOLOGY CENTER
YARBLEY, VA. 19057



CIRCUIT BOARD
1 φ CHARGER

**THIS PAGE
WAS INTENTIONALLY
LEFT BLANK**

APPENDIX C
BIBLIOGRAPHY

APPENDIX C: BIBLIOGRAPHY

- Oughton, G., "New Thyristors Make Series Resonant Inverter Cost Effective", Solid State Power Conversion, published by Powercon Inc., July - August 1977.
- Martin, I., "The Application of ASCR's to High Frequency Inverters", Presented at Powercon 4, Boston, MA, May 13, 1977.
- Schwarz, F. C., "An Improved Method of Resonant Current Pulse Modulation for Power Converters", Transactions on Industrial Electronics and Control Instrumentation, Vol. IECI-23, No. 2, May, 1976.
- Biess, J. J. and Shank, J. H., "High Voltage Series Resonant Inverter Ion Engine Screen Supply", Paper published based on development work performed at TRW, Inc. under contracts NAS12-2183 and NAS3-14383.
- Martin, I., "Operating Characteristics of Self-Commutated Sine Wave SCR Inverters", RCA Thyristors Application Note AN-6745.

APPENDIX D
SNUBBER CIRCUIT COMPUTER SIMULATION

APPENDIX D: SNUBBER CIRCUIT COMPUTER SIMULATION

The snubber circuitry of the high frequency series resonant battery charger was designed with the aid of digital computer circuit simulation. The simulation development is presented below.

The snubber circuit is represented by a step function source, $U(t)$, driving a fourth order passive network. See figure D-1.

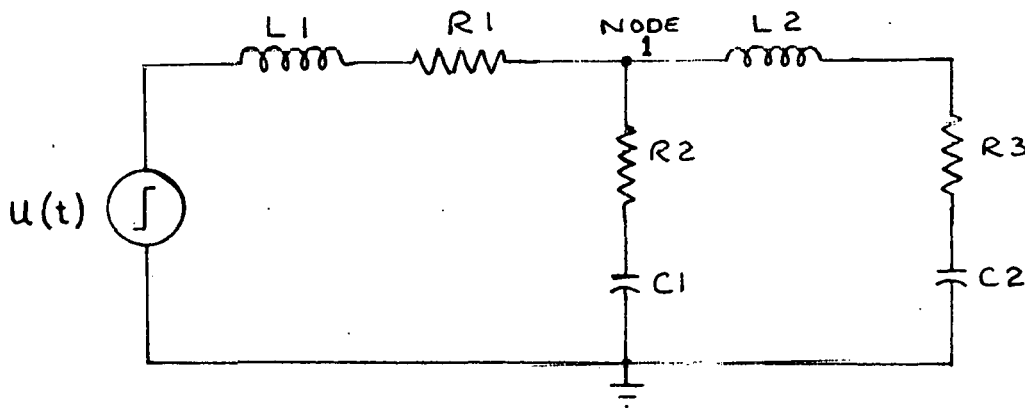


Figure D-1

The SCR would be connected between node number one and the datum node. $L1$ is the main snubber inductor (part of the resonant circuit), $C1$ the snubber capacitor, and $R2$ the snubber resistor. $C2$ represents SCR-to-chassis capacitance and $R1$ and $R3$ represent equivalent series resistances of the series elements. $L2$, ordinarily very small, was included to determine the effectiveness of a fourth order snubber network. The loop equations of the network, including initial conditions, are (voltage normalized):

$$u(t) = L_1 i_1' + R_1 i_1 + R_2(i_1 - i_2) + \frac{1}{C_1} \int_0^t (i_1 - i_2) dt + V_{C_1}[0^+]$$

$$0 = L_2 i_2' + R_3 i_2 + \frac{1}{C_2} \int_0^t i_2 dt + \frac{1}{C_1} \int_0^t (i_2 - i_1) dt + R_2(i_2 - i_1) - V_{C_1}[0^+]$$

where i_1' and i_2' are di_1/dt and di_2/dt respectively.

The initial conditions are:

$$i_1'[0] = \frac{1}{L_1}$$

$$i_2'[0] = \frac{R_2 i_1[0]}{L_2(R_1 + R_2)}$$

The equations above were simulated using Z-transforms and plotted for specific sets of initial conditions of $i_1[0]$ and $i_2[0]$.

The computations were executed on an EAI 640 digital computer; average execution time was six minutes per curve.

A simplified second order model for the snubber network was developed to reduce computer time and allow computation with the ISPICE program available through NCSS. The model is shown in figure D-2.

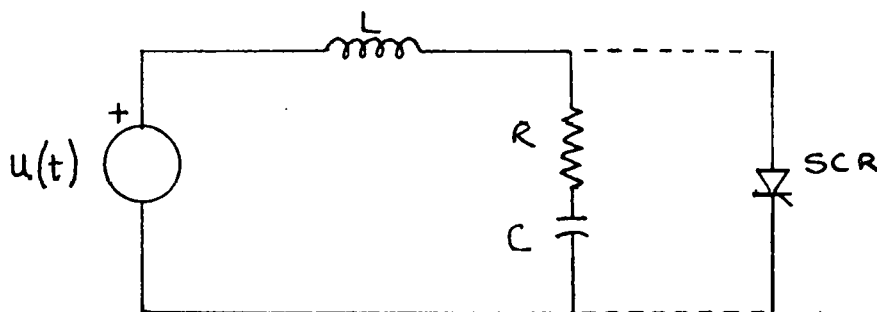


Figure D-2

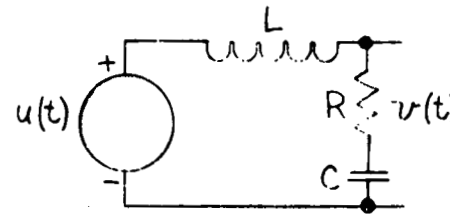
The loop equation is (neglecting SCR junction capacitance):

$$u(t) = L i' + i R + \frac{1}{C} \int_0^t i dt + V_c[0]$$

The network response to a step function was simulated and normalized in terms of damping ratio and natural frequency. Families of design curves were generated to facilitate the trade-offs necessary in choosing snubber components.

Figure D-3 illustrates the relationship between SCR anode voltage and time (normalized). Figure D-4 illustrates the normalized dv/dt vs. time that can be expected. Both families of curves are based on the damping ratio, ζ .

FIGURE D-3



SNUBBER NETWORK
2nd ORDER RESPONSE
NORMALIZED

$$Rcr = 2\sqrt{L/C}$$

$$\xi = \frac{R}{Rcr}$$

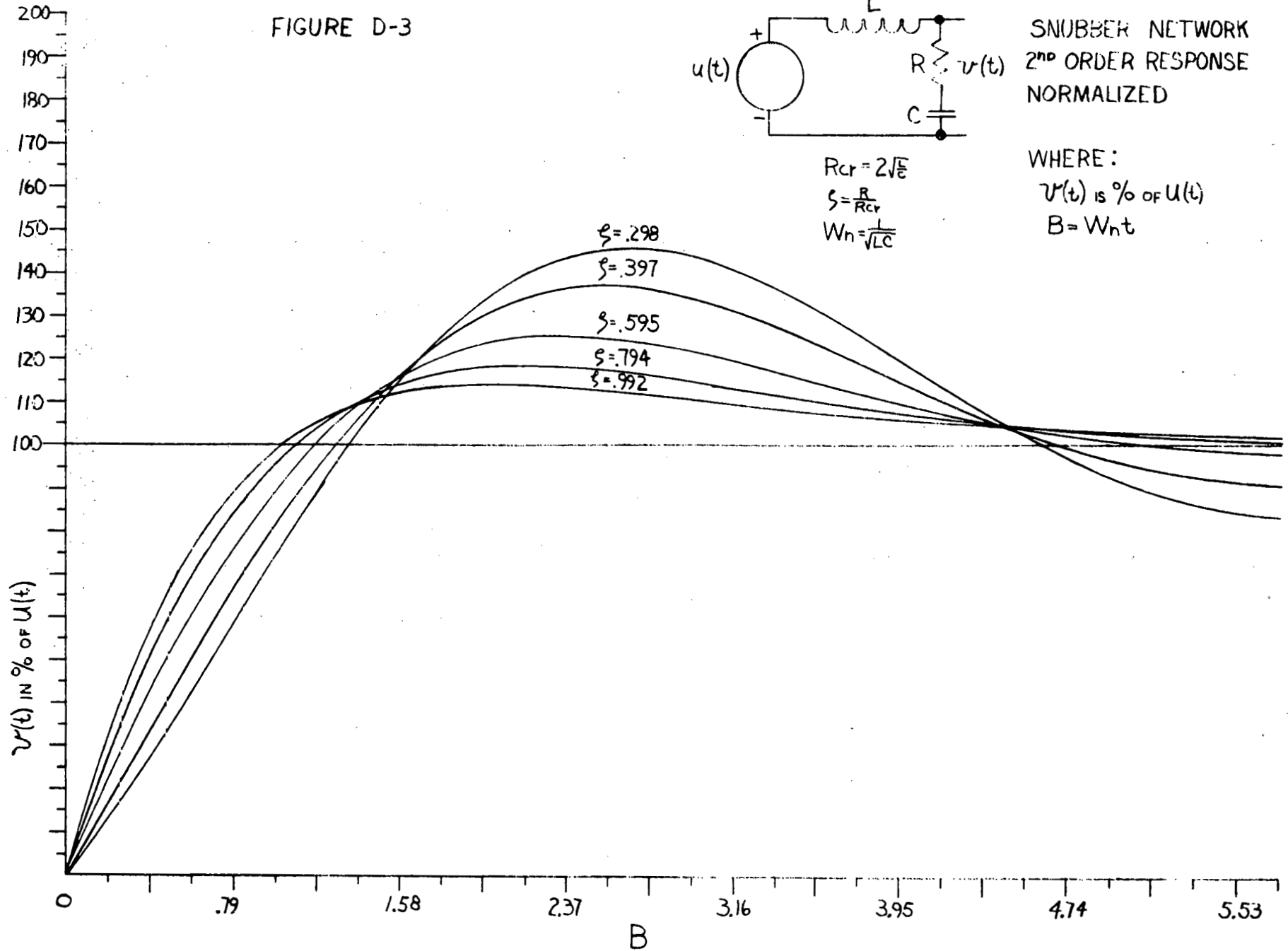
$$Wn = \frac{1}{\sqrt{LC}}$$

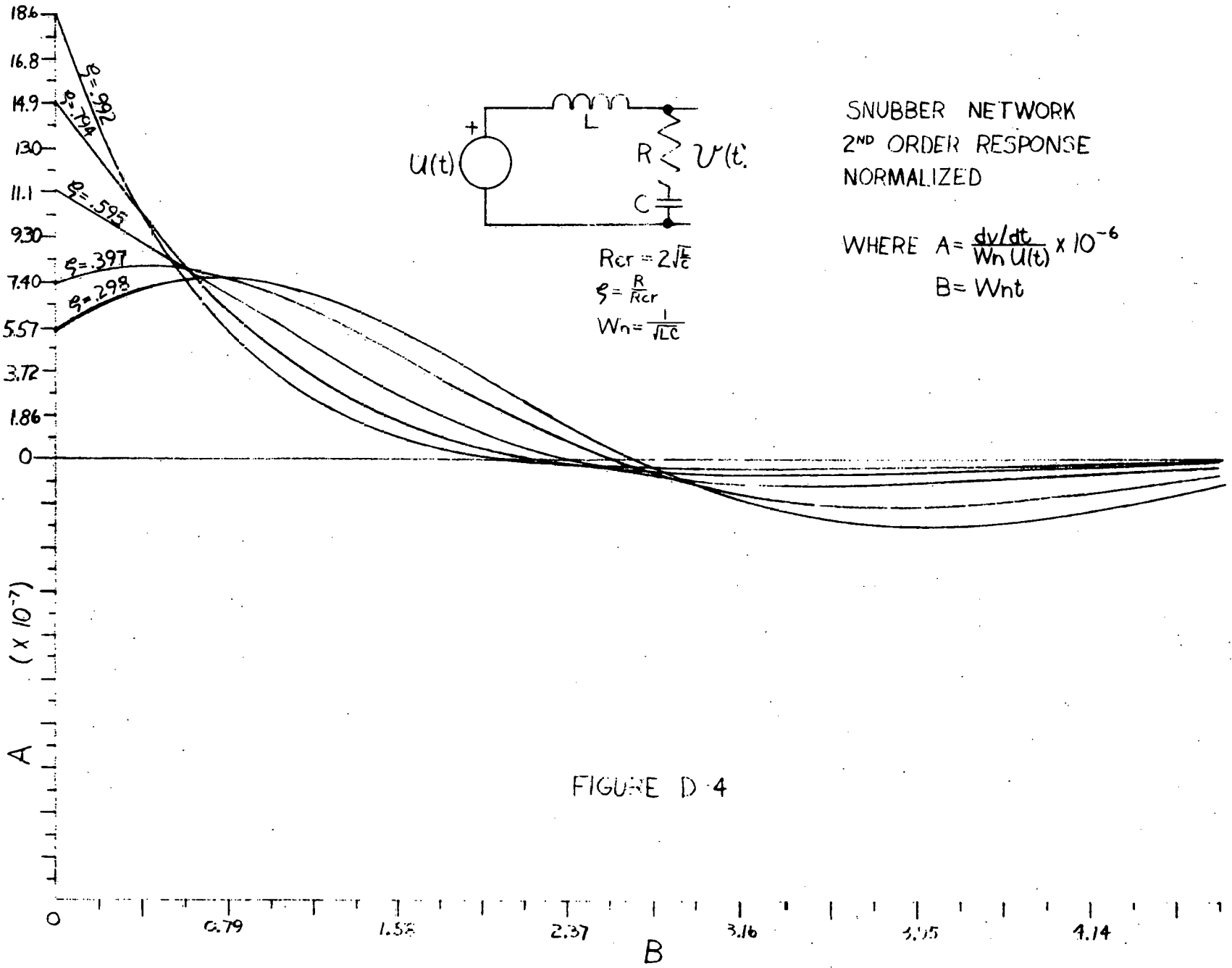
WHERE:

$v(t)$ is % of $U(t)$

$$B = Wnt$$

115





Following is an example of snubber component selection based on the second order model and curves D-3 and D-4. The following assumptions are made:

1. SCR dv/dt will be $1500V/\mu S$.
2. Peak applied line voltage is $368V$ AC, 60 Hz.
3. Snubbing inductor = $20\mu H$.

Step A: Select the damping ratio ζ from figure D-3 on the basis of allowable overshoot and a dv/dt compromise. For this example, $\zeta = 0.595$

Step B: Calculate the maximum $u(t)$. This will be the peak supply voltage ($368V$) plus the resonant ring-up voltage at point A on the power circuit schematic (see figure 2-1). The worst case, under short-circuit conditions, will be a peak of about 2.4 times the supply voltage. But since the next SCR will not be triggered for $5\mu S$ (to allow time for SCR commutation), the voltage at point A will decrease to .707 of its peak value due to ringback current. Thus,

$$u(t) = 368 \times 2.4 \times .707 = 624V$$

Step C: Calculate the natural frequency, ω_n , for the snubber. From curve D-4, choose the value A_n (normalized dv/dt) for the damping ratio $\zeta = .595$. The maximum value is 11.1×10^{-7} .

Since
$$A_n = \frac{dv/dt}{\omega_n u(t)} \times 10^{-6}$$

then
$$\begin{aligned} \omega_n &= \frac{1500}{11.1 \times 10^{-7} \times 624} \\ &= 2.16 \times 10^6 \end{aligned}$$

Step D: To calculate the snubber capacitor, C,

$$\omega_n = \frac{1}{LC}$$

$$C = \frac{1}{L\omega_n^2}$$

For L = 20 μ H,

$$C = 1.066 \times 10^{-8} \text{F}$$

Step E: The snubber resistance is the critical damping resistance, R_{cr} , times the damping ratio ζ .

$$\begin{aligned} R_{cr} &= 2 \sqrt{\frac{L}{C}} \\ &= 86.6 \Omega \end{aligned}$$

Thus,

$$\begin{aligned} R &= .595 \times 86.6 \\ &= 51.5 \Omega \end{aligned}$$

Summarizing the value selections (with standard values chosen):

$$L = 20\mu\text{H}$$

$$C = .01\mu\text{F}$$

$$R = 51\Omega$$

The simulation neglected the effects of reverse recovery current in the anti-parallel (ring-back) diodes, by assuming that initial current in the network was zero. Experience shows that the basic curve shape is unchanged, but the initial dv/dt will be altered. This is at least partly offset by junction capacitance in the SCR's, which is relatively large at low applied voltages.

APPENDIX E
DATA AND DATA REDUCTION

METER READINGS

Photo #	AC V _{IN}	AC I _{IN}	AC W _{IN}	VDC	IDC	VA _{IN} (V _{IN} × I _{IN})	P _{OUT} (Computed)
1	240	4.5	520	144.9	2.75	1080	-
2	240	6.2	1020	144.8	6.25	1488	922
3	240	7.8	1600	144.7	10.0	1872	-
4	240	9.7	2000	144.6	12.25	2328	-
5	240	14.9	3120	144.5	18.25	3576	2723
6	240	18.9	3900	144.4	22.4	4464	-
7	240	19.9	4000	137.2	23.0	4776	3345
8	240	16.6	3690	130.0	23.0	3984	3038
*	240	15.95	3500	124.0	22.75	3828	-
9	240	15.7	3450	120.6	23.0	3768	2904
10	240	14.5	3175	107.3	23.1	3480	-
11	240	13.1	2890	95.6	23.0	3144	2311
12	240	12.1	2610	83.9	23.0	2904	-
13	240	10.8	2350	72.6	23.0	2592	-
14	240	16.7	3700	133.4	22.8	4008	3198
-	264	4.0	500	144.9	2.75	1056	-
-	216	4.3	500	144.9	2.75	929	-
-	216	7.5	1350	144.8	8.50	1620	-
-	264	6.8	1400	144.8	8.5	1795	-
-	264	8.5	2000	144.7	12.1	2244	-
-	216	11.15	2000	144.7	12.1	2408	-
-	264	11.65	2750	144.6	16.5	3076	-
-	216	15.6	2825	144.6	16.5	3370	-
-	264	14.61	3475	144.5	20.25	3857	-
-	216	18.1	3280	140.2	19.0	3910	-
-	216	18.8	3700	130.0	22.8	4061	-

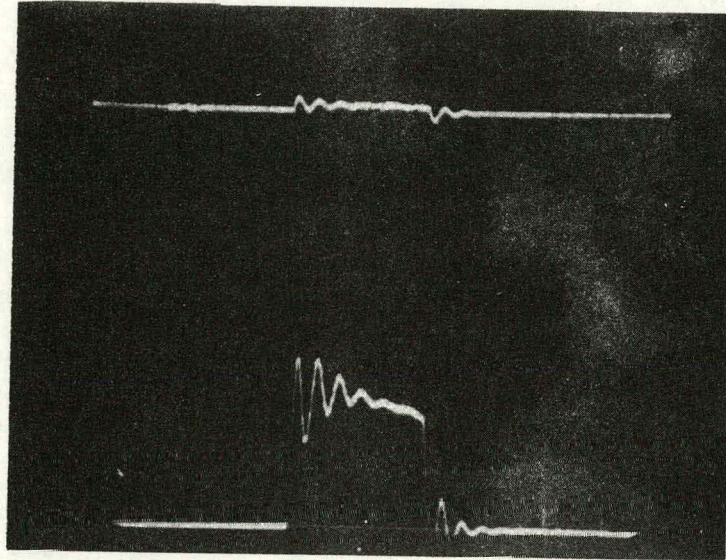
NOTE: *Indicates no photograph included.

This appendix contains the raw data from which the power module performance data were derived (see Section 4.2). The table on page E-1 summarizes these data.

The following pages contain representative oscilloscope photographs of output current and voltage, and the data points used in the calculations of efficiency. Photograph No. 8 repeats the calculation example shown in Section 4.2.2. Output power was computed for selected waveforms.

All of these data were obtained with operation on a 60 Hz utility line. For this reason, the watt-second value for each half cycle is integrated over 8.33 ms, the period at one-half cycle at 60 Hz. The resulting power is the one-half cycle average, which can be considered the long-term average output power for most charge conditions.

PHOTO #2



Data Pt	Time	Voltage	Current	W • mS
1	0	144	0	0
2	0.1	152	29	220.4
3	0.3	147	15	661.3
4	0.5	148	29	649.7
5	0.7	148	20	725.2
6	0.85	148	26	510.6
7	1.1	148	22	888.0
8	1.3	148	23.5	673.4
9	1.5	148	21	658.6
10	1.7	148	21	621.6
11	2.4	148	19	<u>2072.0</u>
				7680.8

$$\text{Average Power} = \frac{7.68}{.00833} = 922\text{W}$$

PHOTO #1

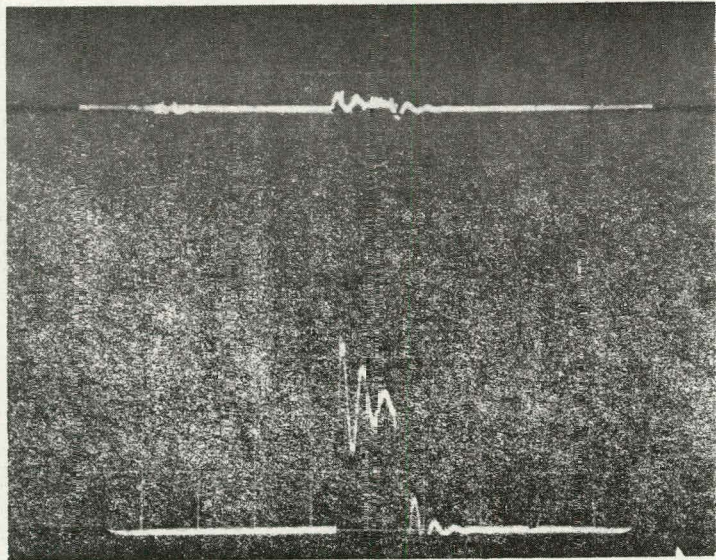
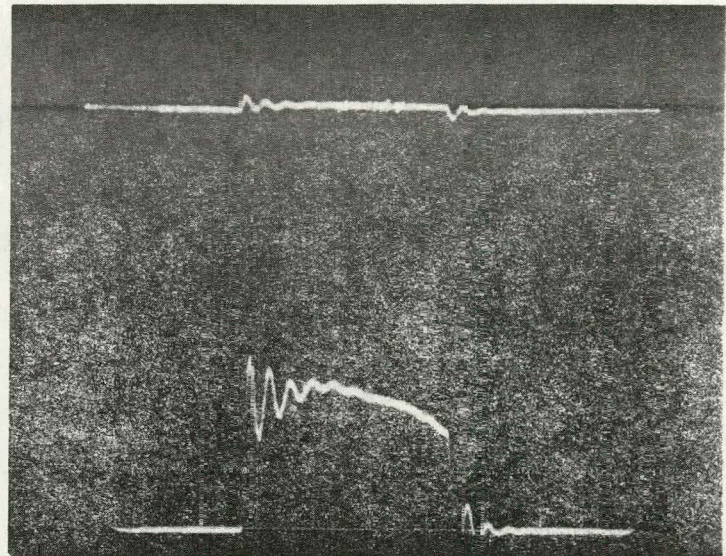


PHOTO #3



123

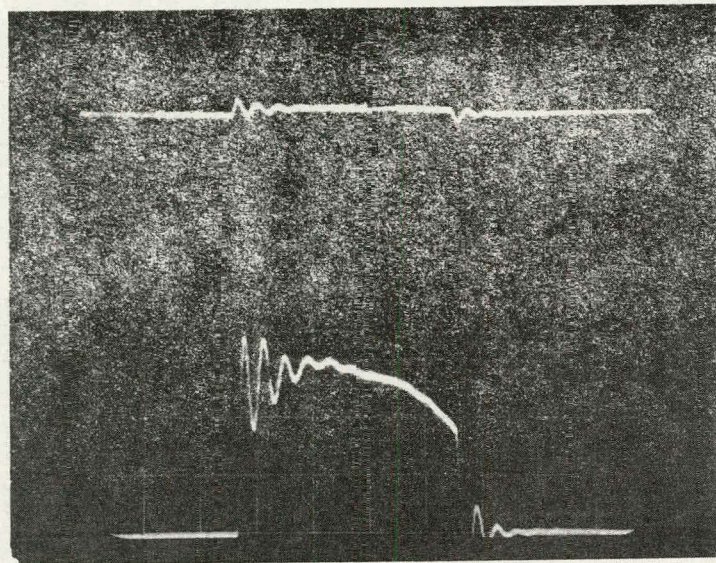


PHOTO #4

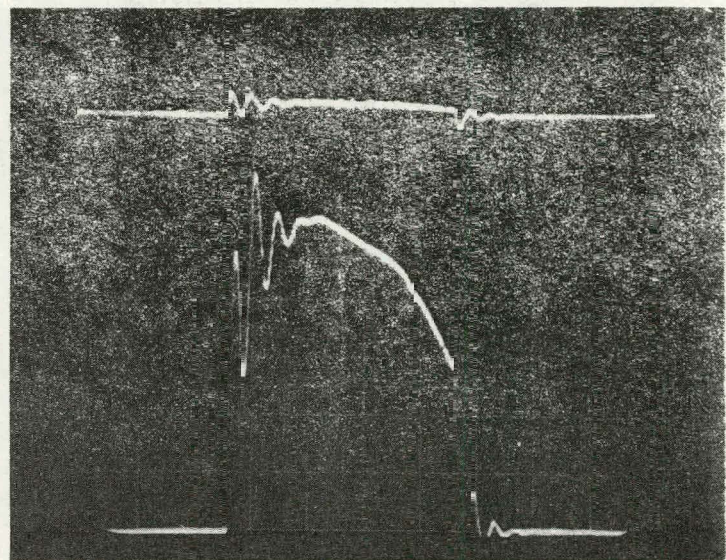
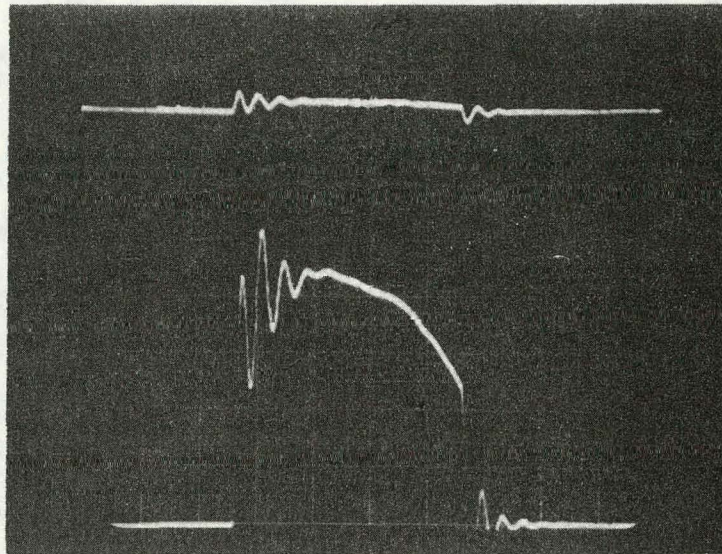
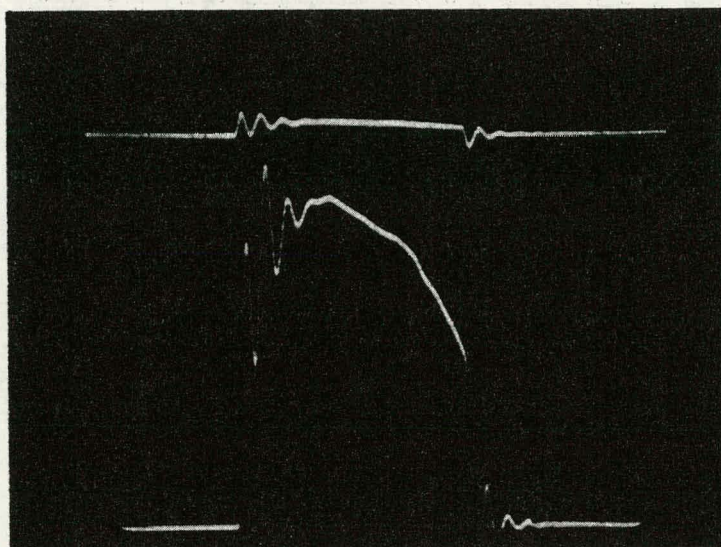


PHOTO #5



Data Pt	Time	Voltage	Current	W • mS
1	0	145	0	0
2	0.1	152	43.5	330.6
3	0.3	146	25.0	1026.2
4	0.5	150	52.0	1145.0
5	0.7	148	35.0	1298.0
6	0.8	150	46.0	604.0
7	1.0	149	40.0	1286.0
8	1.3	149	44.0	1877.4
9	1.4	149	43.0	648.15
10	1.6	149	44.0	1296.3
11	2.9	149	39.0	8038.55
12	3.2	149	34.0	1631.55
13	4.0	148	25.0	<u>3506.40</u>
				22,688.15

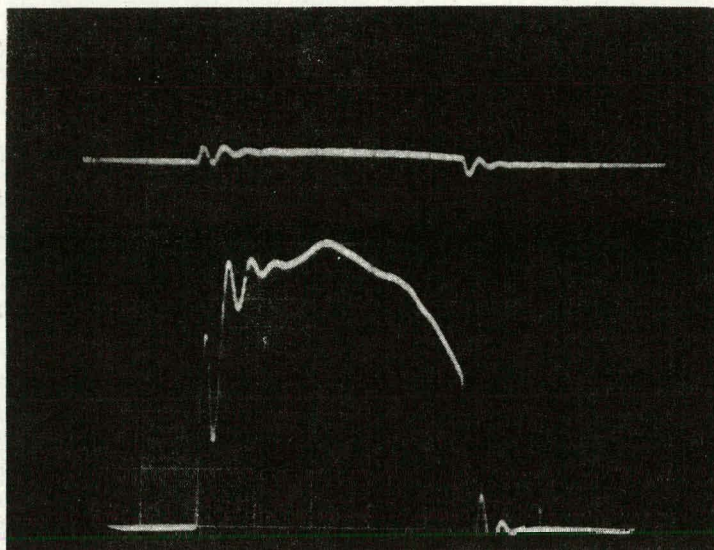
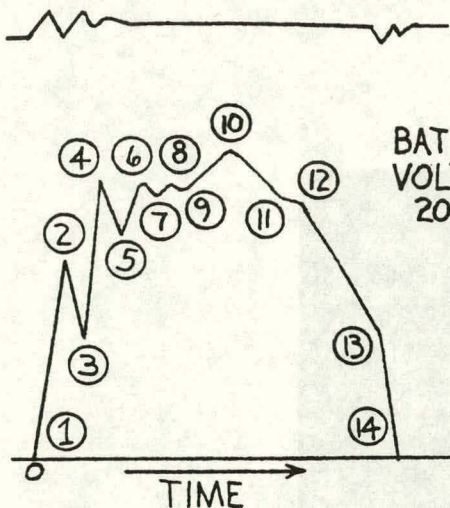
$$\text{Average Power} = \frac{22.69}{.00833} = 2723\text{W}$$



Data Pt	Time	Voltage	Current	W • mS
1	0	138	0	0
2	0.2	148	49	752.2
3	0.28	138	29	450.16
4	0.5	147	64	1475.10
5	0.68	142	45	1421.8
6	0.85	144	58	1253.07
7	1.0	142	53	1190.85
8	1.2	143	57	1567.7
9	1.6	143	58	3289.0
10	2.9	142	50	10,006.1
11	3.2	142	46.5	2005.45
12	4.0	141	30	<u>4,333.20</u>

27,763.63

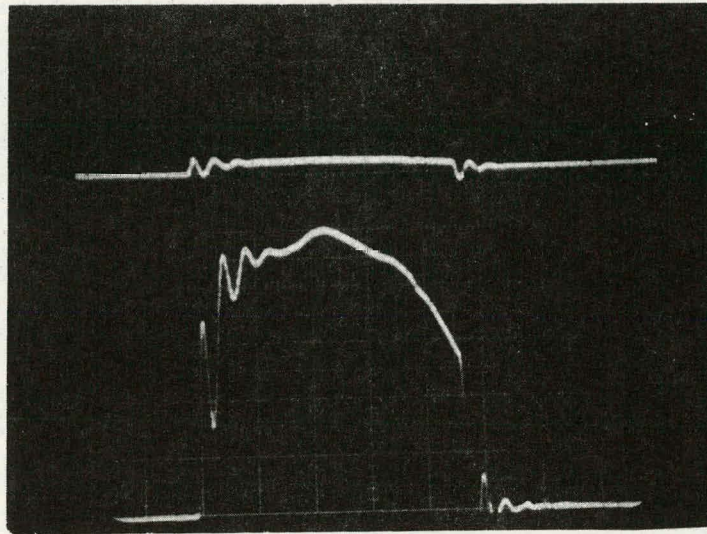
$$\text{Average Power} = \frac{27.76}{.00833} = 3345\text{W}$$



Data Pt	Time	Voltage	Current	W • mS	I • mS
1	0	128	0	0	0
2	0.1	134	33	221.1	1.65
3	0.25	128	16	485.25	3.675
4	0.50	134	47	1043.25	7.875
5	0.65	132	38	848.55	4.25
6	0.85	132	47.5	1128.50	8.55
7	1.05	132	44	1207.8	9.15
8	1.3	132	47	1501.5	11.375
9	1.5	132	46	1227.6	9.3
10	2.2	132	50	4435.2	33.6
11	3.2	132	44.5	6237.0	47.25
12	3.6	132	43	2309.6	17.5
13	4.6	131	28	461.0	35.5
14	4.7	131	0		
				25,316.35	189.67

Meter Readings Manual Integration

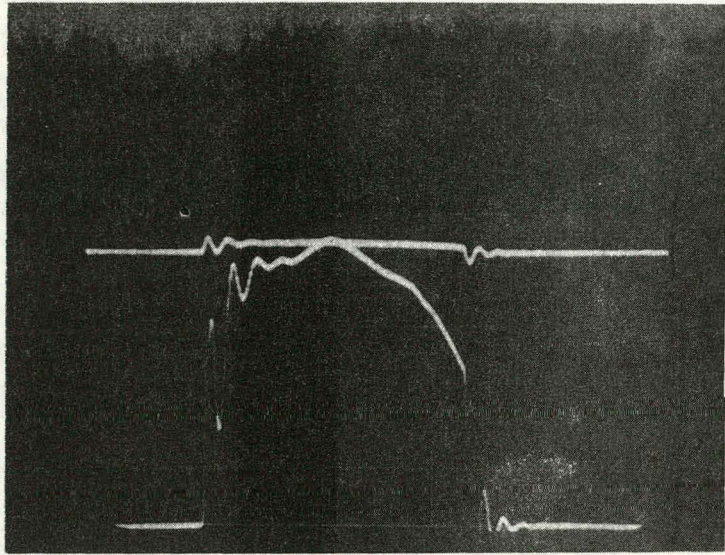
Average Current	23.0	22.76
Average Power, Metered (Average Current* Average Voltage)	2990	
Average Power, Calculated (Integrated Instantaneous Products)		3038



Data Pt	Time	Voltage	Current	W • mS
1	0	121	0	0
2	0.1	126	34	214.2
3	0.25	121	16	466.5
4	0.5	126	45	950.75
5	0.7	124	38	1038.2
6	0.9	126	47	1063.4
7	1.1	124	44	1137.8
8	1.3	124	46	1116.0
9	1.7	124	46	2281.6
10	2.3	125	50	3586.2
11	3.3	125	45	5937.5
12	3.7	125	42	2175.0
13	4.7	124	26	<u>4237.0</u>

24,203.0

$$\text{Average Power} = \frac{24.2}{.00833} = 2904\text{W}$$

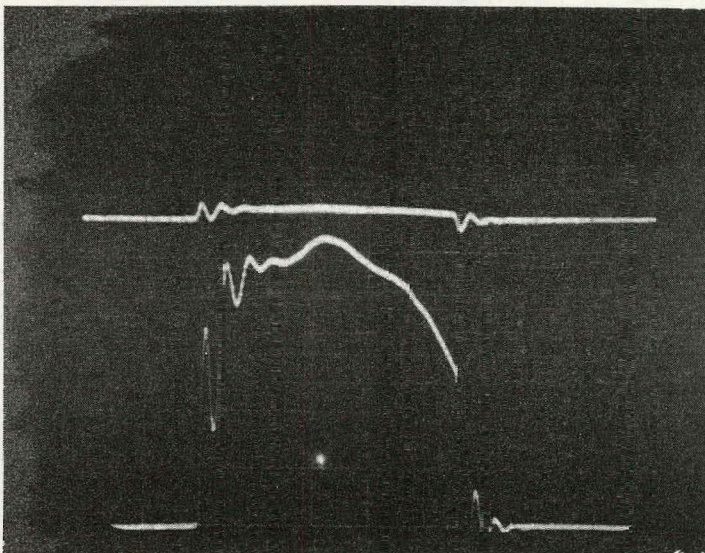


Data Pt	Time	Voltage	Current	W • mS
1	0	85	0	0
2	0.1	101	36	181.8
3	0.25	95	27	465.075
4	0.5	100	45	883.125
5	0.65	98	40	631.5
6	0.85	99	47	857.3
7	1.1	99	46	1150.875
8	1.35	99	47	1150.875
9	1.55	99	46	930.7
10	2.2	99	50	3088.8
11	3.2	99	44.5	4677.75
12	3.7	99	42	2140.875
13	4.05	98	37	1362.2
14	4.6	98	28	<u>1751.75</u>

19,262.0

$$\text{Average Power} = \frac{19.26}{.00833} = 2311\text{W}$$

PHOTO #10



129

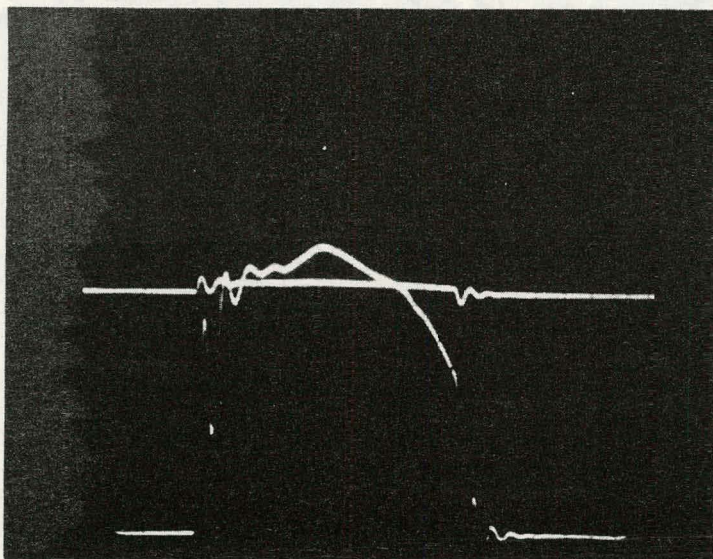


PHOTO #12

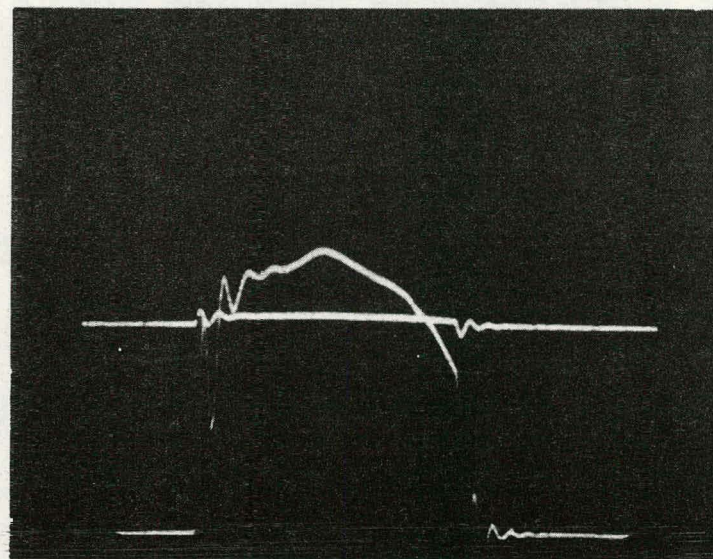
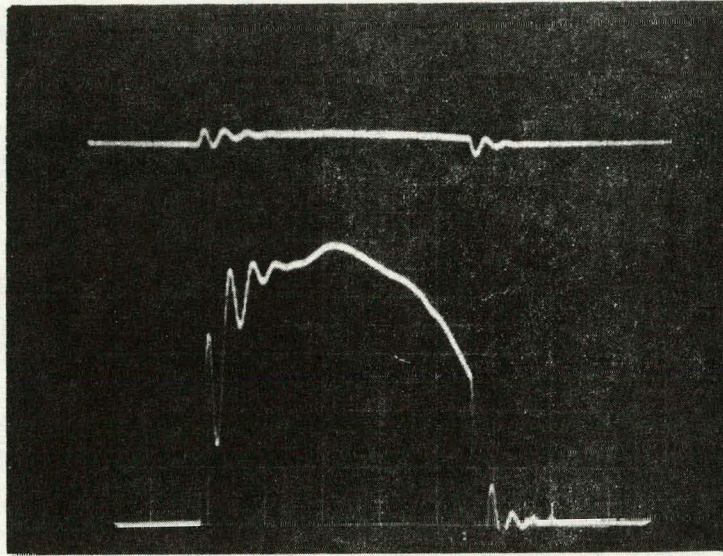


PHOTO #13



Data Pt	Time	Voltage	Current	W • mS
1	0	134	0	0
2	0.2	138	33	455.4
3	0.4	134	14	643.0
4	0.55	138	45	606.45
5	0.75	136	35	1097.0
6	1.0	138	46	1388.5
7	1.15	137	43	917.925
8	1.4	138	46	1529.875
9	1.55	138	45	941.85
10	1.85	138	46	1883.7
11	2.2	138	49	2294.25
12	2.4	138	49.5	1359.3
13	3.9	137	41	9336.0
14	4.3	137	36	2109.8
15	4.8	137	25	<u>2089.25</u>

26,652.3

$$\text{Average Power} = \frac{26.65}{.00833} = 3198\text{W}$$

APPENDIX F
ESTIMATED MATERIAL COST

APPENDIX F.

ESTIMATED MATERIALS COSTS

<u>Description</u>	<u>Quantity</u>	<u>Cost</u>		
		<u>100's</u>	<u>1,000's</u>	<u>10,000's</u>
Printed Circuit Board Ass'y.	1	47.46	37.39	29.78
Power Rectifiers	8	77.98	60.19	40.45
ASCR's, RCA S3710M	4	56.00	56.00	56.00
Bridge Rectifier	1	15.40	15.40	15.40
Free-Wheeling Diode	1	16.35	11.47	5.89
Heat Sinks	4	14.95	12.15	9.35
Varistor (transient suppressor)	1	1.55	1.16	.65
Input Capacitor	1	8.73	7.27	7.06
Resonant Capacitors	4	20.70	17.23	16.65
Output Capacitors	2	42.75	35.80	34.90
Snubber Capacitors	4	2.80	2.80	2.80
Cooling Fan & Filters	1	30.50	24.20	20.35
Control Transformer	1	3.77	3.59	3.42
Output Transformer	1	22.00	20.00	18.00
Input Choke	1	7.00	6.00	5.00
Current Transformer	1	2.50	2.25	2.00
Snubber Inductors	4	6.00	5.00	4.00
Input Circuit Breaker	1	19.70	16.20	16.10
Output Fuse & Block	1	3.27	2.80	2.35
Output Connector	1	3.10	3.10	3.10
Line Cord Set	1	4.67	3.74	2.80
Enclosure*	1	18.70	18.70	18.70
Sub-Total		426.08	362.43	314.75
Indicators (Meters & Shunt)	Set	41.89	38.27	34.70

*This estimate is for an enclosure manufactured in-house. The commercial enclosure supplied with the model for this contract has a cost of \$49.00 in thousands.

APPENDIX G
POWER MODULE OPERATION AND CALIBRATION

APPENDIX G

POWER MODULE OPERATION AND CALIBRATION

I. Safety Considerations

- A. Always connect to a grounded single phase 240 V 60Hz utility line, with a 20A capacity.
- B. Do not operate with covers removed.
- C. Do not block air intake or exhaust openings.
- D. Do not operate with damaged line or output cables.
- E. Clean air filters monthly.
- F. Do not contact output terminals. High voltage exists at these terminals.
- G. High voltages exist at several points within this equipment. Service should be done by qualified personnel only.

II. Physical Installation

- A. The charger cabinet must be fully assembled and all hardware secured prior to operation.
- B. The charger must be mounted securely in a clean location. Sufficient space (4 inches or more) must be provided at front and rear panels for air intake and exhaust.
- C. The charger must not be installed where the ambient temperature exceeds 40°C or where water can fall or be splashed on the cabinet.
- D. Battery fumes must not be drawn into the cabinet.

APPENDIX G (cont'd)

III. Power Requirements

- A. Connect the charger to a single phase, 60Hz, 240V grounded supply. The line breaker must be rated at 20A or more. The service shall be sized according to the breaker rating, but must not be smaller than AWG 12.

IV. Circuit Adjustments

Refer to Schematic Diagram SC6041000, and the Control Circuit Board Assembly, SC6041022.

The charger has been carefully adjusted prior to delivery. If adjustments should be required, they should be made in the following sequence, with the input line at 240VAC and at full output power (23A @ 120V battery) except as noted.

- A. R281 - Adjust the maximum firing interval for zero deadtime between last ringback pulse and the next main pulse, as seen across R206 with <8A output current. (see figure G-1).
- B. R286 - Adjust the minimum commutation time to 7 μ S, as seen on C229 with a CRO. (Adjust at low line). see figure G-2.
- C. R264 - Adjust for total conduction period of 5mS each half cycle at 120V battery. see figure G-3.
- D. R243 - Adjust for maximum charge voltage of 145V (adjust with fully charged battery attached).
- E. R234 - Adjust for an output DC current of 23A at battery voltages \leq 120V.

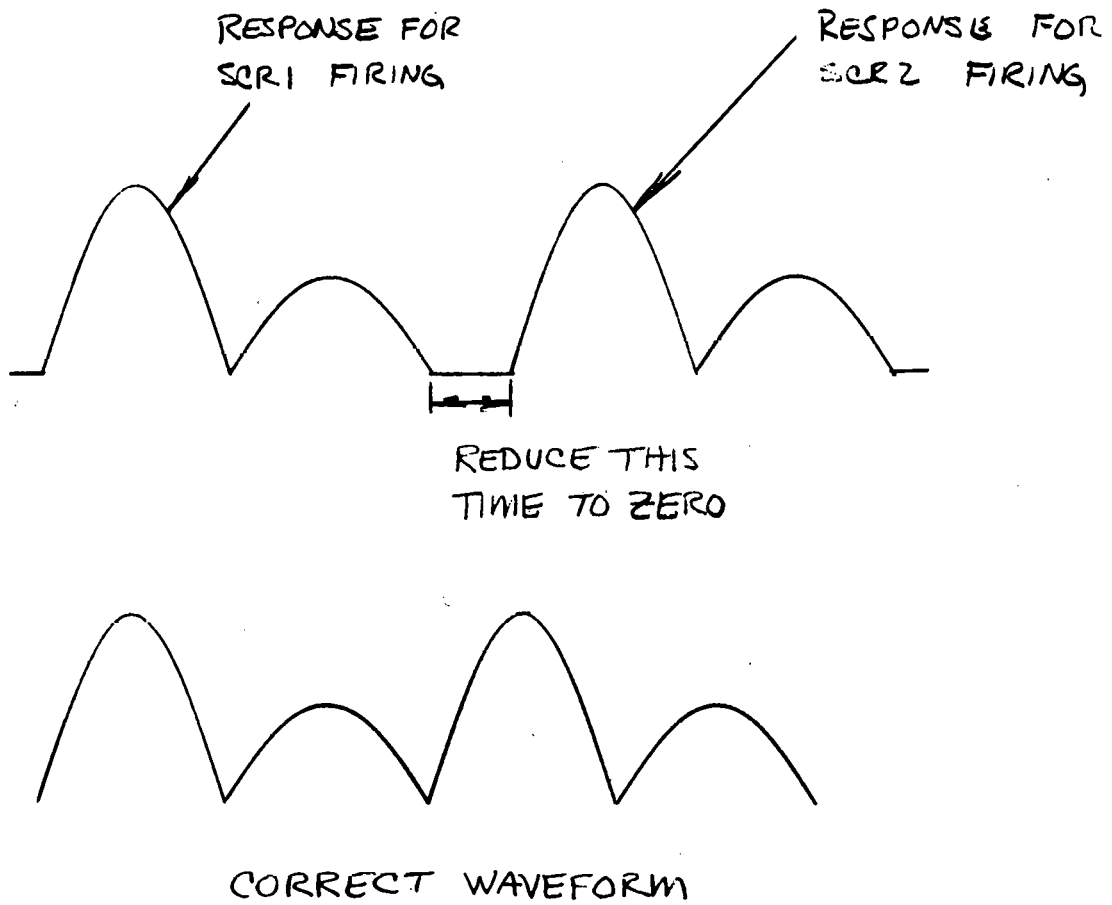


FIGURE 5-1
ADJUSTMENT OF MAXIMUM FIRING ANGLE

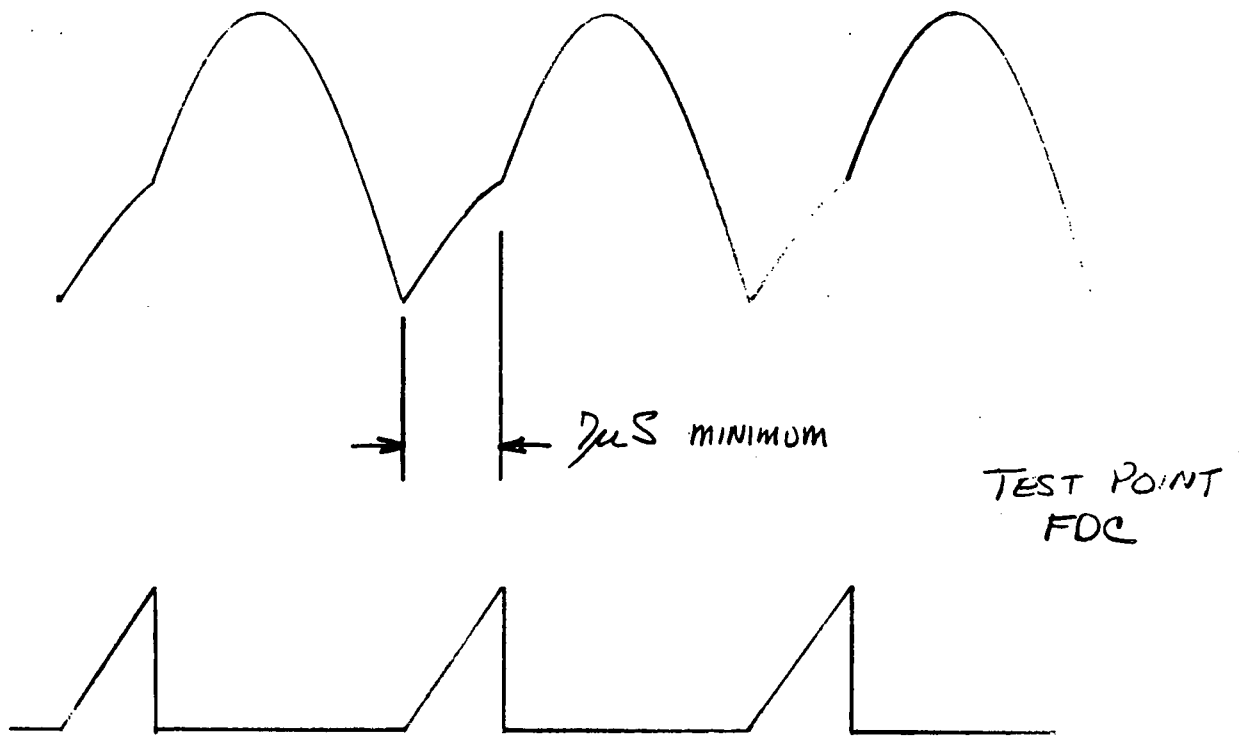


FIGURE 5-2
ADJUSTMENT OF MAXIMUM FIRING INTERVAL

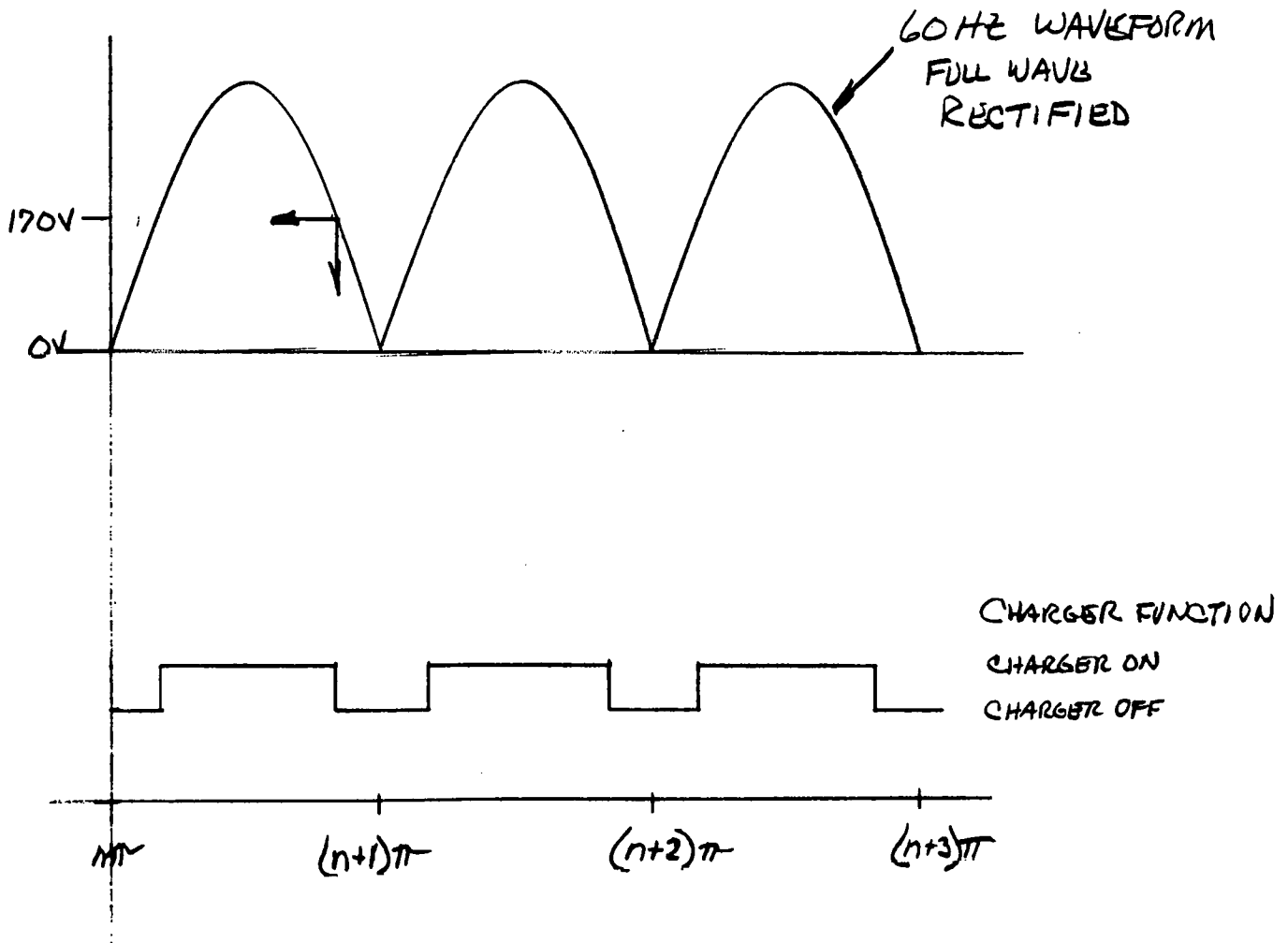


FIGURE 5-3

ADJUSTMENT OF CONDUCTION PERIOD
SHOWN FOR 60 HZ.